37 Copies.

GPO PRICE $ _____

CFSTI PRICE(S) $ _____

Hard copy (HC) 3.00

Microfiche (MF) .65

ff 653 July 65

NASA CR-66529

REGENERABLE ADSORBENT STUDY

By L. C. Spece, F. P. Rudek, T. F. Green, and R. A. Miller

Prepared under Contract No. NAS 1-6574 by
The General Electric Company
King of Prussia, Pa.

for

NATIONAL AERONAUTICS AND SPACE ADMINISTRATION
LANGLEY RESEARCH CENTER
HAMPTON, VA.

CONTENTS

LIST OF ILLUSTRATIONS

LIST OF ILLUSTRATIONS (Cont)

LIST OF TABLES

LIST OF TABLES (Cont)

FOREWORD

This report was prepared by the Life Support Engineering Operation of General Electric's Manned Orbiting Laboratory Department under Contract No. NAS 1-6574. The program was performed under the direction of the Flight Instrumentation Division, Langley Research Center. Contract technical monitor was Rex Martin. The work reported here was performed between August 1966 and December 1967.

Principal investigators for General Electric were: Larry Spece, Engineer, Life Support Equipment; F. P. Rudek, Supervising Engineer, Life Support Equipment; and T. F. Green, Applied Mathematician, Analysis and Techniques Operation.

ABSTRACT

The purpose of this R&D was to describe the performance of a thin film solid regenerable adsorbent, e.g. (determine CO_2 adsorption rates, efficiencies, sizing criteria, and other pertinent system design parameters). The investigations were carried out for a range of environmental conditions which covered the normal operating levels for a typical flight system. The tests were organized into three and four variable factorial designs, and the data were treated by standard statistical techniques.

This type sorber panel is most appropriate for coadsorption of H_2O and CO_2, or for use with a conventional predryer in which CO_2 is desorbed to space. The limiting resistance to CO_2 adsorption is evidently the boundary gas film at the surface of the sieve panel and not within the sieve itself. Equilibrium capacity was nearly 25 percent less than that reported by the manufacturer for pellet beds.

A simplified model was formulated and verified experimentally for the thin film sorber plate. A system weight was derived with this model and the test results which compared favorably with packed bed-type systems. Development of panels with more efficient heat transfer characteristics is possible, and should be completed before a prototype system design is undertaken.

SUMMARY

The experimental investigation reported here was concerned primarily with investigation of uniquely configured regenerable absorbents for carbon dioxide and water vapor removal. The adsorbents, that were evaluated, are adhered by means of a porous binder as a thin continuous film to a metal substrate containing integral heat transfer coils. The resultant assembly or adsorber panel is mounted within a gas tight canister so that the process gas mixture may be directed over the surface of the adsorbent layer. This thin film adsorbent concept gives a "blowby" rather than a "blowthrough" canister arrangement as is the case with the more common packed column bed that contains the adsorbents as individual randomly oriented pellets.

Advantages potentially obtainable from the thin film concept are:

(1) Optimized, uniform, more easily predicted coefficients of heat transmission between the adsorbent sites and the heat source or heat sink fluid. Thus adsorption phenomena that are related to adsorbing temperature may be closely controlled at optimum levels (e.g. adsorb-to-desorb cycle time ratio can be optimized due to minimized thermal lag).

(2) The ventilating gas flow path through the canister can be designed to give minimum flow resistance, thus minimizing the blower power requirement for circulation of process air through the canister. The above mentioned advantages showed the potential for developing an optimized regenerable CO_2/Water Vapor Adsorption System for use with long mission manned space vehicle life support systems.

In order to prove out the validity of the thin film concept, this experimental program was undertaken with the objectives of obtaining design criteria for design of a prototype regenerable adsorbent system. The program experimental approach makes use of statistical techniques to expedite the selection of test runs, so that a maximum of data that bracketed the anticipated performance range for a flight system could be obtained with minimum redundancy in the testing. Test results were corroborated analytically by use of a mathematical model which is based upon the molecular diffusion of the adsorbed gas (CO_2 or water vapor) through the gas boundary layer over the surface of the adsorbent structure. As proven by the test program, this is the primary impedance to the flow of gas into the adsorbent interstices.

The following adsorbents were investigated: Linde Molecular Sieves (13X and 5A), and Silica Gel. Testing of packed column adsorber beds was also performed as a part of this program. Design criteria that were evolved for these adsorbents are presented as well as the performance and physical characteristics for a prototype system for coadsorption of CO_2 and water vapor. Based upon the results obtained to date, it appears that the thin film concept can result in a substantial savings in weight for an operational system for extended mission space vehicle life support systems.

INTRODUCTION

Objective

The evolution of prime hardware optimized for space flight, or for that matter any item, is accomplished by carrying out several distinct developmental phases, i.e., feasibility investigation, laboratory experimentation, a breadboard model, formulation of a prototype design, and flight environment qualification of the prime configuration. If any of these phases are compromised or bypassed, the end item is not likely to be satisfactory. When the product is not adequate for the job, extensive and time consuming backtracking must be accomplished in order to obtain a satisfactory product. In other words, accelerated or so called "high risk" development efforts should be avoided.

Unfortunately in many cases the hardware developmental cycle is "accelerated" with the excuse that "not sufficient time and funds are available to permit performance of all development phases". Invariably such "accelerated" programs end up costing more and taking longer to accomplish than they would if they were done right in the first place. It seems that the phase most commonly slighted is the laboratory experimental effort, perhaps the most important one. It is this phase that provides the design engineer with a set of criteria upon which to base his breadboard and subsequent prototype designs with the confidence that an optimized product will result. When adequate criteria are not determined, the breadboard and prototype models are designed only on the basis of intuition and rules of thumb which are important contributors to a successful effort, but not sufficient in themselves. The resulting design in most cases is finally made to function, but nobody knows precisely why or whether it is performance, weight, or volume optimized.

Adsorbent systems for CO_2 and H_2O vapor control in life sustaining space vehicle environments (e.g., silica gel, the zeolites, and aluminum oxide among others) have been under development for some time. The regenerable adsorbent concept is the most likely candidate for CO_2 adsorption on Advanced Apollo applications and other vehicles of that generation. Their feasibility has been proven, and workable prototypes have been fabricated. To date, a comprehensive laboratory experimental program has not been accomplished for these adsorbents. Thus, state-of-the-art prototypes fall in the category "they work, but nobody really knows why or how well". Scale-up or variations to satisfy particular design requirements with these systems would obviously be a haphazard effort.

For these reasons, a laboratory experimental program to define the performance of various CO_2 and H_2O vapor adsorbents configured as thin continuous films on an internal metal substrate (see figure 1), was initiated. The thin film concept was selected as the primary candidate for evaluation because of its aforementioned potential advantages over packed column pellet beds. Packed column test data were obtained to

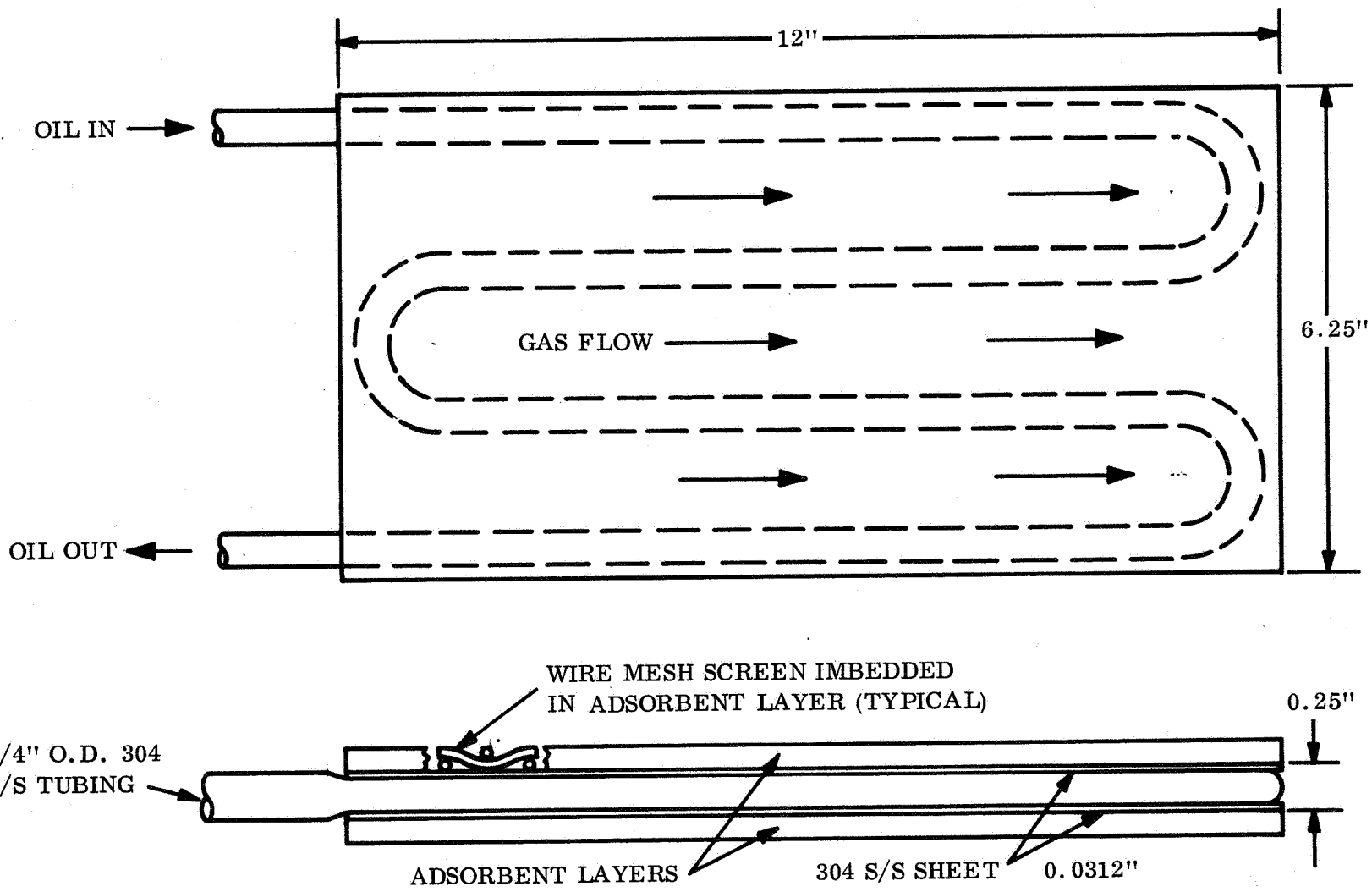

Figure 1. Adsorbent Plate Assembly

validate the program test set up adequacy by comparison of the data with packed column data from other sources. The end result of this program, provides a set of design performance criteria in parametric form. Once the design requirements are known, for a given application, the engineer will need only to compare his requirements with the criteria evolved from the proposed investigation in order to tailor the hardware to the application.

A major shortcoming evidenced with packed column pellet bed configurations, is that the random contact points between the pellets result in poor coefficients of heat transmission between the adsorption sites and the heat source or coolant fluids. Pellet beds inherently exhibit this characteristic. Thermal lag problems and significant temperature gradients throughout the bed are observed. In order to improve the thermal conductance paths within the bed, the idea of utilizing zeolites in the form of a thin continuous film, bonded to a metal heat transfer surface with integral fluid passages was conceived. Figure 1 depicts such a thin film adsorber plate. The CO_2 laden ventilating air stream is directed over the surface of the adsorbent and CO_2 is adsorbed when it diffuses into the porous continuous zeolite layer.

Initial feasibility tests during an inhouse test program indicated that the thin film concept was a promising one. During the initial feasibility testing, adsorption-desorption cycles were manually controlled by alternately valving hot and cold fluid sources as required. A 1 percent CO_2 -dry air mixture was fed to the bed during adsorption. Desorption was accomplished with heat and partial vacuum, (vacuum at room temperature) and nitrogen purge at room temperature. The 1 percent CO_2-air mixture was passed through the sieve plate canister with an MSA Lira Analyzer at the exit to record the CO_2 concentration in the effluent air.

Test results showed that the CO_2-air mixture passes over the sieve plate, with a concentration profile analogous to the flow profile of a fluid, through a smooth conduit. A flow velocity can be reached that allows optimum bed loading efficiency and rate of adsorption. At low velocity, laminar boundary layers mask the CO_2-sieve interface thereby reducing the adsorption rate. High velocities reduce the CO_2-sieve contact time thereby reducing bed efficiency.

Heating and cooling cycles (22.6 minutes total) for the feasibility models were longer than anticipated because of excessive thermal mass, and the use of common lines for cooling and heating. Throughout the testing, pressure drop across the sieve plate assembly was so low as to be non-measurable with an inclined water manometer.

The most significant results of the test, were the demonstration of effective CO_2 adsorption on the thin film molecular sieve plate at controlled bed temperatures, insignificant pressure drop, and rapid desorption of CO_2 at both room temperature and elevated temperatures. In addition, the possibility of applying other adsorbents (i.e., silica gel and aluminum oxide) in a similar configuration appeared likely (since both are formulated by processes which appear to permit deposition of continuous films on

metal surfaces). Based upon the above results, the subject experimental research program was proposed. It centers around establishing a complete set of performance characteristics and design criteria for various adsorbents in the thin film configuration.

EXPERIMENTAL DESIGN

The primary objectives of this program are to generate system design criteria for the thin film adsorber panel CO_2 control concept, which will permit definition of a preliminary system design, and subsequent comparison with packed pellet bed carbon dioxide control systems. In order to achieve these objectives, it is necessary to describe in detail both the physical and operational characteristics of the adsorber panels. Definition of these characteristics are to be in terms of system weight, power, volume, and also in terms of the dynamic operational parameters such as process gas flow rates, process gas pressures, operating temperature, regeneration temperatures, and pressures, weight of sieve per unit of exposed area, etc. Data required to describe the adsorber panel system in these terms can best be obtained by a carefully integrated experimental and analytical program.

To this end, the program described herein was formulated and performed utilizing statistical techniques and procedures where applicable. The experimental program was structured along the following broad task categories.

(1) Selection of variables to be considered and definition of ranges.

(2) Determination of the significance of these variables in terms of their effect on adsorber panel performance and their interactions with each other.

(3) Formulation of quantitative relationships between adsorber panel performance, the variables selected, and system design criteria.

The subsequent sections describe the methods used to perform each of these tasks, the analysis and quantification of the results, and the empirical and theoretical basis (where applicable) for all factors of significance.

Selection of Variables

Consideration of all the variables that could conceivably be of significance leads to a rather large, unwieldy tabulation of factors. There are, however, practical limitations which when considered serve to reduce the number of variables and in some cases the range of interest. One such limitation was the decision to limit the program to evaluation of one "type A" and one "type X" molecular sieve, silica gel, and activated alumina for various adsorption functions. These are tabulated in table 1 along with other variables associated with the selected adsorber panel configuration and size.

Variables presented in table 2 represent those shown to be most significant during early feasibility tests, and analyses of typical adsorption system characteristics. Selection of the ranges, and the levels within each range were based upon the consideration of test equipment limitations, practical limitations of typical spacecraft systems,

TABLE 1

ADSORBER PANEL CHARACTERISTICS

Adsorbent	Configuration (a)	Weight of adsorbent pounds	Weight of panel assembly pounds	Function
Linde 13X	1/8" thick	0.677	5.31	These panels to be tested separately for adsorption of carbon dioxide and water vapor, and as a coadsorber for carbon dioxide and water vapor.
	1/4" thick	1.45	6.73	
Linde 5A	1/8" thick	0.650	5.15	This panel assembly to be tested as a carbon dioxide adsorber in a relatively low dewpoint atmosphere.
Davison silica gel, no. 05	1/8" thick	0.586	5.07	To be tested as a predryer.
	1/4" thick	1.17	6.44	To be tested as a predryer.
Alcoa activated alumina, H-151	1/4" thick	1.34	5.98	To be tested as a predryer.
	1/2" thick	2.80	8.06	To be tested as a predryer.

a — Thicknesses shown are for two 6" x 12" layers/panel.

and the anticipated problems associated with correlation of theoretical and empirical relationships. The rationale associated with the selection of each variable, its range, and intermediate points is briefly described in the following paragraphs. Specifics regarding verification of the applicability of the ranges (and/or intermediate points) selected will be discussed in detail in the report sections concerned with the particular variable.

TABLE 2

DYNAMIC TEST PARAMETERS

Variable	Units	Minimum value	Maximum value	Comments
Velocity	ft/min	25	375	Intermediate points are 200 and 275 feet/minute. Velocity is calculated rate across the face of the adsorber panel.
Carbon dioxide partial pressure	mm Hg	3.1	21	Intermediate points are 4.0, 5.3, and 7.6 mm Hg. Pressure specified is at canister inlet.
Plate temperature Adsorption	^{o}F	30	75	Maximum value is range from 72^{o} to 75^{o}F and represents naturally attained steady-state level.
Desorption	^{o}F	75	300	Desorption was performed at ambient temperature as well as 150^{o}F.
Inlet dewpoint	^{o}F	- 30	+ 40	Inlet dewpoint controlled at two levels.
Path length	feet	2	4	Length varied by placing canisters in series.
Total pressure adsorption	mm Hg	380	760	Several runs made at low total pressure. Change in performance seemed insignificant.
Desorption	mm Hg	20×10^{-3}	50	Regeneration at 200 microns was also achieved.

Adsorber Panel Characteristics

Selection of adsorbents to be tested were based upon the specific functional characteristics of each material as generally reported in the beginning of this section. That is the "type A" was tested primarily as a carbon dioxide adsorber. The "type X" sieve was tested as a carbon dioxide adsorber and as a coadsorber, performing the function of carbon dioxide removal in the presence of appreciable quantities of water vapor (i.e., + 40°F dewpoint). Silica gel and activated alumina were slated for tests as dryers (some silica testing was performed, activated alumina was not tested).

Configuration of the adsorber panels as flat plates, with either 1/8 inch or 1/4 inch layers of adsorbent bonded to them, was a selection based upon prior development testing with similar assemblies and the recommendations of the Linde Division of Union Carbide to limit adsorbent thickness to 1/4 inch. The recommendation not to exceed 1/4 inch was based upon current limits of technology at Linde and, since it did not appear to seriously limit the scope of this program the advice was accepted. The one square foot adsorbent area (i.e., two 6 x 12 layers per assembly) was selected to provide flexibility to the program by providing easily measureable quantities of dynamic process variables and such results as flow rates, temperatures, carbon dioxide, and water vapor adsorbed, etc.

Test Variables

For any given adsorbent-adsorbate system the parameters effecting the adsorption process can be generally categorized as those concerned primarily with mass and heat transfer. The variables listed in table 2 represent these factors as applied to the test system. Velocity, path length, absolute pressure, and carbon dioxide partial pressure clearly are critical parameters affecting the rate of transfer of carbon dioxide. Plate temperature and inlet dewpoint are parameters more directly concerned with the carbon dioxide capacity of any given adsorber panel. In the carbon dioxide adsorption cycle, water vapor acts as an interfering contaminant effecting adsorbent capacity.

The range of velocity selected is intended to cover both the laminar and turbulent flow regimes to provide data on the variation in adsorption rates which may be attributed to velocity. The lower level (i.e., 25 feet/minute) results in a Reynolds number of 440 for a rectangular duct at one atmosphere total pressure and 75°F. Initially 200 feet/minute (Reynolds number, 3530) was selected as the upper limit but preliminary screening tests indicated little effect on the performance of the adsorber test assembly. Tests at 275 feet per minute had greater effect on adsorption rates so a change in the upper limit to 375 feet/minute was made.

Changing the total pressure from one atmosphere to one-half atmosphere had little effect on the performance of the adsorber test assembly. Since elimination of this factor as a variable effecting adsorption would produce at worst a conservative

estimate of adsorber performance, total pressure was eliminated as a variable for the adsorption process. The range of pressures studied during desorption were designed to provide information on performance in two distinct modes. First, vacuum desorption (20 to 200 microns) with carbon dioxide dump to space, and second the recovery of carbon dioxide by regeneration at a moderate pressure level (50 mm Hg) more closely approximating performance of an onboard pumping system.

Carbon dioxide partial pressure is of course the major factor to be considered. The level of partial pressure affects both rate and capacity. Physiological limitations dictate that CO_2 level not exceed 7.6 mm Hg in areas inhabited over long periods of time. Spacecraft system designs specify CO_2 levels no greater than 3.8 mm Hg (or 0.5 percent of a sea level atmosphere). This therefore is the level at which the adsorber system must operate and represents the low end of the range tested. Testing at 21 mm Hg was performed primarily to aid in the formulation of a suitable mathematical model and to insure the validity of data collected by purposely providing for an easily discernable change in adsorber performance.

Range of inlet dewpoints selected simulates two potential operating conditions. The low dewpoint accounting for operation with a predryer, the high level for operation without a separate predryer -- i.e., performing in a coadsorption mode.

Adsorber plate temperatures of 30°F and 75°F were designed to bracket a reasonable operating range for a spacecraft environmental control system. The lower level was selected to determine the degree of gain in capacity so that the overall system penalty of operation at this level could be assessed. Regeneration temperatures were selected on the basis of other studies reporting on the availability of heat sources in a typical spacecraft.

Test Design

Following selection of pertinent variables and levels of interest the problem becomes one of determining the possible effects of these variables on the performance of the adsorber panel. Rather than utilize the traditional approach to experimentation in which one factor is varied while all others are held constant, the number of runs required was reduced by using factorial design techniques. In this way several factors can be varied at one time in accordance with a prearranged pattern thereby obtaining a comparable amount of data with fewer runs. Factorial designs also permit estimation of the size of the error variation in the data, and an evaluation of interactions between variables if they exist.

Before proceeding to the factorial designs utilized in this program, a quick review of the terminology used in describing experimental designs may provide for easier understanding of the following text.

Experimental variables are usually called "factors". The particular value of the variable is called the "level" of the factor. The "yield" is the overall result of a run, in this case the weight of CO_2 adsorbed, or the efficiency per pass, etc. For any given run the impact of the specific variable on yield is the "effect". Each grouping of runs (or tests) examining a series of variables in the prescribed pattern is called a "block", and repetitions of the same experiment under identical conditions are called "replications".

As previously presented, the initial cut at delineating significant factors resulted in a list of seven for each material tested. The experiments are designed so that the effects of each factor can be measured and independantly tested for significance. The term "factorial designs" covers several statistical techniques for the design of the experiment. In general the factorial design is useful in making a survey of system variables. It does not in itself yield a quantitative relationship showing the effect of a variable. However, in conjunction with a regression analysis a quantitative relationship among the important variables can be established. This program utilized for the most part 2^n type factorial designs which are structured on a much simpler scale than the often used central composite designs.

Figure 2 is a composite schematic of the testing performed during this program. Figures shown in each block represent the factors tested in that particular block and the two levels of each factor. The number shown in parenthesis is the number of individual tests run in the block.

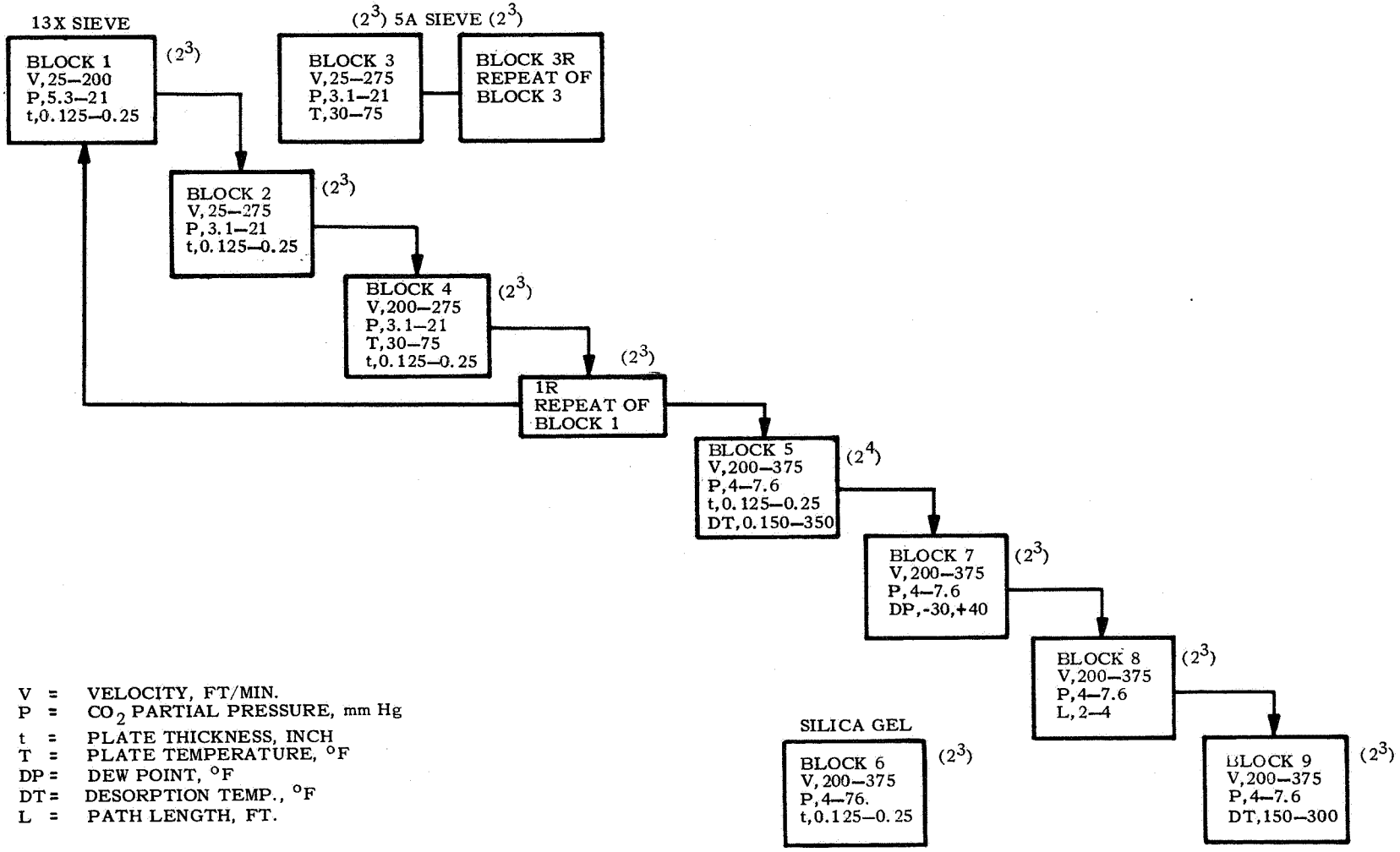

Figure 2. Test Sequence for Regenerable Adsorbent Study

TEST HARDWARE DESCRIPTION

Adsorber Plate Design and Development

Figure 3 shows an assembly of a typical adsorber plate used in the tests. The plates were assembled in two variations having adsorbent layer thicknesses of 1/8 inch and 1/4 inch applied to the outer surfaces of the plate. The 1/8 inch assembly was developed as follows:

Woven wire screen, made from 304 stainless steel, was brazed to a thin metal substrate 32 mils in thickness. The wire screen contained 0.063-inch diameter wire strands with a spacing of four wire strands per inch. The screen gave an adsorbent-to-substrate bond that assures optimum thermal conductance paths and maximum structural integrity. The primary problem associated with the brazing process was getting the wire screen to lay flat enough so that point contact could be maintained between the wire screen and the metal substrate. Annealing of the wire screen for a period of one hour and a temperature of $1800^{o}F$, softened the wire screen to the point where all warpage was eliminated from the wire screen and a level surface was achieved.

The plates were weighed and sent to the Linde Division of Union Carbide where a layer of adsorbent material was spread on the surface in the form of a slurry, completely filling the void volume in the metal screen. The moisture was driven out of the slurry by means of a refractory process (the details are proprietary to Union Carbide) leaving a solid layer of adsorbent material encapsulating the wire mesh screen. Upon return of the plates by the vendor, a second weighing was performed. The amount of sieve added to the plate was calculated as the difference between the two weighings.

The integral heat transfer fluid coils are made from 1/4-inch o.d. 304 stainless steel tube bent into the shape shown in figure 1. After bending, the tube was placed into a press and flattened to give an elliptical cross section so that a greater heat transfer surface area could be obtained between the tube and metal substrate. The bonding of the 1/4 inch tubing to the adsorbent plates was accomplished by using an aluminized epoxy cement. This cement, composed of 80 percent aluminum and 20 percent epoxy, required a total cure time of 21 hours at a maximum temperature of $320^{o}F$. In order to minimize plate contamination during this process, a purge gas of 100 percent nitrogen gas (dewpoint less than $-60^{o}F$) was flowing continuously through the curing oven. After allowing the oven to cool to room temperature, the plates were removed and a flanged, gasketed faceplate was added to the assembly as shown in figure 3. This plate, made from teflon, thermally isolated the adsorber plates from the canister walls during testing and facilitated plate installation and removal from the canister.

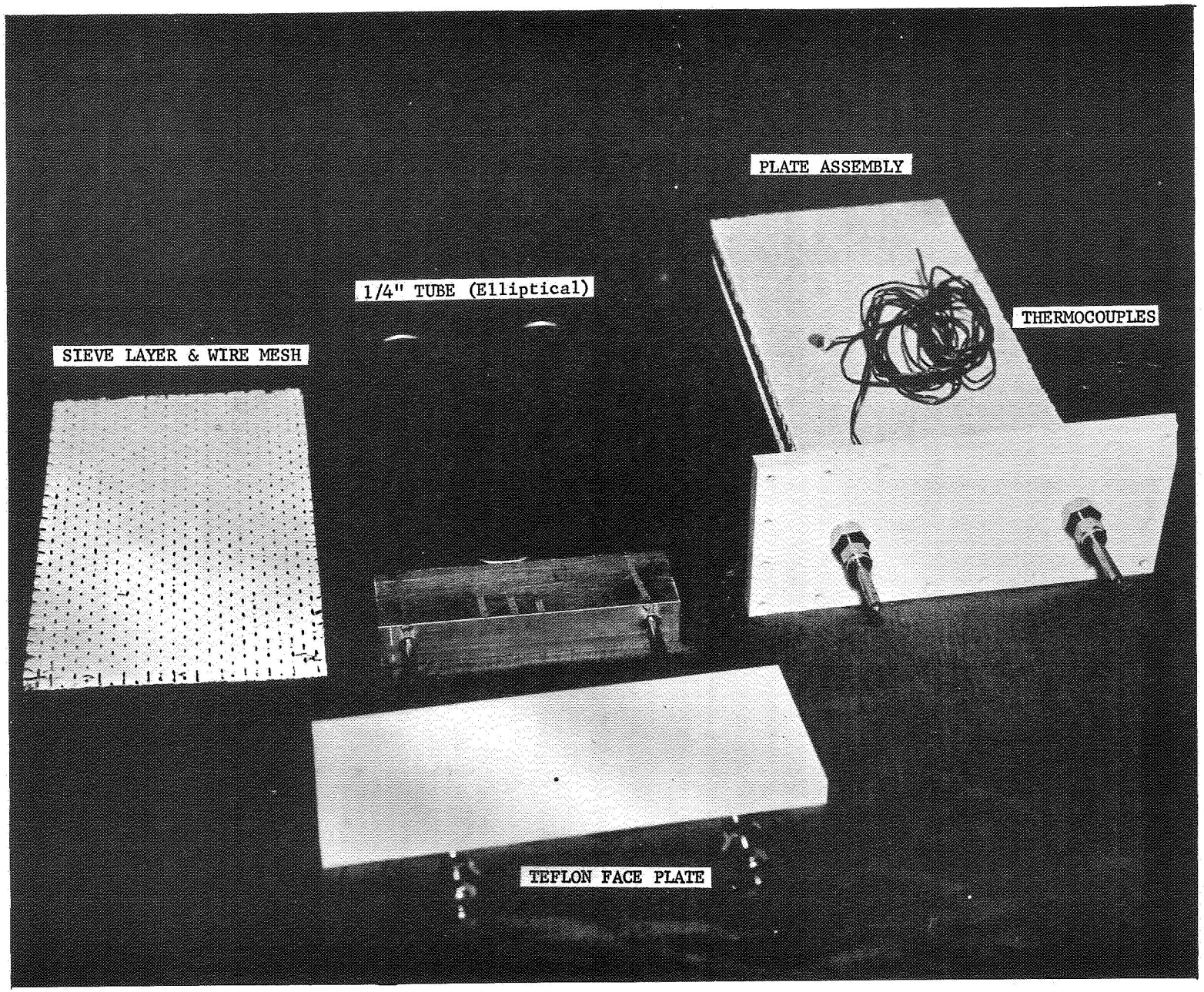

Figure 3. Adsorber Plate

The 1/4 inch assemblies were fabricated by methods similar to those used for the 1/8 inch assemblies, the only major differences being the dimensions of the wire screen and the weight of adsorbent added to the layer. The 1/4 inch wire screen was made from 304 stainless steel and contained wire strands 0.12-inch in diameter. The spacing of the wire strands was two per inch amounting to a wire separation distance of 0.5 inch.

Canister Design

The canister assembly shown in figure 4 houses the adsorbent plates and is comprised of a main housing, a front flange, inlet/outlet manifolds to permit flow of process gas through the canister, and a vacuum port located at the rear of the housing. Six teflon stringers are attached to the sides, top, and bottom of the housing to position the adsorbent plate during installation and to thermally isolate the plate from the canister walls. The stringers also serve as vanes to straighten the flow of process gas as it proceeds along the plate surface. The adsorbent plate, after insertion into the canister, is attached to the rectangular flange on the front of the canister by 20 mounting screws. A 1/16-inch silicone-rubber, rectangular gasket is placed between the teflon face plate and the aluminum flange to provide a leak-free sealing surface. The dimensions of the gasket and teflon face plate are shown in figure 4. The adsorbent canister assembly is shown schematically in figure 5.

The inlet manifold made from 1.0-inch o.d. 6061-T6 aluminum tubing is welded to the top surface of the canister housing. The process air enters the canister through three oblong orifices, 0.25 X 1.0 inch cut through the canister wall. The process gas exits from the canister, through an identical manifold welded to the bottom surface of the canister.

The vacuum port located at the rear of the canister is made from a section of 2.0-inch o.d. aluminum tube attached to a 6.0-inch diameter flange. The 6.0-inch flange served as the mounting surface for the entire canister assembly and connected with a 2.0-inch shut off valve located on the vacuum.

Instrumentation

This section covers the choice of instruments used to measure the process variables investigated in the regenerable adsorbent study.

The flow meter used to measure CO_2 inlet gas rates was a Brooks 8940 flow controller connected to a Model 1355 rotameter with tantalum float. This combination has a maximum capacity of 840 cc/min of CO_2 at 20 psig and 70°F (0.515 lb CO_2/hr) with an accuracy of $\pm$ 1 percent of maximum scale reading. The maximum flow rate of 0.515-lb/hr gives adequate capacity for the test setup where CO_2 adsorption rates did

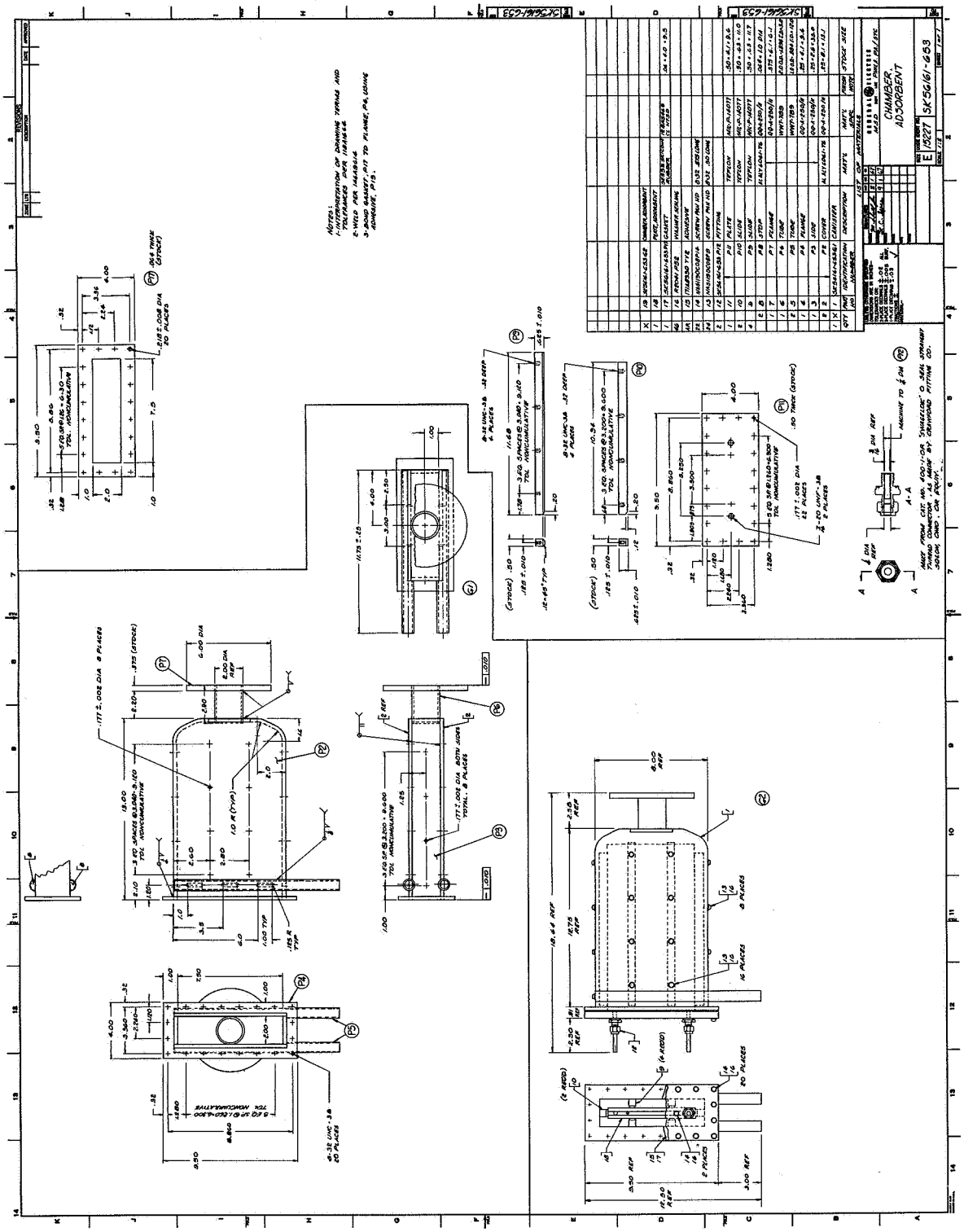

Figure 4. Canister Assembly

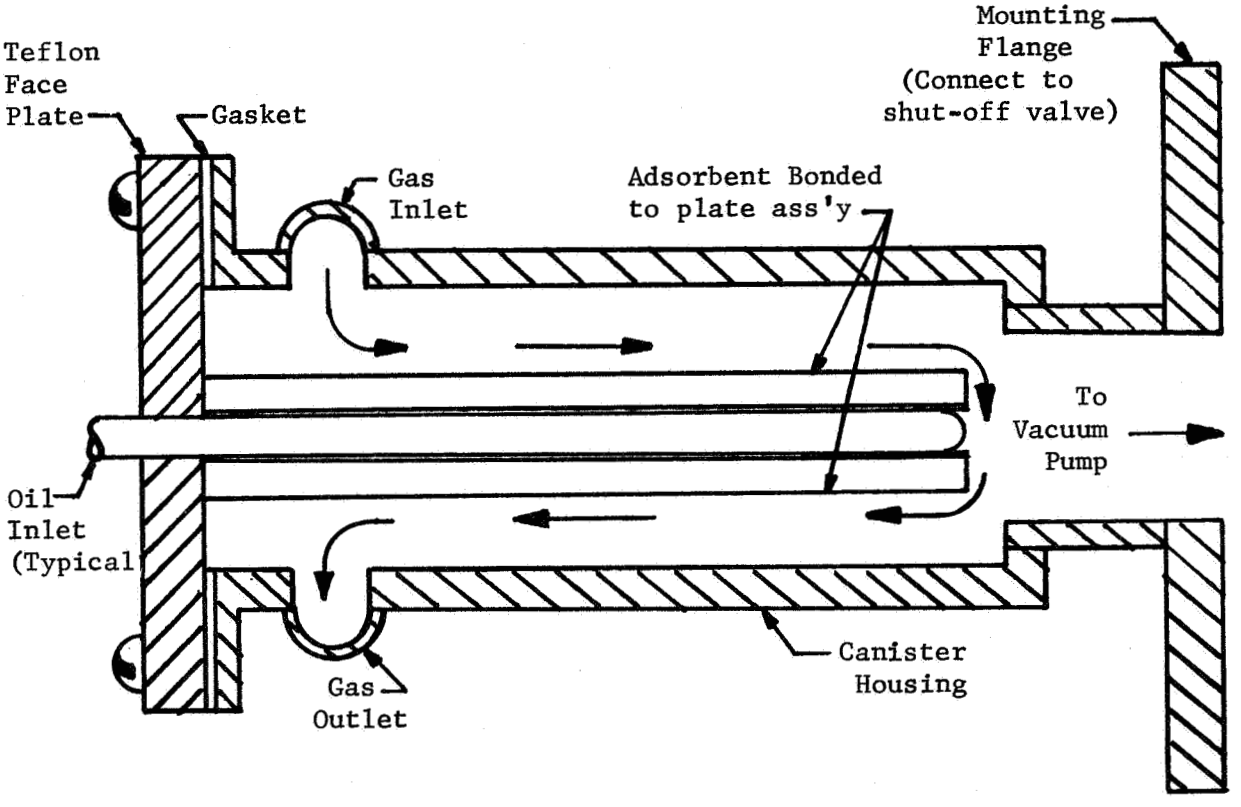

Figure 5. Cross Section of Adsorbent Canister

not exceed 0.2-lb CO_2/hr. The calibration curve for the instrument is shown in figure 6.

The instrument used to detect CO_2 concentration was a LIRA 300 Infrared Analyzer, manufactured by the Mine Safety Appliances Company. The instrument was calibrated at the beginning of each day by using certified calibration gases containing one, two, and three percent by volume of CO_2 mixed with nitrogen gas. The sampling lines connecting the LIRA to the flow system were 1/4-inch o.d. copper tubing approximately 2 feet long. The sample flow rate was 1 SCFH which is in accordance with the manufacturer's recommendations. The output signal from the LIRA was connected to a Model 6702 Multipoint Recorder, manufactured by Weston Instrument Company, so that a continuous trace of the CO_2 concentration could be obtained. In order to control the CO_2 concentration at a constant level in the system during testing, two relays located on the recorder were preset, one to start CO_2 flow when the CO_2 concentration fell below the desired setpoint and the other to terminate CO_2 flow when the CO_2 concentrations exceeded the setpoint. The bandwidth for this control setup was found to be $\pm$ 0.1 mm or a maximum error of $\pm$ 3.2 percent.

Two dewpoint hygrometers, supplied as GFE, were used during the testing, the Model 992-C1-T1-R1 unit manufactured by Cambridge Systems, Inc., and the Model DHGL-3P unit manufactured by the Bendix Corporation. Both instruments measure dewpoint to an accuracy of $\pm$ 1°F. The inlet and outlet sampling lines were 1/4 inch-o.d. 304 stainless steel approximately 4 feet in length. The Cambridge unit was used to monitor the canister inlet humidity because control relays, which were an integral part of the unit, could be connected to the water control solenoid valve and used to maintain the constant 40°F inlet dewpoint required for the tests. The Bendix unit had a faster response time and for this reason, was used to monitor the canister outlet humidity. Both units were connected to a Weston Model 6702 Multipoint Recorder to provide continuous readout capability.

It should be noted here that the inlet sample lines to the CO_2 and dewpoint detectors were located approximately 2 feet downstream of the cabin simulated volume (see figure 9). The outlet sample lines were located about 3 feet downstream of the canister outlet.

The meter used to monitor process gas flow rates was a Brooks 1 inch Venturi, Model 20660. The venturi was permanently installed in the flow system 3 feet upstream of the canister and connected to a water manometer graduated in 0.1 inch increments and readable to 0.05 inch. The lower flow of 25 ft/min approached the accuracy limits of the device since a Δ P of only 0.1 inch of water was required to provide this rate. This item is discussed further in the data analysis. The difficulty did not arise in measurements at the higher velocities of 200 to 375 ft/min since the calibration curve (see figure 7) possessed a much steeper slope in this range.

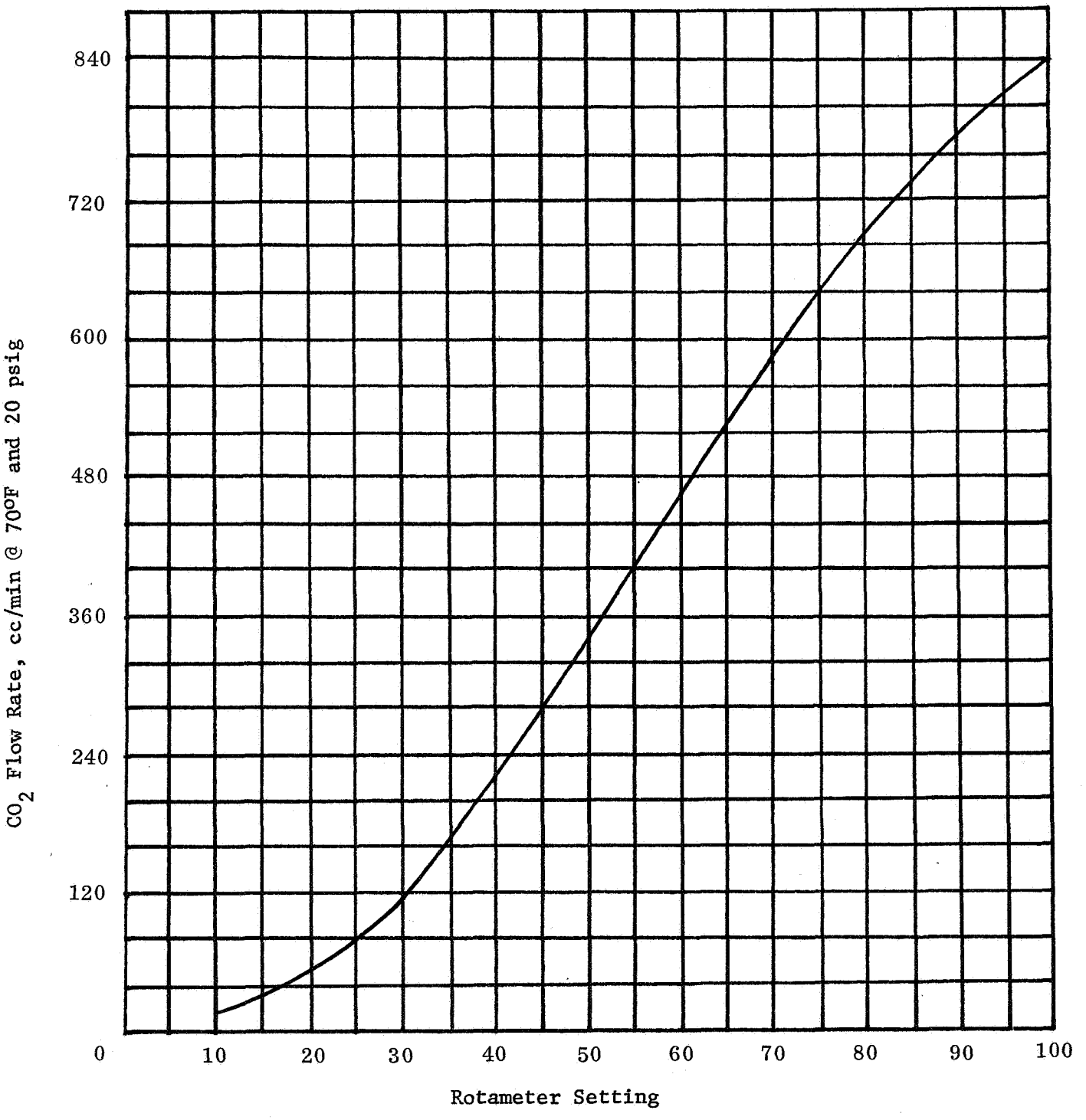

Figure 6. Calibration Curve for CO_2 Rotameter

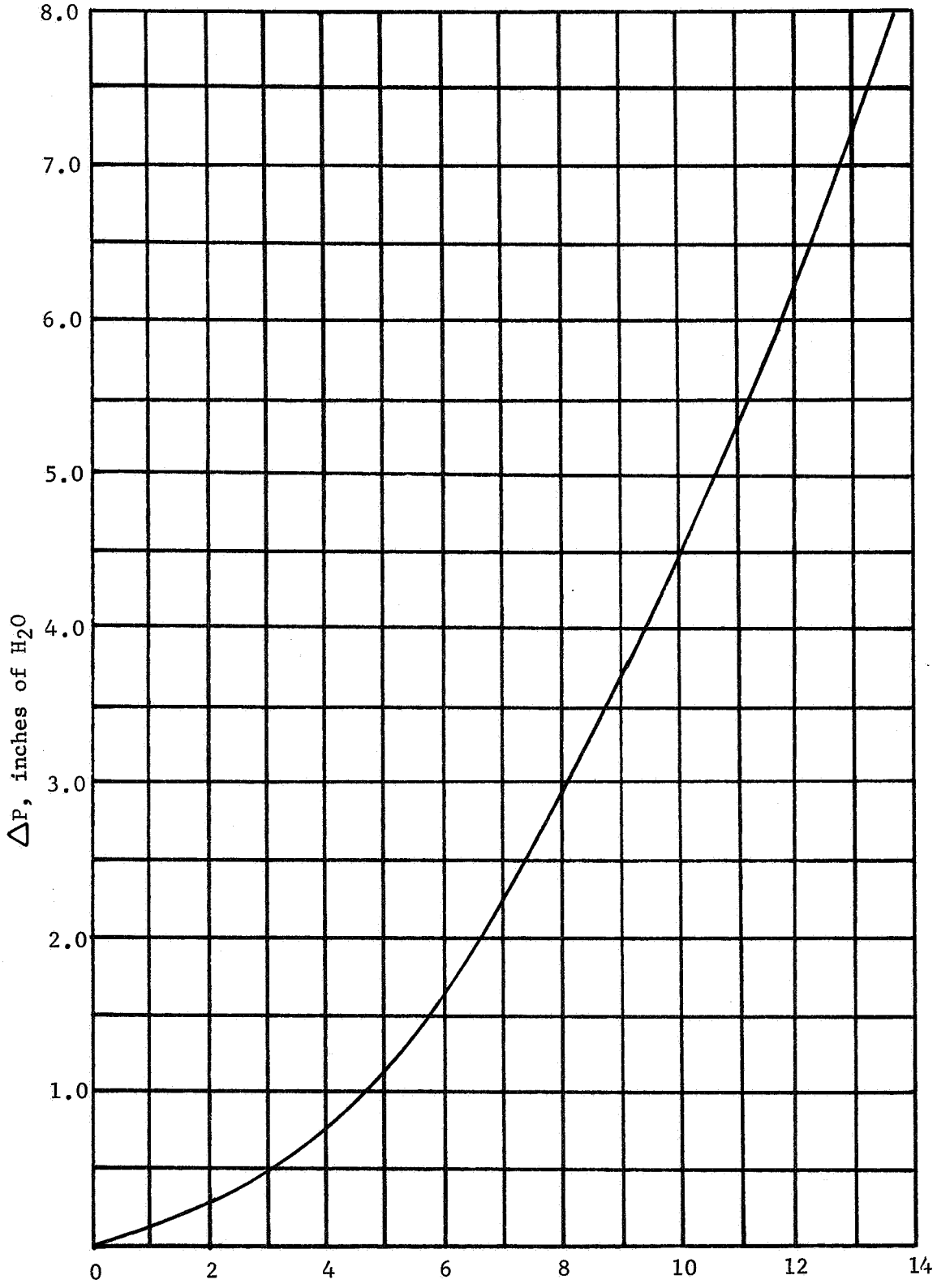

Figure 7. Calibration Curve, Air Venturi

The pressure transducer used to monitor canister pressure during regeneration was the Model 6081-1 unit manufactured by Electro Optical Systems, Inc., and was supplied as GFE. This device was mounted in the center of the canister wall. The inlet port to the device was 6 inches from the front and rear of the adsorbent plate and approximately 0.625 inches above the plate surface. The output signal from the device was monitored on an Esterline Angus, Series S, recorder to obtain a continuous recording trace. The accuracy of the two units in combination was found from vendor specifications to be $\pm$ 1.5 percent.

The absolute pressure was monitored by a Wallace-Tiernan Model FA-160 gauge. The full scale range of 0-800 mm Hg covered the operating range of 380-760 and was used during the testing. The gauge was mounted 1.5 feet upstream of the canister and has an accuracy of $\pm$ 1 percent.

Test Setup and Procedures

In order to define both static and dynamic characteristics of the adsorber plates, two separate test setups were utilized. Figure 8 shows the static test setup used for determining the CO_2 equilibrium loading curves and heats of adsorption for both 5A and 13X molecular sieve adsorber plates. Figure 9 shows the dynamic test setup used to determine CO_2 adsorption rates, desorption characteristics, pressure drops and other system design parameters.

Static system (CO_2 equilibria).-The CO_2 adsorption capacity of the adsorber plates was determined at temperatures of 35° and 72°F and at CO_2 partial pressures varying from 2.0 mm of Hg to 49.2 mm Hg. The effect of a diluent gas was investigated by adding dry nitrogen (dewpoint less than -30°F) to the system until a total pressure of one atmosphere was attained.

Figure 8 shows in schematic form the essentials of the static equilibrium test system employed. Prior to each test, each plate was regenerated by exposure to a vacuum of 20-60 microns Hg and an elevated temperature of 300°F to insure the same starting point for each test run. The following describe in detail the procedure followed during the test. Numbers shown in parenthesis correspond to identification numbers on the schematic. A bell jar (6), of known volume (3.51 ft^3) was evacuated through pump (7). Hot silicone oil at 350°F was pumped (11) through the adsorber plates until thermal equilibrium is attained. Pressure in the jar was monitored continuously by a transducer (5) until no further outgassing was detected, as evidenced by a decrease in the rate of change of the pressure decay curve to less than 50 μ/minute. The flow of hot oil was then stopped and cooled silicone oil was valved through the plate, continuing until the desired temperature level for the test was attained. At this point coolant flow

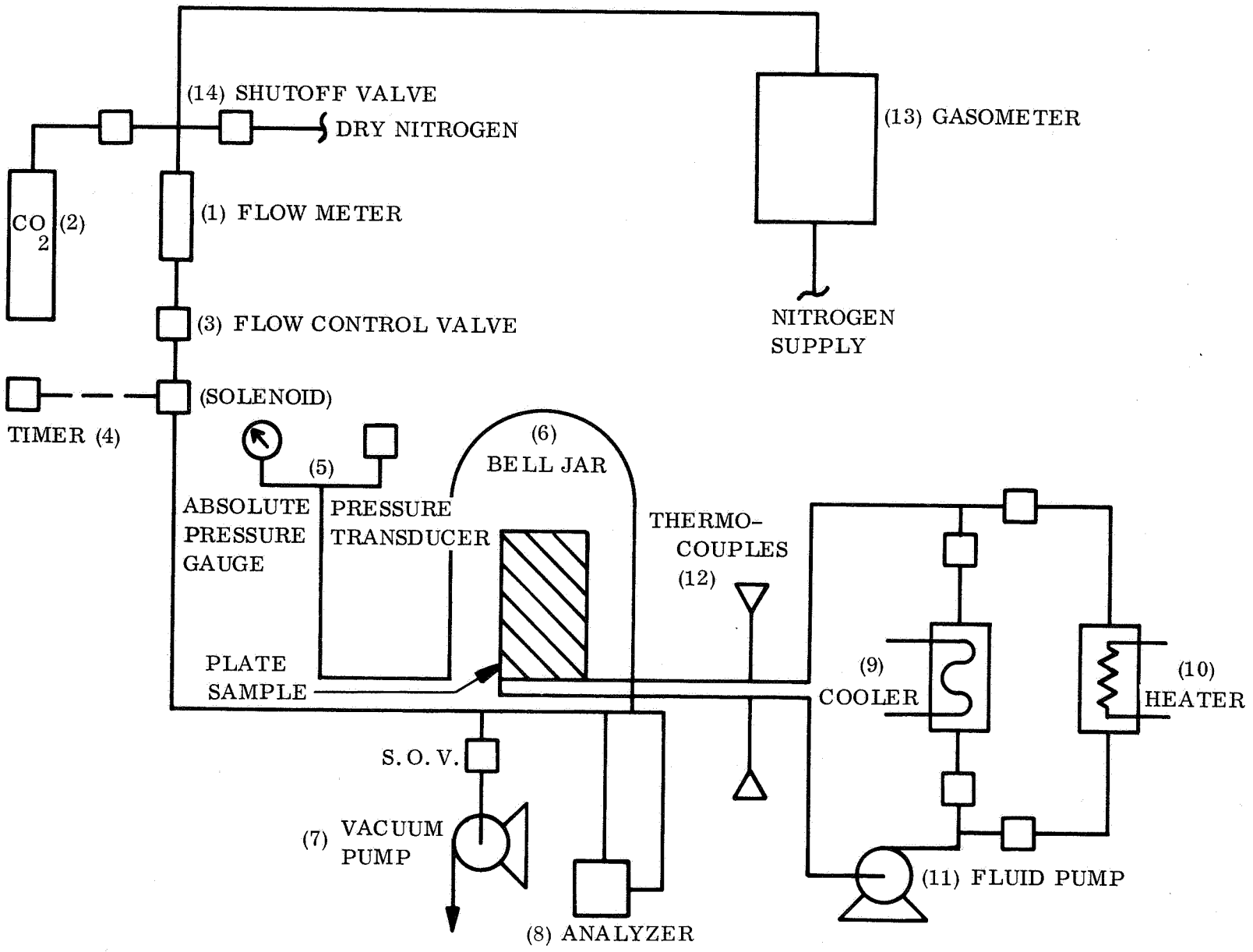

Figure 8. Static Test Stand

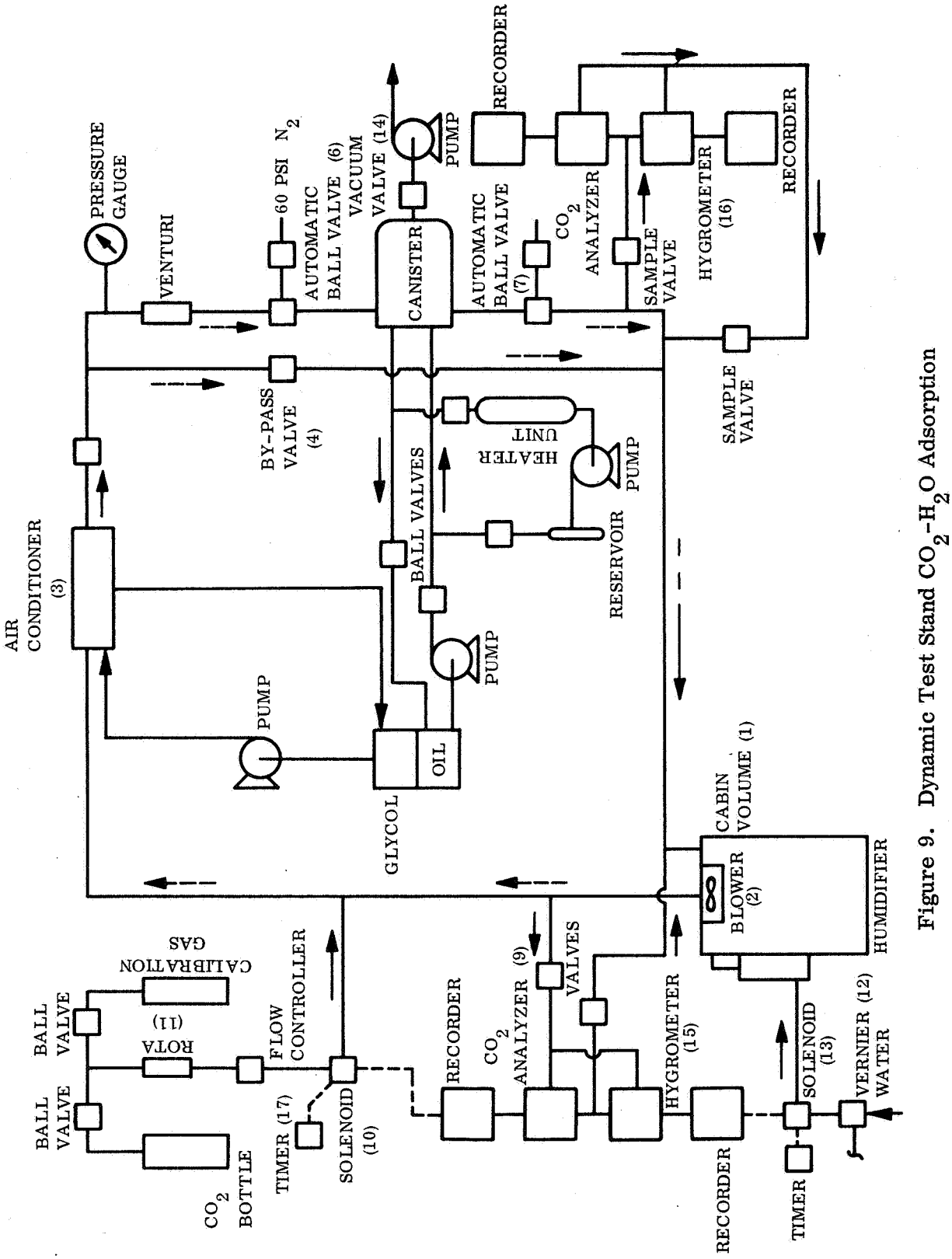

Figure 9. Dynamic Test Stand CO_2-H_2O Adsorption

was stopped and a fixed amount of carbon dioxide gas was metered into the system as follows:

A two-stage regulator located in the CO_2 supply (2) was adjusted to give a 20 psig outlet pressure. The CO_2 gas after leaving the regulator flowed through the flow meter (1) and flow controller (3). The flow controller was preset to give a constant flow rate during the test which was independent of the pressure in the bell jar. The flow rate was determined by noting the rotameter reading and referring to the calibration curve supplied with the instrument, included in figure 6 of this report. The electrically operated shutoff valve (4) was in series with a timer, so that the exact period of time during which the valve was open could be recorded. The precise amount of CO_2 added to the system was calculated by multiplying the flow rate by the time which the valve was open. When the required amount of CO_2 gas was added to obtain the planned test conditions, the flow was terminated and pressures in the bell jar were continuously recorded until no further adsorption was noted (as determined by a stabilization of pressure within bell jar). The final pressure was recorded and the amount of CO_2 adsorbed by the plate was calculated by the methods described in a later section of this report. To determine the effect of absolute pressure on the overall equilibrium process, a diluent gas, in this case nitrogen, was introduced into the system. The CO_2 analyzer pump was then turned on, so that a continuous sample of the bell jar gas could be taken. Upon reaching a steady reading on the CO_2 analyzer the test was terminated and the regenerative process was begun. The tests were repeated for several pressures and temperatures which are discussed in a later section.

Dynamic test setup.-The second and major phase of the testing was concerned with dynamic system parameters and definition of operating characteristics. Figure 9 shows the finalized configuration of the system used for the dynamic portion of the testing.

The air flow loop was composed of 1.0-inch i.d. copper pipe. A simulated cabin volume of 7.5 ft^3 (1) housed the blower unit (2) for the system. The blower was powered by a 115 vac., 400 cps electric motor and was capable of producing a maximum pressure rise of 8.0 inch H_2O and a maximum flow of 40 CFM. Interior mounting of the blower eliminated the possibility of leakage through the fan housing during test runs at pressures less than atmospheric and resulted in better mixing of the process gas, thereby minimizing the possibility of stratification.

The gas, upon exiting from the cabin volume entered the air conditioner (3) where it was cooled to a wet bulb temperature of $40^{\circ}F$ measured at the coil outlet. The cabin air (1) was preconditioned by means of a bypass circuit (4) which valves the canister out of the flow. When the adsorption tests were begun, valve (4) was closed and valves (6) and (7) were opened. Flow rates were adjusted by changing motor speeds and through closing and opening of manual valve (8). During the test, a continuously operating analyzer (9) monitored concentration until it reached a preset minimum value. At this point a relay actuated the solenoid (10), admitting CO_2 at a constant flow rate into the flow loop. Quantities of CO_2 added were calculated by

using the timer reading (17) and the reading on the rotameter (11). Water content of the system was controlled by the electrical heater and a calibrated vernier valve (12).

The vernier valve was used to regulate the water flow rate into the humidifier unit. A rate of 1 cc/min was used during the tests. Water flow rates greater than this value overloaded the humidifier and forced a mixture of steam and water into the cabin volume. Flow rates less than this value caused an overheated condition within the humidifier. When the dewpoint of the process gas dropped below the minimum value of $40^{\circ}F$, a relay in the hygrometer sampling unit opened the solenoid (13) allowing water to flow through the vernier and into the heater where it was vaporized to steam. As the system humidity increased to $1^{\circ}F$ above the nominal $40^{\circ}F$ setting the valve was closed by a relay which was actuated by the hygrometer, thus terminating the makeup of water flow. Water vapor removal could then be calculated by taking the difference between canister inlet and outlet dewpoint as measured by the hygrometers (15 and 16).

Upon completion of any given test run, the canister was isolated from the flow loop and the vacuum valve (14) was opened for regeneration of the plate assembly. The vacuum pump evacuated the canister volume to a minimum of 20 microns.

DISCUSSION OF TEST DATA

Equilibrium Testing

The test equipment previously described and shown in figure 8 was used to determine the equilibrium conditions for CO_2 loading capacity on both 5A and 13X sieves. The results are summarized in tables 3 and 4 and figures 10 and 11. The experimental procedure followed can be summarized briefly as follows:

(1) Desorb plate at 300°F and 20 microns pressure

(2) Calibrate bell jar volume

(3) Add known quantity of CO_2 gas

(4) Monitor pressure until equilibrium is attained

(5) Calculate amount adsorbed by plate

Since a considerable time period (1 hour) was required to achieve pressure equilibrium during adsorption, an analytical method was used to predict the final pressure so that test times could be shortened. To predict this value, a pressure trace covering a time period of 30 minutes is used from which a system time constant or response time can be calculated (see figure 12).

The equation used to determine the system time constant is:

$$\ln\left(\frac{P_1 - P_2}{P_2 - P_3}\right) = \frac{\Delta t}{a} \qquad (1)$$

where

P = partial pressure of CO_2

Δt = time interval

a = time constant

The time constant "a" is calculated by substituting pressure decay data into equation (1). The time constant "a" is defined as the time required for the CO_2 pressure to decay 36.7 percent of its initial value, P_0. Selecting the pressure, P_a at $t = t_a$, from test data then permits use of the relationship $(P_o - P_a)/1 - 0.367)$ to determine the total pressure change in the system from P_o to P_{eq}. The equilibrium pressure, P_{eq}, determined in this manner is the value listed in Tables 3 and 4.

TABLE 3

EQUILIBRIUM LOADING ON 13X SIEVE

Test no.	Equilibrium CO_2 pressure (mm Hg)	CO_2 inlet rate (lb/min.)	Time (minutes)	Total * CO_2 added (lb)	Sieve loading (lb CO_2/lb)	Temperature (^oF)
1	2.1	0.0086	3.7	0.0317	0.045	35
2	3.5		4.7	0.0406	0.057	35
3	5.1		6.7	0.0575	0.081	35
4	40.3		13.3	0.1142	0.137	35
5	1.6		1.9	0.0164	0.0229	72
6	2.9		2.7	0.0233	0.032	72
7	4.4		3.2	0.0275	0.037	72
8	49.2	0.0086	10.1	0.0868	0.090	72

* Quantity of CO_2 added to the system Sieve loading determined by considering residual system CO_2 level.

TABLE 4

EQUILIBRIUM LOADING ON 5A SIEVE

Test no.	Equilibrium CO_2 pressure mm Hg	CO_2 inlet rate lb/min.	Time (minutes)	Total CO_2 added lb	Loading lb CO_2/lb	Temperature (^{o}F)
9	2.0	0.0086	4.8	0.0413	0.063	35
10	2.9		5.4	0.0465	0.069	35
11	4.9		6.6	0.0564	0.083	35
12	19.6		10.4	0.0889	0.121	35
13	1.3		2.5	0.0214	0.032	72
14	2.7		3.1	0.0268	0.039	72
15	4.2		3.6	0.0308	0.044	72
16	35.6	0.0086	9.4	0.0810	0.096	72

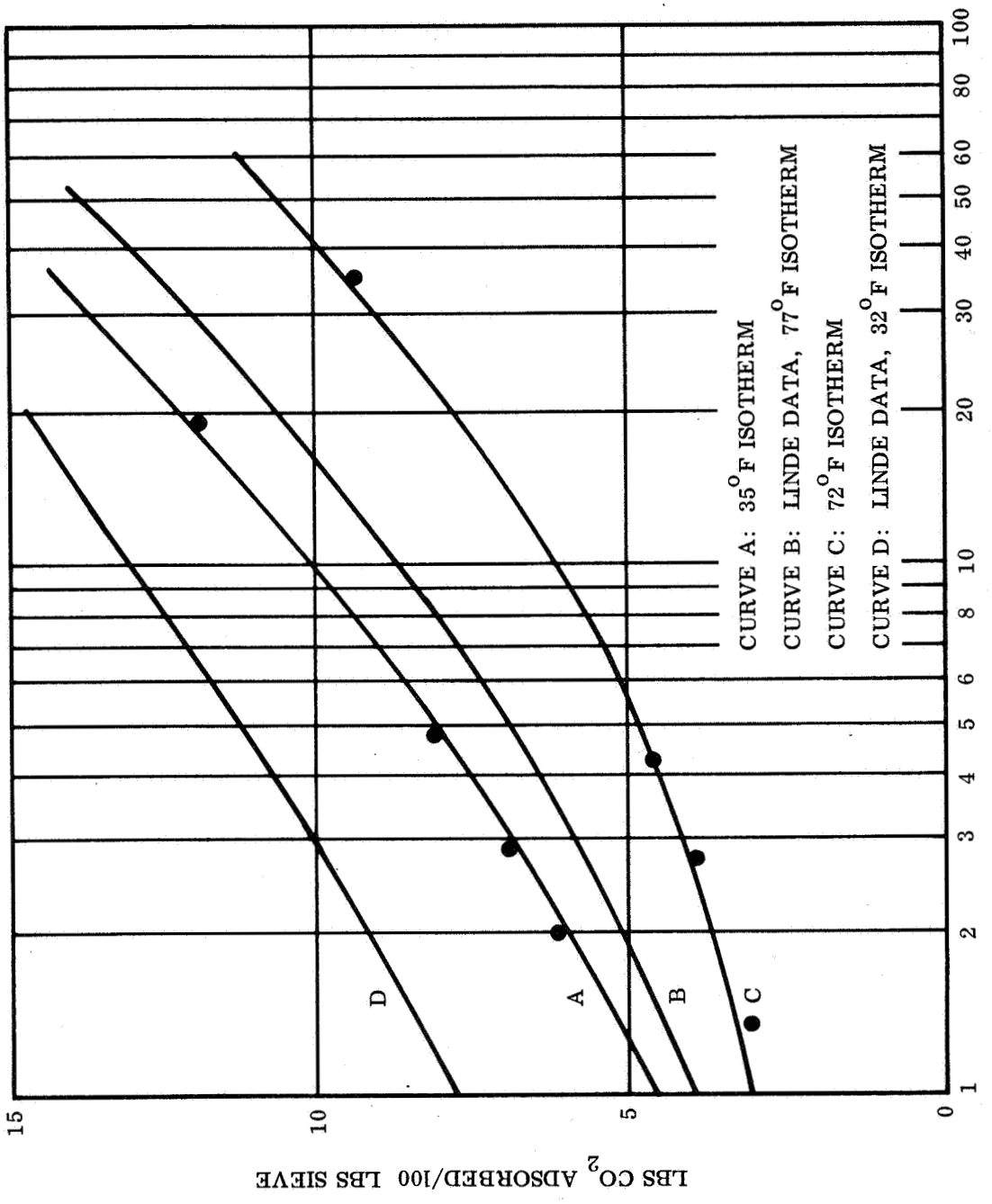

Figure 10. CO_2 Equilibrium Loading on 5A Sieve

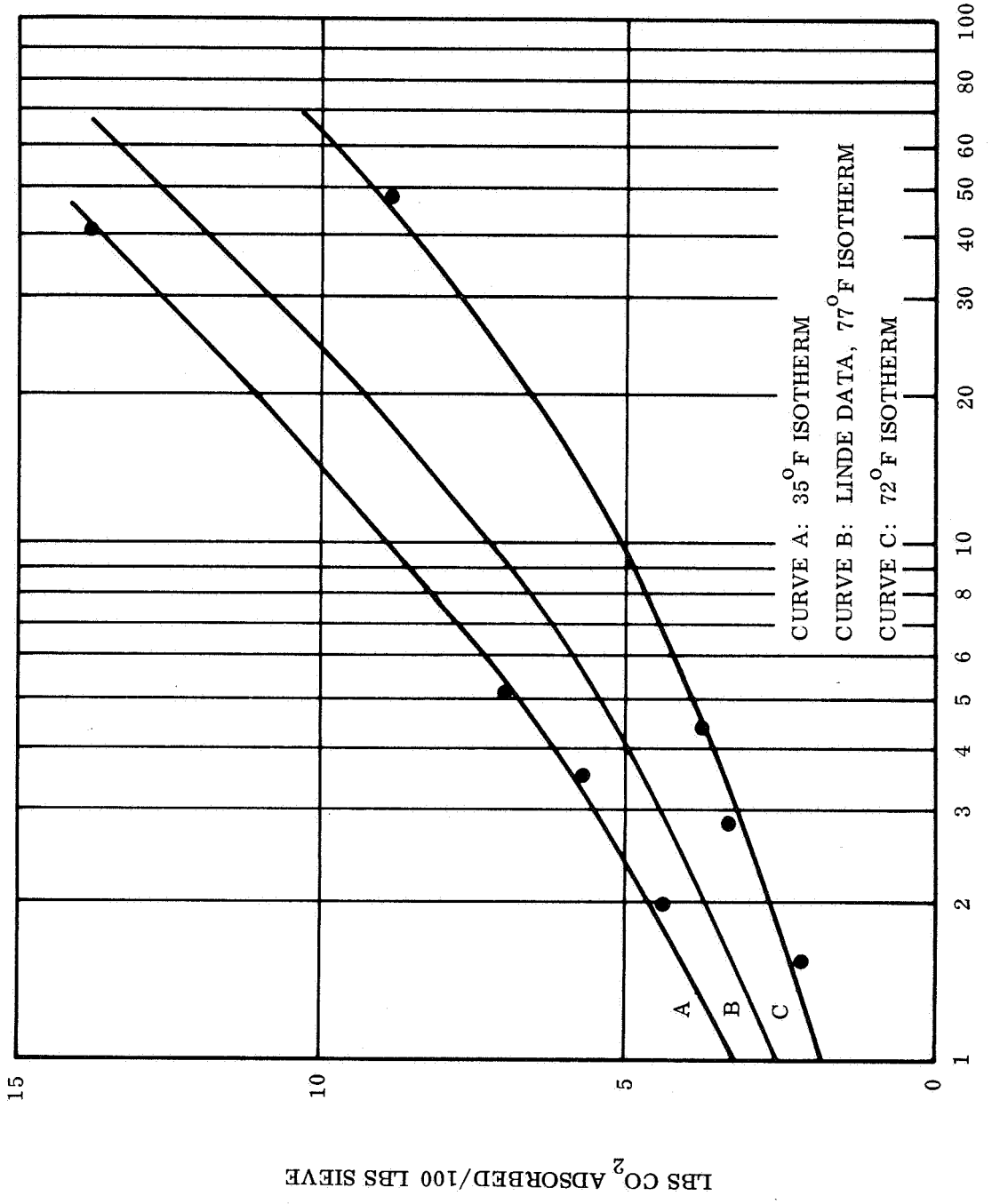

Figure 11. CO_2 Equilibrium Loading on 13X Sieve

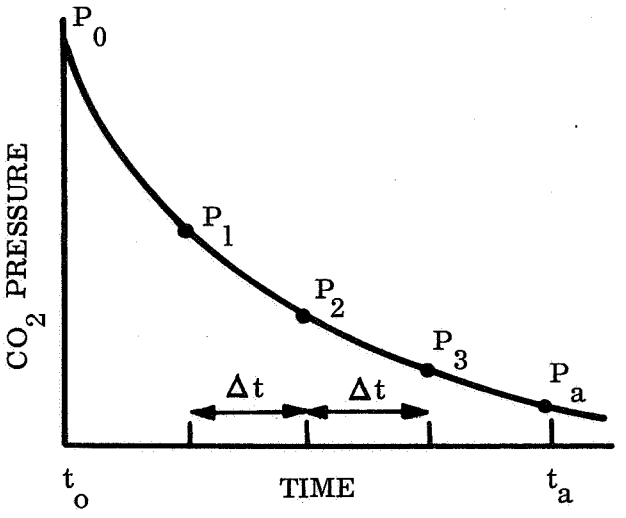

Figure 12. Pressure Decay

A sample calculation for the equilibrium loading of the plate is given below for run no. 5 in table 3.

Total amount of CO_2 added:

$$W = Q \times t \tag{2}$$

where:

W = weight of CO_2 added

Q = CO_2 inlet rate, lb/min

t = Time

$$W = 0.0086\text{-lb/min} \times 1.9 \text{ minutes}$$

$$W = 0.0164\text{-lb}$$

Amount of CO_2 in bell jar:

$$PV = \frac{WRT}{M} \tag{3}$$

where:

P = pressure at equilibrium

V = bell jar volume

W = weight of CO_2

R = gas constant

T = absolute temperature

M = molecular weight of CO_2

$$W = \frac{(44\text{-lb/mol})\ (1.6/760\text{-atm})\ (3.51\text{-ft}^3)}{(0.73\text{-ft}^3\ \text{atm/mole}\ ^{\circ}\text{R})\ (532^{\circ}\text{R})}$$

W = 0.00084-lb

Amount adsorbed by plate:

$$W = 0.0164 - 0.00084 = 0.01556\text{-lb adsorbed}$$

Plate loading:

$$\frac{0.01556}{0.68\text{-lb sieve}} = 0.0229\text{-lb } CO_2/\text{lb sieve}$$

A comparison of the plate performance at 72°F with the Linde data for sieve pellets (curve B, figure 10 and 11) shows the plate equilibrium to be about 70 percent of the Linde reported values.

This difference may have been caused by the accumulation of hydrocarbon contaminants during plate fabrication. For example, the aluminized epoxy used to bond the 1/4-inch tubing to the plate metal substrate (see "Adsorber Plate Design" section) was known to contain epoxy binders and solvents. The exact composition of these compounds could not be obtained from the manufacturer; however, a distinct odor was noted during the curing procedure which showed them to be present inside the oven.

Prior to testing, the plates were heated to 300°F and subjected to a vacuum of 20 μ Hg for 4 hours. While this preconditioning decreased the water loading on the plates to less than 0.01-lb H_2O/lb adsorbent based upon Linde data, the 300°F temperature may not have been high enough to drive off the hydrocarbon compounds.

The 300°F preconditioning temperature was the maximum that could be tolerated by the aluminized epoxy adhesive.

The effect of a diluent gas, in this case nitrogen, was also studied. Based upon the results this diluent has no measurable effect on the equilibrium loading as discussed below. Upon reaching the initial steady state condition, dry nitrogen was added until the absolute pressure reached atmospheric. The CO_2 concentration was monitored by the LIRA analyzer for approximately 15 minutes. Small percentage changes were noted but they appeared to be within the instrument accuracy of ±2 percent of scale reading. The procedure was repeated for several different CO_2 partial pressures with no change in the equilibrium conditions being observed.

Differential Heat of Adsorption

The heats of adsorption presented were not determined by calorimetric techniques. Instead estimates were calculated as follows:

The adsorption of carbon dioxide by a solid adsorbent is an exothermic reaction. The attendant energy release can be determined in several ways. For this analysis the method chosen is based on the use of the Clausinus-Clapeyron equation, which is shown below:

$$(\ln P) = \frac{\Delta Ha}{R} \quad d \quad \left(\frac{1}{T}\right) \tag{4}$$

P = CO_2 partial pressure, mm Hg

T = absolute temperature, ^{o}R

ΔH_a = differential heat of adsorption

R = gas constant

By integrating and rearranging terms equation (4) becomes:

$$\Delta H_a = \frac{R(T_1\ T_2)}{(T_2 - T_1)} \quad \ln \left(\frac{P_2}{P_1}\right) \tag{4a}$$

Equation a can now be used to estimate heats of adsorption from the experimental adsorption data shown in figures 10 and 11. Values of ΔH_a calculated in this manner are tabulated in table 5 for Linde 5A and 13X sieve at constant loading over the temperature range 35° to 72°F. These calculations cover the expected operating range of the adsorbents.

TABLE 5

HEAT OF ADSORPTION FOR 13X AND 5A MOLECULAR SIEVES

Loading Lbs CO_2/100 lbs sieve	ΔH_a Btu/lb	
Sieve	13X	5A
3.0	374	---
4.0	351	---
5.0	---	491
6.0	---	479

The calculated heats of adsorption are seen to be larger for the 5A sieve, which is probably due to its greater affinity for CO_2. Unless this energy generated during adsorption is removed by cooling, isothermal conditions cannot be maintained on the plate and the adsorbent capacity for CO_2 actually decreases as the plate temperature rises.

The heats of adsorption were observed to decrease as the equilibrium loading increases. Operation of the plate at lower capacities (i.e., shorter cycle times) would require less energy removal during the adsorption process. Although the values of ΔH_a are quite large, when considered in terms of an operating system where the CO_2 adsorption rate is on the order of 0.3 lb/hr, the total heat load on the vehicle heat rejection system would be quite small.

Dynamic Testing

Analysis of the dynamic test data for CO_2 adsorption was accomplished by performing the following tasks:

(1) Application of statistical analysis techniques to the data in order to identify major effects and interactions.

(2) Construction of a theoretical diffusion model that was employed to corroborate test data and

(3) Comparison of the test data with the model.

Statistical Analysis

For purposes of analysis it is necessary to select an appropriate measure of adsorber panel performance. The raw test data is in the form of the rate of carbon dioxide added to the system as a function of time. Adsorption rate in lbs/hour as a function of time is then calculated. From this, three measures of adsorber panel performance were calculated.

(1) Time to a selected fraction of the maximum rate (which is at time zero).

(2) Total CO_2 adsorbed versus time.

(3) Efficiency: That is, the ratio of CO_2 adsorbed to the total amount of CO_2 passing over the sieve.

It is these data that are further processed to determine the effects and interactions as a function of the yield, i.e., for the analyses performed here, the total CO_2 adsorbed.

As previously noted the experimental designs were of the 2^{n-k} factorial type. These designs are the simpliest to run and analyze, and do in view of their orthogonal nature provide a considerable amount of information, concerning the effects of factors on performance, relative importance of factors and sum of squares permitting estimates of residual error to be made.

The sum of squares is a measure of the variation ascribed to that particular factor. To be validly determined however, replications are required. Since only two blocks were completely replicated a pseudo-form of replication was used to get at least some insight into this basic quantity. The technique will be explained in detail later in this section, but it involved the designation of elapsed time within a run as a block effect, a technique not in conflict with accepted practices.

The effect of a factor has a simple geometric meaning. Consider the case of two factors: X_o, X_i, Y_o, Y_i. The quantity Z_{ij} refers to the yield at levels i and j of the x and y factors respectively.

The effect of x at level y_o is,

$$e_{x_o} = Z_{10} - Z_{00}$$

and at level y_1,

$$e_{x1} = Z_{11} - Z_{01}$$

The net effect is the average of these or,

$$e_x = 1/2\ (e_{x_o} + e_{x_1})$$

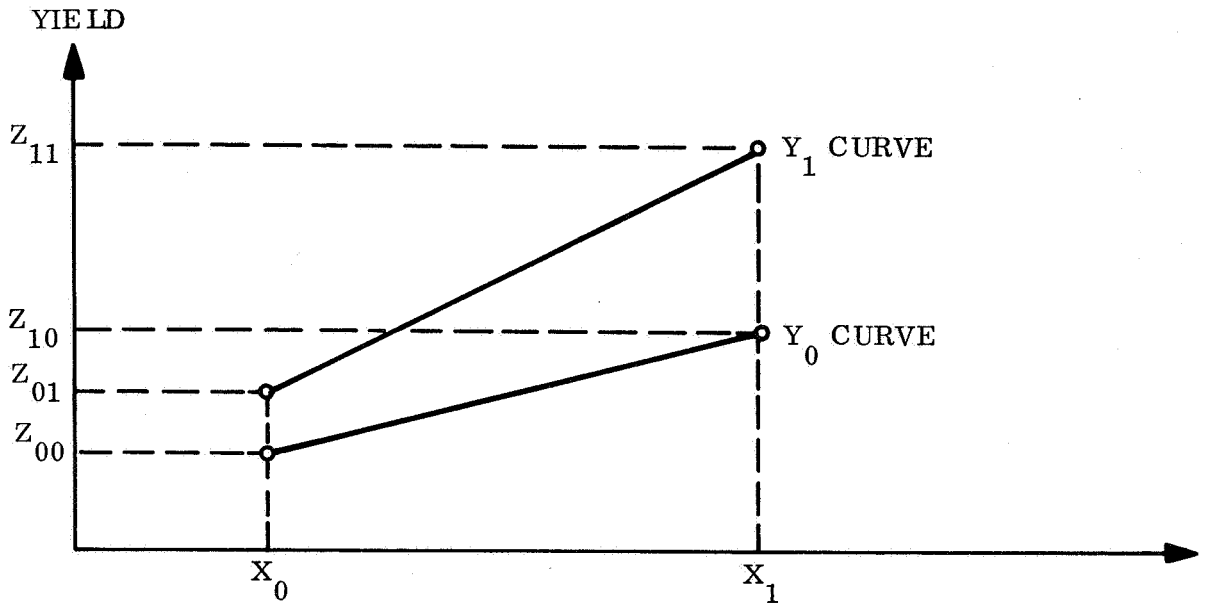

Figure 13. General Example of Interaction

A similar analysis holds true for the factor y. From this we proceed to an evaluation of the interaction between x and y. Interaction is a measure of the disparity of the effects of y for example at the two levels of x. This is the average difference or,

$$e_{xy} = 1/2 \quad (Z_{11} - Z_{10}) - (Z_{01} - Z_{00})$$

Similarly we can reverse x and y to obtain,

$$e_{yx} = 1/2 \quad (Z_{11} - Z_{01}) - (Z_{10} - Z_{00}) \qquad = e_{xy}$$

If the lines are parallel, the interaction therefore is zero.

In the Regenerative Adsorbent study most of the experiments involved three factors at two levels. The concept of effect for three factors bears a direct relationship to the simple two factor case mentioned previously.

Consider the most frequently encountered variables: velocity v_o, v; partial pressure CO_2 p_o, p; and plate thickness t_o, t.

The effect of plate thickness can be measured at four combinations of the other two factors.

TABLE 6
EXAMPLE OF MAIN EFFECTS

Velocity	Partial pressure	Effect of thickness
v_o	p_o	$v_o p_o t_1 - v_o p_o t_o$
v_1	p_o	$v_1 p_o t_1 - v_1 p_o t_o$
v_o	p_1	$v_o p_1 t_1 - v_o p_1 t_o$
v_1	p_1	$v_1 p_1 t_1 - v_1 p_1 t_o$

The notation $v_i\ p_j\ t_k$ symbolically represents the observed yield for that particular combination of levels.

The average effect of thickness is then:

$$C = 1/4 \left[v_o p_o t_1 + v_1 p_o t_1 + v_1 p_1 t_1 - v_o p_o t_o - v_1 p_o t_o - v_o p_1 t_o \right]$$

This can be used as a first cut design tool, for it represents the expected change in the yield for an increase ($\Delta t = t_1 - t_o$) in plate thickness.

If the sum of squares is divided by its degrees of freedom then this quantity becomes a measure of the variability due to its related factor. If the ratio of this quantity to the residual mean square is subsequently computed, the size of this ratio becomes a measure of the significance of the related factor. This ratio can then be compared (under the usual assumptions concomitant with analysis of variance techniques) with percentage points of the F distribution.

The following paragraphs present the results of the analysis of variance performed on the test data covering the sample space previously delineated. These results provide a strong indication of the significance of the factors selected over the ranges studied. The yield selected as being most representative of adsorber canister performance is total weight of CO_2 adsorbed.

The Analysis of Variance

The computer program used in this analysis is a general purpose program which aids in the development of a design matrix and also performs the necessary computations for full or fractional design and design analyses of variance.

A full variety of designs can be handled by the program but it is used here only for full factorials and an occasional fractional.

Block 1 (table 7) for which the factors of interest are:

(1) Velocity: 200, 25 feet/minute (V)

(2) Partial pressure: 21, 5.3 mm Hg (P)

(3) Plate thickness: 1/4, 1/8 inches (T)

Table 8 which is from block 1R is a set of replicated runs at the same conditions as block 1. As previously noted, the quantity "CO_2 Adsorbed" will be considered as the primary yield variable in the following analyses. As previously noted to gain insight into the error terms these runs were analyzed at 1, 5, 10, and 15 minutes of elapsed time. The observations taken at each time considered as replicated.

The program Frac 1, Frac 2 was then used on the three factors for the four time periods. The results for the final time period should be considered the most significant since it represents the cumulative response of the adsorber panel. A brief summary of the results are shown in table 9 in the form of effect estimates and F-ratios. The consistency of the results for all four time periods may be viewed as a verification of the validity of the analytical technique in this application.

The effect of partial pressure is highly significant for the range studied in all four cases. Plate thickness was significant at the 95 percent level but dropped below this at the 15 minute run. It may be concluded that at best, plate thickness is a marginally significant factor over the range studied. In all four cases, all the interaction terms were insignificant. This provides a strong indication that the effects of partial pressure and plate thickness are additive over the range of experimentation for blocks 1 and 1R.

The consistency of results between time periods indicated that running a 2 x 2 x 2 x 4 factorial could be used to provide for a residual sum of squares term with 32-degrees of freedom permitting formulation of an estimate of residual error possible now because of the larger statistical sample. A brief summary of the results of this analysis is shown tabulated in table 10.

As a result the factor "time" can now be tested for significance and any variability due to time can be separated out in the analysis of variance leaving the remaining factors on an equivalent basis. The mean squares (M-square) shown in table 10, based upon analysis of data at various time increments during the runs of "blocks" 1 and 1R are in general agreement with those obtained for the analysis of variance performed on the data at the end of each run. The emergence of plate thickness as a significant

TABLE 7 BLOCK 1.

CO_2 ADSORPTION ON 13X MOLECULAR SIEVE AS A FUNCTION OF VELOCITY, PP CO_2 AND PLATE THICKNESS

Run number	Variables			Total run time, min.	CO_2 inlet rate, lb/hr x 10^3	Total CO_2 adsorbed (W) and removal efficiency (Eff)										Initial CO_2 adsorption rate, lb/hr
						t = 1 min.		t = 5 min.		t = 10 min.		t = 15 min.		t = 19 min.		
	Velocity, ft/min.	PP CO_2, mm Hg	Plate thickness, inch			W, lbs x 10^3	Eff, %	W, lbs x 10^3	Eff, %	W, lbs x 10^3	Eff, %	W, lbs x 10^3	Eff, %	W, lbs x 10^3	Eff, %	
1	200	21	0.125	20	22.9	2.18	9.53	10.4	9.1	19.1	8.4	27.2	7.9	32.7	7.5	0.131
2	~25	21	0.125	16	2.86	2.02	70.46	9.07	63.4	16.0	55.9	21.9	51.0			0.121
3	200	5.3	0.125	16	5.78	1.15	19.9	5.53	19.2	10.1	17.4	12.9	14.9			0.069
4	~25	5.3	0.125	18	0.72	0.97		4.75		8.53		10.8		11.5	83.9	0.058
7	200	21	0.25	20	19.1	1.58	8.3	7.65	8.0	14.1	7.4	19.0	6.7	23.3	6.4	0.095
8	~25	21	0.25	20	2.40	1.48	62.2	7.23	60.7	14.1	59.2	20.1	56.2	23.9	52.7	0.089
9	200	5.3	0.25	16	4.8	8.17	16.9	3.55	14.8	6.05	12.6	7.87	10.9			0.049
10	~25	5.3	0.25	16	0.60	0.67	~100	2.78	92.5	4.69	79.9	6.25	69.3			0.040

Constants: Plate temp., 30°F; Dew point, -30°F
Regeneration, 300°F and 20μ; Path length, 2 ft.
Absolute press, 760 mm Hg

TABLE 8 BLOCK 1R.

CO_2 ADSORPTION ON 13X MOLECULAR SIEVE AS A FUNCTION OF VELOCITY, PP CO_2 AND PLATE THICKNESS

Run number	Variables			Total run time, min.	CO_2 inlet rate, lb/hr x 10^3	Total CO_2 adsorbed (W) and removal efficiency (Eff)										Initial CO_2 adsorption rate, lb/hr
						t = 1 min.		t = 5 min.		t = 10 min.		t = 15 min.		t = 19 min.		
	Velocity, ft/min.	PP CO_2, mm Hg	Plate thickness, inch			W, lbs x 10^3	Eff, %	W, lbs x 10^3	Eff, %	W, lbs x 10^3	Eff, %	W, lbs x 10^3	Eff, %	W, lbs x 10^3	Eff, %	
60	200	21	0.125	16	22.9	1.50	6.6	7.05	6.2	12.6	5.5	16.6	4.8	20.4	37.5	0.090
61	~25	21	0.125	20	22.9	1.52	52.6	7.12	49.7	12.9	45.1	17.5	40.9			0.091
62	200	5.3	0.125	18	5.78	1.08	18.8	4.6	15.9	7.62	13.2	9.48	10.9	10.0	9.1	0.065
63	~25	5.3	0.125	18	0.72	0.97		4.37		7.11		8.65		9.07	66.1	0.058
64	200	21	0.25	16	19.1	1.48	7.8	7.0	7.34	12.7	6.7	17.4	6.1			0.089
65	~25	5.3	0.25	16	0.60	0.62	~100	2.67	88.7	4.53	75.2	5.92	65.6			0.037
66	200	5.3	0.25	16	4.8	0.72	14.9	3.20	13.3	5.52	11.5	7.27	10.1			0.043
67	~25	21	0.25	18	2.38	1.32	55.2	6.12	51.3	10.8	45.5	14.1	39.3	15.1	33.3	0.079

Constants: Plate temp., 30°F; Dew point, -30°F
Regeneration, 300°F and 20μ; Path length, 2 ft.
Absolute press., 750 mm Hg

TABLE 9

SUMMARY OF ANALYSIS OF VARIANCE FOR BLOCKS 1 AND 1R

	1 minute		5 minutes	
Source	Effect	F-ratio	Effect	F-ratio
Average	0.00125	-------	0.00581	
Velocity (V)	0.000120	1.20	0.000606	1.33
Partial pressure (P)	0.000762	48.28**	0.00376	51.57**
Thickness (t)	-0.000337	9.45*	-0.00158	9.08*
VP	-1.67×10^{-5}	-------	2.71×10^{-5}	
Pt	-2.5×10^{-7}	-------	1.81×10^{-4}	
Vt	8.49×10^{-6}	-------	4.38×10^{-5}	
VPt	2.07×10^{-5}	-------	-2.71×10^{-5}	
	10 minutes		15 minutes	
Average	0.0104		0.0137	-------
Velocity (V)	0.00113	1.11	0.00160	-------
Partial pressure (P)	0.00728	46.15**	0.0106	38.35**
Thickness (t)	-0.00267	6.22*	-0.00335	3.83
VP	3.344×10^{-5}		1.24×10^{-4}	-------
Pt	4.53×10^{-4}		2.74×10^{-4}	-------
Vt	-7.4×10^{-5}		-2.20×10^{-4}	-------
VPt	-1.52×10^{-4}		-2.20×10^{-4}	-------

*Significant at the 95% level

**Significant at the 99% level

TABLE 10

BLOCK 1 AND 1R SUM OF SQUARES

Source	SS	DF	M-square	(F-ratios)
A (V)	1.203764E-05	1	1.203764E-05	2.74
B (P)	5.035200E-04	1	5.035200E-04	114.98
C (t)	6.325037E-05	1	6.325037E-05	14.44
D (time)	1.462629E-03	3	4.875429E-04	111.33
AB	2.852175E-08	1	2.852175E-08	
AC	5.873153E-08	1	5.873153E-08	
AD	4.985835E-06	3	1.661945E-06	
BC	8.277129E-07	1	8.277129E-07	
BD	2.192431E-04	3	7.308104E-05	16.68
CD	2.096023E-05	3	6.986743E-06	
ABC	1.436565E-07	1	1.436565E-07	
ABD	4.243338E-08	3	1.414446E-08	
ACD	1.662411E-07	3	5.541369E-08	
BCD	4.300964E-07	3	1.433655E-07	
ABCD	1.485460E-07	3	4.951532E-08	
SSE	1.401271E-04	32.0	4.378973E-06	
SST	2.428599E-03	63.0	3.854919E-05	

factor in the latter analysis is most logically explained by reviewing the significance (from tables 7 and 8) as a function of time. It appears that early in the run adsorption does not occur as quickly for the one-quarter inch panel as it does on the one-eighth inch panel. Since this characteristic does not hold throughout the run it appears that the degree of regeneration may not be equivalent, there being nearly equivalent quantities of sieve regenerated on each panel (i.e., assuming the degree of regeneration for the 1/8-inch panel to be 1.0, then the 1/4-inch panel might be expected to have a relative regeneration factor of 0.5). The total quantities of CO_2 adsorbed on each panel further substantiate this hypothesis.

The factor time is of course significant as is the interaction between time and partial pressure there being the obvious correlation between loading, the driving force (ΔpCO_2), and elapsed time.

An indication of the degree of interaction shown can be obtained by observing the size of the effect compared with the overall effect, or rather the change from one time period to the next.

Following analysis of blocks 1 and 1R, and noting the relative insignificance of velocity on the quantity of CO_2 adsorbed, the "block" 2 experiments were designed. The range of velocity studied was expanded upward in an attempt to determine at what level (if any) velocity becomes an important factor.

Partial pressure range was also expanded but in the opposite direction to begin determination of the effects of lower partial pressures.

Block 2 consisted of a 2^3 test on 13X molecular sieve panels for which the following factors were tested for significance.

(1) Velocity: 275, 25-ft/min (V)

(2) Partial pressure CO_2: 21, 3.1-mm Hg (P)

(3) Plate thickness: 1/4, 1/8-inches (T)

The data is summarized for elapsed times 1, 5, 10, 15 minutes in table 11 as done previously for blocks 1 and 1R.

The data is not replicated, but it is again assumed that the elapsed times are "block" effects which interact little with the main variables providing once more a pseudo-replication. The analysis of variance is shown in table 12.

TABLE 11, BLOCK 2.

CO_2 ADSORPTION ON 13X MOLECULAR SIEVE AS A FUNCTION OF VELOCITY, PP CO_2, AND PLATE THICKNESS

Run number	Variables			Total run time min	CO_2 inlet rate lb/hr x 10^3	Total CO_2 adsorbed (W) and removal efficiency (Eff)										Initial CO_2 adsorption rate lb/hr
						t = 1 min		t = 5 min		t = 10 min		t = 15 min		t = 19 min		
	Velocity, ft/min.	PP CO_2, mm Hg	Plate thickness, inch			W, lbs x 10^3	Eff, %	W, lbs x 10^3	Eff, %	W, lbs x 10^3	Eff, %	W, lbs x 10^3	Eff, %	W, lbs x 10^3	Eff, %	
17	25	21	0.25	24	2.40	1.60	67.1	6.82	57.2	11.5	48.2	14.4	40.3	15.8	34.8	0.096
18	25	3.1	0.25	14	0.35	0.80	22.7	3.92	22.3	6.86	19.5	7.9	15.0			0.048
19	275	3.1	0.25	20	3.90	0.83	21.5	4.02	20.8	7.21	18.6	9.15	15.8	9.97	13.6	0.050
20	275	21	0.25	16	26.2	2.16	8.2	10.2	7.8	17.1	6.5	21.6	5.5	23.6	4.7	0.128
31	275	3.1	0.125	16	4.70	0.83	17.9	3.87	16.6	6.69	14.4	7.9	11.4	8.22	9.3	0.050
32	25	3.1	0.125	16	0.42	0.90	21.3	3.98	18.9	5.7	13.5	6.8	10.7			0.034
33	275	21	0.125	20	31.5	2.08	6.6	9.67	6.1	16.3	5.17	20.8	4.4	23.0	3.9	0.125
34	25	21	0.125	12	2.86	2.03	71.1	9.0	62.9	15.9	55.6	17.1	39.8			0.122

Constants: Plate temp., 30°F
Regeneration, 300°F and 20μ
Path length, 2 ft.
Absolute press, 760 mm Hg
Dew point, - 30°F

TABLE 12

BLOCK 2 ANALYSIS OF VARIANCE

Source	Effect	F-Ratio
Average	0.00799	
(V) Velocity	0.00157	-------
(P) Partial pressure	0.00630	9.84**
(T) Plate thickness	-0.000219	-------
VP	1.11×10^{-3}	-------
PT	-7.19×10^{-4}	-------
VT	7.32×10^{-4}	-------
VPT	7.58×10^{-4}	-------

Residual Mean Square = 3.23×10^{-5} with 24 d.f.

With the increased range for V and P, the effects remain additive (compare with 1, 1R) with little interaction and only partial pressure significant. The results here are simple to interpret. The partial pressure range is great enough to "overpower" the other suspected factors. A more detailed exploration of the sample space will require a cutting down of the CO_2 partial pressure range.

Although the velocity effect is still not indicated as significant, a review of raw data and subsequent comparison with similar data from Blocks 1 and 1R indicate a definite increase in the relative rates of adsorption between velocities.

Blocks 1 and 2 were performed with adsorber panel temperatures of $30^{\circ}F$. Since this does represent a constraint on the system, the following, block 4 was designed to obtain data on performance at $75^{\circ}F$ at the same levels of carbon dioxide partial pressure and plate thickness but over a narrower temperature range. The data tabulation is shown in table 13.

Block 4 was a 2^{4-1} fractional factorial type experiment for which the fourth factor; namely plate temperature is confounded with the three way interaction term for purposes of analysis. By maintaining the other factors at previously explored levels the validity of the confounding is enhanced.

TABLE 13 BLOCK 4.

CO_2 ADSORPTION ON 13X MOLECULAR SIEVE AS A FUNCTION OF VELOCITY, CO_2 P.P., PLATE TEMPERATURE AND THICKNESS

Run number	Variables				CO_2 Inlet rate, lbs/hr x 10^3	Total CO_2 adsorbed (W) and removal efficiency (Eff)										Initial CO_2 adsorption rate lb/hr
						t = 1 min		t = 5 min		t = 10 min		t = 15 min		t = 19 min		
	Velocity, ft/min	PP CO_2, mm Hg	Plate temp., ^oF	Plate thickness, inch		W, lbs x 10^3	Eff, %	W, lbs x 10^3	Eff, %	W, lbs x 10^3	Eff, %	W, lbs x 10^3	Eff, %	W, lbs x 10^3	Eff, %	
44	275	21	75	0.25	26.2	1.97	7.50	9.0	6.9	14.6	5.6	18.3	4.8	19.6	3.9	0.118
45	200	21	30	0.25	19.1	1.83	9.61	8.73	9.2	15.7	8.2	21.2	7.4	24.7	6.8	0.110
46	275	3.1	30	0.25	3.87	0.83	21.5	3.77	19.5	6.89	17.8	9.35	16.1	10.9	14.8	0.050
47	200	3.1	75	0.25	2.82	0.70	24.9	3.30	23.5	5.92	21.0	7.90	18.7			0.042
48	275	21	30	0.125	31.5	2.33	7.4	11.0	6.9	19.8	6.3	26.6	5.6			0.140
49	200	21	75	0.125	22.9	2.08	9.1	10.1	8.8	18.6	8.1	25.0	7.3			0.125
50	275	3.1	75	0.125	4.70	1.18	25.5	5.60	24.1	9.6	20.7	11.9	17.1			0.071
51	200	3.1	30	0.125	3.38	1.83	54.3	8.73	51.7	15.6	46.4	21.2	41.8	24.7	38.5	0.110

Constants: Regeneration at 300°F and 20μ Dew point, -30°F
Absolute Pressure, 760 mm Hg Path length, 2 ft

The data was again processed for the times; 1, 5, 10, and 15 minutes.

With this confounding structure the results are as shown in table 14.

TABLE 14

BLOCK 4 ANALYSIS OF VARIANCE

Source	Effect	F-Ratio
Average	0.01	
(V) Velocity	-0.000989	-------
(P) Partial pressure	0.00577	4.76*
(t) Thickness	-0.00383	2.09
(T) Temperature + VPt	-0.00184	-------
VP + tT	0.00102	-------
Pt + VT	0.000796	-------
Vt + PT	0.000918	-------

Residual mean square = 5.60×10^{-5} with 24 d.f.

The partial pressure effect as indicated (and anticipated) was again significant although somewhat less than in previous runs. The interactions all appeared as insignificant supporting the conclusions reached from the analysis of variance for blocks 1 and 2 for which variable ranges were similar. Velocity, which had narrower range here, did not appear significant in either block 2 or 4, indicating that the range should be further expanded. The sign on the temperature effect was as expected (i.e., for an increase in temperature the yield, carbon dioxide adsorbed, is expected to decrease) and the relative insignificance of the effect indicated that cooling of the adsorber panel below normal ambient operating conditions was not warranted. Subsequent adsorption was therefore performed at 70^{o}F to 75^{o}F.

The Block 5 experiments represent narrowing down of the sample space by limiting the range of pCO_2 studied to a practical spacecraft system operating region. At the same time the search for an optimum velocity continued upward to 375 ft/min, the upper limit of the existing test equipment. Tables 15A and B is a summary of the data and test conditions for block 5.

TABLE 15A BLOCK 5.

CO_2 - H_2O COADSORPTION ON 13X MOLECULAR SIEVE AS A FUNCTION OF VELOCITY, PP CO_2, PLATE THICKNESS AND REGENERATION TEMPERATURE

Run number	Variables: Velocity ft/min.	Variables: PP CO_2, mm Hg	Variables: Plate thickness, inch	Total run time min	CO_2 Inlet rate lb/hr x 10^3	Total CO_2 adsorbed (W), total H_2O adsorbed (W^o) and CO_2 removal efficiency (Eff): t = 1 min, W, lbs x 10^3	t = 1 min, Eff, %	t = 5 min, W, lbs x 10^3	t = 5 min, Eff, %	t = 10 min, W, lbs x 10^3	t = 10 min, Eff, %	t = 10 min, W^o, lbs x 10^3	t = 15 min, W, lbs x 10^3	t = 15 min, Eff,%	t = 15 min, W^o, lbs x 10^3	Initial CO_2 adsorption rate lb/hr
68	375	4.0	.125	16	8.2	0.70	8.6	3.3	8.1	5.81	7.1	7.64	7.12	5.8	11.6	0.042
69	200	4.0	.125	16	4.4	0.58	13.4	2.67	12.2	4.64	10.6	6.47	5.28	8.1	10.0	0.035
70	375	7.6	.125	16	15.5	0.73	4.7	3.3	4.3	5.41	3.5	7.13	6.52	2.8	11.1	0.044
71	200	7.6	.125	16	8.3	0.67	8.1	3.0	7.2	5.04	6.1	6.23	6.17	4.9	9.7	0.040
72	375	4.0	.25	16	3.6	0 53	7.8	2.40	7.1	3.85	5.7	7.96	4.33	4.2	12.3	0.032
73	200	4.0	.25	16	12.9	0.57	15.6	2.42	13.3	3.81	10.5	5.91	4.27	7.8	9.0	0.034
74	375	7.6	.25	18	6.9	0.78	6.1	3.62	5.6	6.39	4.9	7.93	8.28	4.3	12.1	0.047
75	200	7.6	.25	18	8.2	0.77	11.1	3.42	9.9	5.88	8.5	5.75	7.42	7.2	9.5	0.046

Constants: Regeration at 200 μ, 300°F
Path length, 2 ft
Absolute Pressure, 760 mm Hg
Dew point, 40°F
Plate temp, 75°F

TABLE 15B BLOCK 5.

CO_2 - H_2O COADSORPTION ON 13X MOLECULAR SIEVE AS A FUNCTION OF VELOCITY, PP CO_2, PLATE THICKNESS AND REGENERATION TEMP.

Run number	Variables			Total run time min	CO_2 Inlet rate lb/hr x 10^3	Total CO_2 adsorbed (W), total H_2O adsorbed (W^o) and CO_2 removal efficiency (Eff)										Initial CO_2 adsorption rate lb/hr
						t = 1 min		t = 5 min		t = 10 min			t = 15 min			
	Velocity ft/min.	PP CO_2, mm Hg	Plate thickness, inch			W, lbs x 10^3	Eff, %	W, lbs x 10^3	Eff, %	W, lbs x 10^3	Eff, T	W^o, lbs x 10^3	W, lbs x 10^3	Eff, %	W^o, lbs x 10^3	
76	375	4.0	0.125	16	8.2	0.58	7.1	2.77	6.8	4.79	5.9	6.83	5.82	4.7	10.3	0.035
77	200	4.0	0.125	16	4.4	0.52	11.9	2.28	10.5	3.75	8.6	6.57	4.62	7.1	10.1	0.031
78	375	7.6	0.125	16	15.5	0.77	4.9	3.50	4.5	5.9	3.8	6.72	7.58	3.3	10.3	0.042
79	200	7.6	0.125	16	8.4	0.58	6.4	2.38	5.8	4.0	4.8	6.04	4.48	3.6	9.5	0.032
80	375	4.0	0.25	16	6.8	0.48	7.1	2.18	6.4	3.48	5.12	7.31	4.10	4.0	11.3	0.029
81	200	4.0	0.25	16	3.6	0.48	13.3	2.13	11.8	3.45	9.5	5.10	4.07	7.5	8.1	0.029
82	375	7.6	0.25	16	12.9	0.67	5.2	3.08	4.7	4.82	3.7	6.90	5.57	2.9	10.4	0.040
83	200	7.6	0.25	16	8.9	0.57	8.3	2.41	6.9	3.76	5.5	5.71	4.38	4.2	8.7	0.034

Constants: Regeneration at 200μ , 150°F
Path length, 2 ft.
Absolute Pressure, 760 mm Hg.
Dew point, 40°F
Plate temp., 75°F

While varying the factors as noted above it was decided to begin the phase of investigation involving regeneration of the panels and operation at high humidity. All regenerations to this point in time had been done at 300°F and approximately 20 microns absolute pressure. Block 5 regenerations were performed at low pressure (200 microns) but at 150°F and 300°F. The regeneration pressure of 200 microns was a limitation of the pumping system which could not handle the water vapor loads. This block is a 2^4 factorial involving 16 tests.

Only partial pressure and the "Pt" interaction indicated a greater than unity F-Ratio; however using the statistical definitions of significance as depicted by "F" Ratios no significant effects were observed as shown in table 16.

The fundamental conclusion here is that the selected ranges were too small to produce a large enough incremental change in the yield. Examination of the data in tables 15A and 15B do however show a significant decrease in the amount of CO_2 adsorbed when regeneration is performed at 150°F indicating incomplete removal of CO_2 and a subsequently lower loading swing during adsorption. Velocity still remains relatively insignificant although again there is an increase in the adsorption rates by as much as 25 percent for the 1/8-inch panel (runs no. 68 and no. 69).

Addition of water vapor resulted in a decrease in CO_2 capacity of approximately 50 percent.

Block 7 represents a further expansion of the sample space to include the performance of the panels under high inlet humidity conditions and longer path length. Operation in this mode is a coadsorption function where both water and carbon dioxide are concurrently removed from the process gas. The attempt here is to define the degree of interference of the water vapor and the compensating effect of more sieve since CO_2 adsorption remains as the primary function of the adsorber.

This block is a 2^3 factorial with 13X under the conditions noted in table 17.

The same assumptions made for block 2 regarding time are made for this case as well. A complete 2^3 factorial analysis of variance was run with the results shown in table 18.

Again it is noted that the interaction effects are not significant. The effects of the variable V, and P are also not significant, possibly due, in part, to the decreased range as compared to previous runs. The effects of humidity are decidedly significant and should therefore be considered as a factor in further quantitative investigation.

Path length was not a variable but a review of the data shows that the numerical effects of relative humidity and path length (or quantity of sieve) are nearly equal in magnitude but opposite in sign. The net effect is that capacity of the "system" was comparable to the system operating at the low humidity levels previously tested.

TABLE 16

BLOCK 5 ANALYSIS OF VARIANCE

Source	Effect	F-Ratio
Average	0.00350	-------
(V) Velocity	0.000449	-------
(P) Partial pressure	0.00615	1.18
(t) Plate thickness	-0.000496	------
(T) Regeneration temp	0.000464	-------
VP	0.000321	-------
Vt	-0.000155	-------
VT	-0.0000426	-------
Pt	0.000584	1.06
PT	0.000332	-------
tT	0.000356	-------
VPt	-4.83×10^{-5}	-------
VPT	-3.88×10^{-4}	-------
VtT	-4.73×10^{-5}	-------
PtT	2.64×10^{-4}	-------
VPtT	3.07×10^{-4}	-------

Residual mean square = 5.13×10^{-6} with 48

TABLE 17 BLOCK 7.

CO_2 ADSORPTION ON 13X MOLECULAR SIEVE AS A FUNCTION OF VELOCITY, PP CO_2, AND INLET DEW POINT

Run number	Variables: Velocity ft/min	Variables: PP CO_2, mm Hg	Variables: Inlet dew point, ^oF	Total run time, min	CO_2 Inlet rate lb/hr x 10^3	Total CO_2 adsorbed (W), total H_2O adsorbed (W^o) and CO_2 removal efficiency (Eff): t = 1 min, W, lbs x 10^3	t = 1 min, Eff, %	t = 5 min, W, lbs x 10^3	t = 5 min, Eff, %	t = 10 min, W, lbs x 10^3	t = 10 min, Eff, %	t = 10 min, W^o, lbs x 10^3	t = 15, W, lbs x 10^3	t = 15, Eff, %	t = 15, W^o, lbs x 10^3	Initial CO_2 adsorption rate lb/hr
95	375	7.6	40	18	12.9	1.53	10.8	6.28	8.8	9.12	6.4	12.9	11.0	5.1	21.2	0.092
96	200	7.6	40	18	6.9	1.5	19.7	6.33	16.7	9.6	12.6	11.6	11.1	9.8	20.3	0.090
97	200	4.0	40	16	3.6	0.87	21.7	3.88	19.4	6.48	16.2	14.0	7.8	12.9	24.1	0.055
98	375	4.0	40	16	6.8	0.92	12.2	4.10	10.9	6.90	9.2	12.7	8.47	7.5	21.0	0.052
108	375	4.0	-30	16	6.8	1.83	24.4	8.32	22.2	14.1	18.8		16.7	14.9		0.026
109	200	4.0	-30	18	3.6	1.68	42.1	7.23	36.2	11.9	29.7		14.6	24.4		0.020
110	375	7.6	-30	18	12.9	3.0	21.0	13.6	19.1	24.5	17.2		32.0	14.9		0.047
111	200	7.6	-30	18	6.9	2.57	33.8	12.2	31.9	20.7	27.2		25.9	22.8		0.034

Constants: Path length, 4 ft
Absolute Pressure, 760 mm Hg
Plate temp., 75^oF
Regeneration, 20 μ and 300^oF

TABLE 18

BLOCK 7 ANALYSIS OF VARIANCE

Source	Effect	F-Ratio
Average	0.00958	
(V) Velocity	0.00112	-------
(P) Partial pressure	0.00469	3.54
(H) Humidity	-0.00719	8.33**
VP	2.64×10^{-4}	-------
PH	-2.57×10^{-3}	1.06
VH	-1.03×10^{-3}	-------
VPH	-5.16×10^{-4}	-------

Residual mean square = 4.96×10^{-5} with d.f.

Of additional significance is the apparent ability of the adsorber panel to be cycled without additional processing to remove water vapor. The inference here specifically is that additional sieve could be used to increase overall capacity and eliminate the need for a predryer in an operating system.

Block 8 consisted of a 2^3 test on a dual canister for which the following factors were tested:

(1) Velocity: 375, 200 ft/min (V)

(2) Partial pressure CO_2: 7.6, 4.0 mm Hg (P)

(3) Path length: 4, 2 ft.

The data for the four times; 1, 5, 10, 15 minutes is listed along with other test parameters in table 19. The extension of path length for this test also has the effect of increasing the capacity of the system by doubling the amount of sieve used. The panels are however now a hybrid system with one 1/8-inch and one 1/4- inch panel. Dew-point was again reduced to -30°F to provide data on path length for a single component adsorption system.

TABLE 19 BLOCK 8.

CO_2 ADSORPTION ON 13X MOLECULAR SIEVE AS A FUNCTION OF VELOCITY, PP CO_2, AND PATH LENGTH

Run number	Variables			Total run time, min	CO_2 Inlet rate, lbs/hr x 10^3	Total CO_2 adsorbed (W) and removal efficiency (Eff)										Initial CO_2 adsorption rate lbs/hr
						t = 1 min		t = 5 min		t = 10 min		t = 15 min		t = 19 min		
	Velocity, ft/min	PP CO_2, mm Hg	Path length, ft			W, lbs x 10^3	Eff, %	W, lbs x 10^3	Eff, %	W, lbs x 10^3	Eff, %	W, lbs x 10^3	Eff, %	W, lbs x 10^3	Eff, %	
92	375	7.6	2	18	12.9	1.43	11.1	6.62	10.2	11.6	8.9	15.2	7.8	17.3	7.0	0.086
93	200	7.6	2	18	6.3	0.85	12.3	3.85	11.2	6.58	9.5	8.32	8.0	8.78	6.7	0.051
94	375	4.0	2	16	6.8	0.93	13.7	4.23	12.4	7.38	10.8	9.52	9.3	10.7	8.3	0.056
99	200	4.0	2	18	3.6	0.80	22.0	3.72	20.5	6.38	17.6	7.97	14.6	8.38	12.2	0.048
108	375	4.0	4	18	6.8	1.83	24.4	8.32	22.2	14.1	18.8	16.7	14.9	17.5	12.3	0.110
109	200	4.0	4	18	3.6	1.68	42.1	7.23	36.2	11.9	29.7	14.6	24.4	15.4	20.3	0.101
110	375	7.6	4	18	12.9	3.0	21.0	13.6	19.1	24.5	17.2	32.0	14.9	35.5	13.1	0.18
111	200	7.6	4	18	6.9	2.57	33.8	12.2	31.9	20.7	27.2	25.9	22.8	28.7	19.9	0.154

Constants: Regeneration at 20μ and 300°F
Plate temp., 75°F
Dew point, -30°F

Absolute Pressure, 760 mm Hg

Again using pseudo-replicated data as a basis the analysis of variance becomes:

TABLE 20

BLOCK 8 ANALYSIS OF VARIANCE

Source	Effect	F-Ratio
Average	0.00956	
(V) Velocity	0.00223	-------
(P) Partial pressure	0.00447	3.10
(L) Path length	0.00722	8.10**
VP	1.14×10^{-3}	-------
PL	2.78×10^{-3}	1.20
VL	-7.0×10^{-5}	-------
VPL	-3.6×10^{-4}	-------

As previously inferred the factor "path length" seems to effect the resulting yield in a fashion almost identical to that of humidity in block 7. In fact, the effects are even numerically close, with reversed signs of course. The other factors and interactions are not significant; again repeating the pattern of block 7.

Block 9 is a series of tests performed over a narrow range of parameters to determine the ability of the panels to be cycled while operating with a predryer but being regenerated at 50 mm Hg and elevated temperatures. As shown in table 21 the panels performed well and the results are comparable with similar runs at lower regeneration pressures.

Blocks 3 and 3R are an evaluation of a 5A panel operating as a CO_2 adsorber in a dry atmosphere. The tests performed are inconclusive in that the number of variables tested was minimal. The 13X panels as anticipated had better capacity. Tests were terminated with 5A plates because of severe contamination as a result of a blower fire. Blocks 3 and 3R tables 22 and 23 are a replicated experiment which considers velocity (V), Partial Pressure (P) and Plate Temperature (T), as variable factors with all others held at constant levels.

TABLE 21 BLOCK 9.

CO_2 ADSORPTION ON 13X MOLECULAR SIEVE AS A FUNCTION OF VELOCITY, PP CO_2 AND REGENERATION TEMPERATURE

	Variables					Total CO_2 adsorbed (W) and removal efficiency (Eff)										
						t = 1 min		t = 5 min		t = 10 min		t = 15 min		t = 19 min		
Run number	Velocity, ft/min	PP CO_2, mm Hg	Regen. temp., ^oF	Total run time, min	CO_2 Inlet rate, lbs/hr x 10^3	W, lbs x 10^3	Eff, %	W, lbs x 10^3	Eff, %	W, lbs x 10^3	Eff, %	W, lbs x 10^3	Eff, %	W, lbs x 10^3	Eff, %	Initial CO_2 adsorption rate lb/hr
100	375	7.6	300	16	15.5	1.27	8.2	5.38	6.9	8.37	5.4	9.92	4.3	10.3	3.5	0.076
101	200	7.6	300	16	8.3	1.18	14.3	5.08	12.3	8.09	9.8	9.32	7.5			0.071
102	375	7.6	150	16	15.5	0.75	4.8	3.50	4.5	5.98	3.9	7.27	3.1			0.045
103	200	7.6	150	16	8.3	0.63	7.6	2.90	7.0	5.02	6.1	6.22	5.0			0.038
104	375	4.0	300	16	8.2	1.23	15.1	5.37	13.1	8.34	10.2	9.9	8.1	10.3	6.6	0.074
105	200	4.0	300	16	4.4	1.20	27.5	5.15	23.6	7.99	18.3	9.2	14.1	9.47	11.4	0.072
106	375	4.0	150	16	8.2	0.72	8.8	3.32	8.1	5.62	6.9	6.82	5.6	7.05	4.5	0.043
107	200	4.0	150	16	4.4	0.65	14.9	3.01	13.8	5.09	11.7	6.27	9.6			0.039

Constants: Plate Temp., 75°F
Absolute Pressure, 760 mm Hg
Dew point, -30°F
Plate thickness, 0.125
Regenerated at 30 mm Hg - 50 mm Hg

TABLE 22 BLOCK 3.

CO_2 ADSORPTION ON 5A MOLECULAR SIEVE AS A FUNCTION OF VELOCITY, PP CO_2, AND PLATE TEMPERATURE

Run number	Variables			Total run time, min	CO_2 Inlet rate, lb/hr x 10^3	Total CO_2 adsorbed (W) and efficiency (Eff)										Initial CO_2 adsorption rate lb/hr
						t = 1 min		t = 5 min		t = 10 min		t = 15 min		t = 19 min		
	Velocity, ft/min	PP CO_2, mm Hg	Plate temp., ^oF			W, lbs x 10^3	Eff, %	W, lbs x 10^3	Eff, %	W, lbs x 10^3	Eff, %	W, lbs x 10^3	Eff, %	W, lbs x 10^3	Eff, %	
21	275	3.1	30	22	4.6	0.58	12.6	2.75	11.8	4.83	10.4	6.3	9.0	7.14	8.1	0.035
22	25	3.1	30	12	0.42	0.53	126.2	2.42	114.4	4.03	95.3	4.32	68.1			0.032
23	275	3.1	75	16	4.6	0.62	13.3	2.9	12.5	4.66	10.0	5.53	7.9			0.037
24	25	3.1	75	12	0.42	0.42	98.6	1.68	79.7	2.63	62.3					0.025
25	225	21	75	18	2.86	0.89	31.2	4.16	29.1	7.16	25.0	9.67	22.5	10.4	19.2	0.054
26	25	21	30	18	2.86	0.63	22.1	3.03	21.2	5.22	18.3	7.03	16.4	7.52	13.8	0.038
27	275	21	30	18	31.5	1.43	4.5	6.74	4.3	10.9	3.5	13.1	2.8	13.6	2.3	0.085
28	275	21	75	18	31.5	1.07	3.4	5.17	3.3	8.19	2.6	10.2	2.2	10.8	1.8	0.064

Constants: Plate thickness, 0.125 in.
Regeneration, 300°F and 20 μ
Pressure Abs., 760 mm Hg
Dew point, -30°F
Path length, 2 ft

TABLE 23 BLOCK 3R.

CO_2 ADSORPTION ON 5A MOLECULAR SIEVE AS A FUNCTION OF VELOCITY, PP CO_2, AND PLATE TEMPERATURE

Run number	Variables			Total run time, min	CO_2 Inlet rate, lbs/hr x 10^3	Total CO_2 adsorbed (W) and removal efficiency (Eff)										Initial CO_2 adsorption rate, lb/hr
						t = 1 min		t = 5 min		t = 10 min		t = 15 min		t = 19 min		
	Velocity, ft/min	PP CO_2, mm Hg	Plate temp., ^oF			W, lbs x 10^3	Eff, %	W, lbs x 10^3	Eff, %	W, lbs x 10^3	Eff, %	W, lbs x 10^3	Eff, %	W, lbs x 10^3	Eff, %	
52	275	21	75	18	31.5	1.14	3.6	5.28	3.4	8.61	2.7	10.5	2.2	11.0	1.8	.069
53	~25	21	75	18	2.9	0.77	26.8	3.63	25.4	6.43	22.5	8.7	20.3	9.5	17.5	.046
54	275	3.1	30	22	4.65	0.70	15.1	3.15	13.6	5.23	11.2	6.57	9.4	7.25	8.2	.042
55	~25	3.1	75	10	4.22	3.83	90.7	1.72	81.3	2.57	60.8					.023
56	~25	21	30	16	2.86	0.72	25.0	3.43	23.9	6.02	21.1	7.82	18.2	8.23	15.1	.043
57	275	21	30	18	31.5	1.35	4.3	6.35	4.0	10.9	3.5	13.4	2.8			.081
58	275	3.1	75	14	4.65	0.65	13.9	3.02	12.9	4.75	10.2	5.58	8.0			.039
59	~25	3.1	30	14	0.42	0.58	138.1	2.60	123.1	4.35	102.8	4.88	77.1			.035

Constants: Plate thickness, 0.125 in.
Regeneration, 300°F and 20 μ
Absolute pressure, 760 mm Hg
Dew point, -30°F
Path length, 2 ft

The velocity range is greater to a degree in this case as compared to blocks 1, 1R (25 to 275 ft/min) and similarly for partial pressures (3.1 to 21. mm Hg).

The consideration of temperature as an effect has introduced a degree of non-additivity into our model, for velocity and partial pressure interact with each other in all four cases. Also, a 3-way interaction between all three variables is observed at the marginal 95 percent level as shown in the effects table.

In a fashion similar to 1 and 1R, the abbreviated results for the four elapsed time periods are listed below:

Elapsed Time = 1 minute

Source	Effect	F-Ratio
Average	0.000801	
(V) Velocity	0.000370	69.40**
(P) Partial pressure	0.000485	119.00**
(T) Temperature	-0.0000288	--------
VP	2.12×10^{-4}	22.75**
PT	5.41×10^{-5}	1.47
VT	-2.71×10^{-5}	--------
VPT	-1.02×10^{-4}	5.26

Elapsed Time = 5 minutes

Source	Effect	F-Ratio
Average	0.00372	
(V) Velocity	0.00178	68.86**
(P) Partial pressure	0.00239	124.09**
(T) Temperature	-0.00168	--------
VP	9.31×10^{-4}	18.82**
PT	2.31×10^{-4}	1.16
VT	-9.57×10^{-5}	--------
VPT	-5.04×10^{-4}	5.51*

Elapsed Time = 10 minutes

Source	Effect	F-Ratio
Average	0.00620	
(V) Velocity	0.00280	72.45
(P) Partial pressure	0.00414	158.33**
(T) Temperature	-0.000466	1.99
VP	1.33×10^{-3}	16.34**
PT	4.86×10^{-4}	2.17
VT	-2.58×10^{-4}	--------
VPT	-8.91×10^{-4}	7.30*

Elapsed Time = 15 minutes

Source	Effect	F-Ratio
Average	0.00761	
(V) Velocity	0.00332	77.15**
(P) Partial pressure	0.00563	221.86**
(T) Temperature	-0.00064	2.86
VP	9.28×10^{-4}	6.01*
PT	7.97×10^{-4}	4.43
VT	-5.24×10^{-4}	1.91
VPT	-1.08×10^{-3}	8.24*

Partial pressure, again, is highly significant, which may be due to the fairly wide interval of interest. Velocity now appears as a highly significant factor. In the determination of a quantitative model, indications are that the relationship between CO_2 adsorbed and the three variables (V, P, T) enter in a strongly non-linear fashion. The extension of the velocity from an upper limit of 200 to 275-ft/min may indicate that this region is critical and should be investigated further.

A repetition of the consistent pattern again encouraged us to combine all the data and include time as factor (a 2 x 2 x 2 x 4 design).

A summary of the analysis of variance is shown in table 24.

The significant interaction terms encountered in the four runs reflect in a more complex structure for the combined analysis of variance. As in the 1-1R case, time is a highly significant factor along with velocity and partial pressure. The factor, temperature, however now becomes marginally significant at the 95 percent level. This was not observed for the four runs, but the interaction with time may have influenced the result. Velocity and partial pressure again interact strongly. Also each of these interact with time, individually and combinationally (that is VPT). Partial pressure and temperature also interact, which is related to the appearance of temperature as a significant factor.

In summary, it is evident that temperature does not enter into our mathematical relationship in simple form. The effect of temperature as a main factor is not clearly indicated, but its introduction caused significant interaction terms to appear.

Further analysis would probably be simplified by holding temperature constant and selecting levels for other suspected factors. A repetition of the experiments at different temperature levels may allow us to study the other effects in a simpler manner.

Diffusion Model

The phenomena of diffusion and mass transfer have been well documented in the literature. The following analytical procedure is taken in large part from reference no. 1. Consider a fluid flowing parallel to the solid surface of a flat plate. Assume the bulk velocity of the gas to be in the turbulent flow region and the place under observation on the plate to be relatively far removed from the edge of the plate so that special flow conditions caused by geometry such as container walls need not be considered. The velocity of the fluid particles at various distances from the solid surface is not uniform but varies from zero at the surface to larger values at positions removed from the plate finally reaching the bulk flow conditions of the main gas stream. Figures 14 and 15 show the construction of a typical film and the velocity profile for the gas at different locations.

TABLE 24

BLOCKS 3 AND 3R ANALYSIS OF VARIANCE

Source	DF	Mean-square	F-Ratio
(V) Velocity	1	6.86×10^{-5}	228.69**
(P) Partial pressure	1	1.60×10^{-4}	534.50**
(T) Temperature	1	1.70×10^{-6}	5.67
(C) Time periods	3	1.43×10^{-4}	477.62**
VP	1	1.15×10^{-5}	38.65**
VT	1	8.20×10^{-7}	2.73
VC	3	6.78×10^{-6}	22.60**
PT	1	2.46×10^{-6}	8.20**
PC	3	1.98×10^{-5}	66.02**
TC	3	3.08×10^{-7}	1.02
VPT	1	6.67×10^{-6}	22.25**
VPC	3	8.70×10^{-7}	2.90
VTC	3	1.95×10^{-7}	--------
PTC	3	4.17×10^{-7}	1.39
VPTC	3	7.59×10^{-7}	2.53

Residual mean square = 3.00×10^{-7} with 32 d.f.

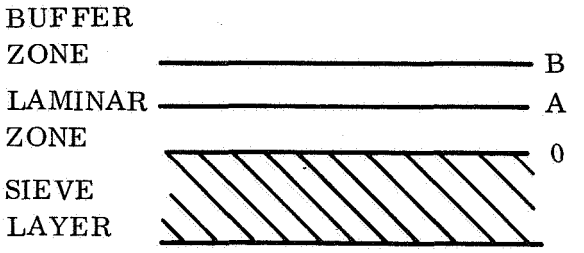

Figure 14. Mass Transfer Zone

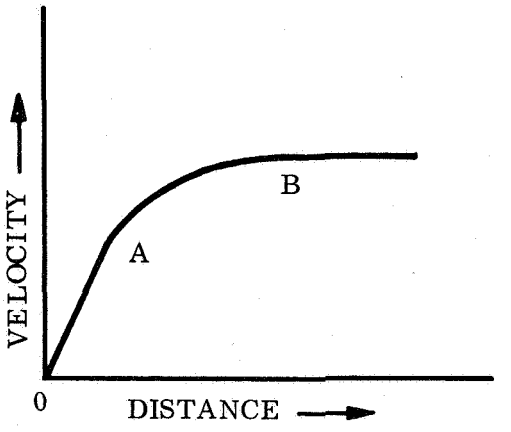

Figure 15. Velocity Profile

The velocity of the gas in the laminar regime, OA, is linear beginning at zero and increasing until the velocity reaches the limits of laminar flow (Reynolds No. < 2100). This laminar film is characterized by an orderly movement of gas particles in persistant, well-defined streamlines which parallel the contours of the surface, and there is no bulk movement of gas in a direction perpendicular to the surface. The middle zone or buffer region (AB) is characterized principally by the formation of eddy currents which result in large velocity vectors being perpendicular to the plate surface. There are no well defined streamlines in this area, velocity does not increase linearly with distance, and considerable mixing of gas particles is accomplished in this area. At the outer limits of the zone, flow finally reaches the maximum value. The relative thickness of the zones depends upon the degree of turbulence existing, which in turn depends upon the surface smoothness and Reynolds number.

$$R_e^{o} = DV \rho / \mu$$

where:

D = Diameter

V = Velocity

ρ = Density

μ = Viscosity

These same phenomena are found wherever a fluid flows past a solid surface, flat or round, so it is apparent that any substance diffusing through the various zones must involve two separate mechanisms. Diffusion in the laminar region is called "molecular diffusion", and diffusion in the turbulent zone is generally known as "eddy diffusion".

Molecular diffusion is the transport of individual gas particles through a fluid which is stagnant or, if laminar flow, in a direction perpendicular to the flow streamlines.

The kinetic theory provides some added insight into the process. A molecule of gas is pictured as traveling in a straight line at a uniform velocity until it collides with another molecule, where the velocity is changed in both magnitude and direction. The average distance the molecule travels between collisions is called the "mean free path" and the average velocity of the molecule is dependant upon the temperature. The molecule is thus seen to travel a highly complex path, with the net distance it moves being only a small fraction of its actual path length. For this reason, the net rate of diffusion is very slow.

From reference no. 1 the basic equation for determining the molecular diffusion rate of one gas (a) through another gas (b) is:

$$-d_{p_a} = \frac{RT}{D_{ab}P} \quad (N_a P - N_a P_a - N_b P_a) \quad dZ \qquad (6)$$

where

dP_a = pressure drop of diffusing gas across dZ

R = gas constant

D = diffusion constant

T = absolute temperature

N_a = moles of gas diffusing per unit time and area

dZ = film thickness

It is reasonable to assume that for the case of CO_2 diffusing through N_2 into a zeolite layer, N_b approaches zero. Figure 16 depicts schematically this diffusion process.

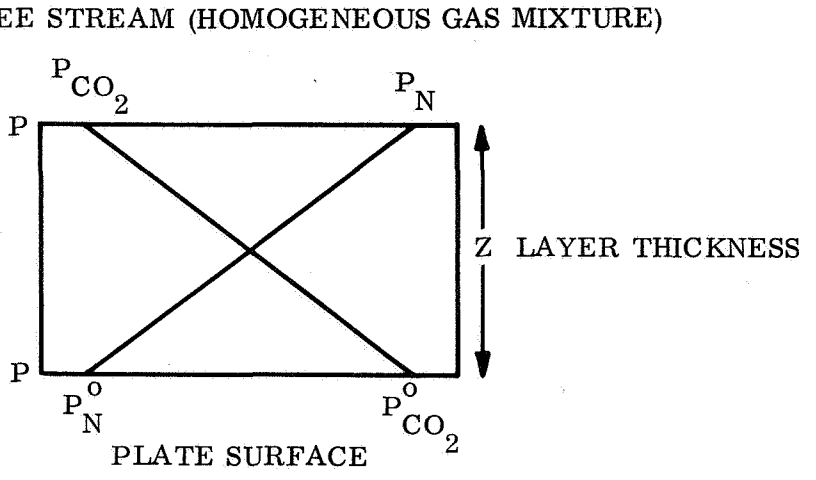

Figure 16. Pressure Drop Across Film

By integration of equation 6, the relationship for CO_2 diffusion is obtained:

$$N_{CO_2} = \frac{D_{ab}P}{RTZP_b}\left(P_{CO_2} - P^o_{CO_2}\right) \qquad (6a)$$

where

$$P_b = \frac{P^o_N - P_N}{\log\ (P^o_N/P_N)}$$

P_N = partial pressure of N_2 in freestream

P^o_N = partial pressure of N_2 at plate surface

Equation (6a) can now be used (with a suitable prediction for the film thickness) to evaluate the data from the experiments.

The prediction of accurate film thicknesses is difficult in that under actual conditions a constant value is never achieved.

Average film thicknesses were determined from figure 17. This figure (reproduced from reference no. 2, p. 153) shows the effect of velocity on film thickness for air flowing parallel to a flat, horizontal plate. Experimental data for a number of different gas velocities have been plotted to show how the gas velocity increases from essentially zero at the plate surface to the maximum or free stream velocity outside the film

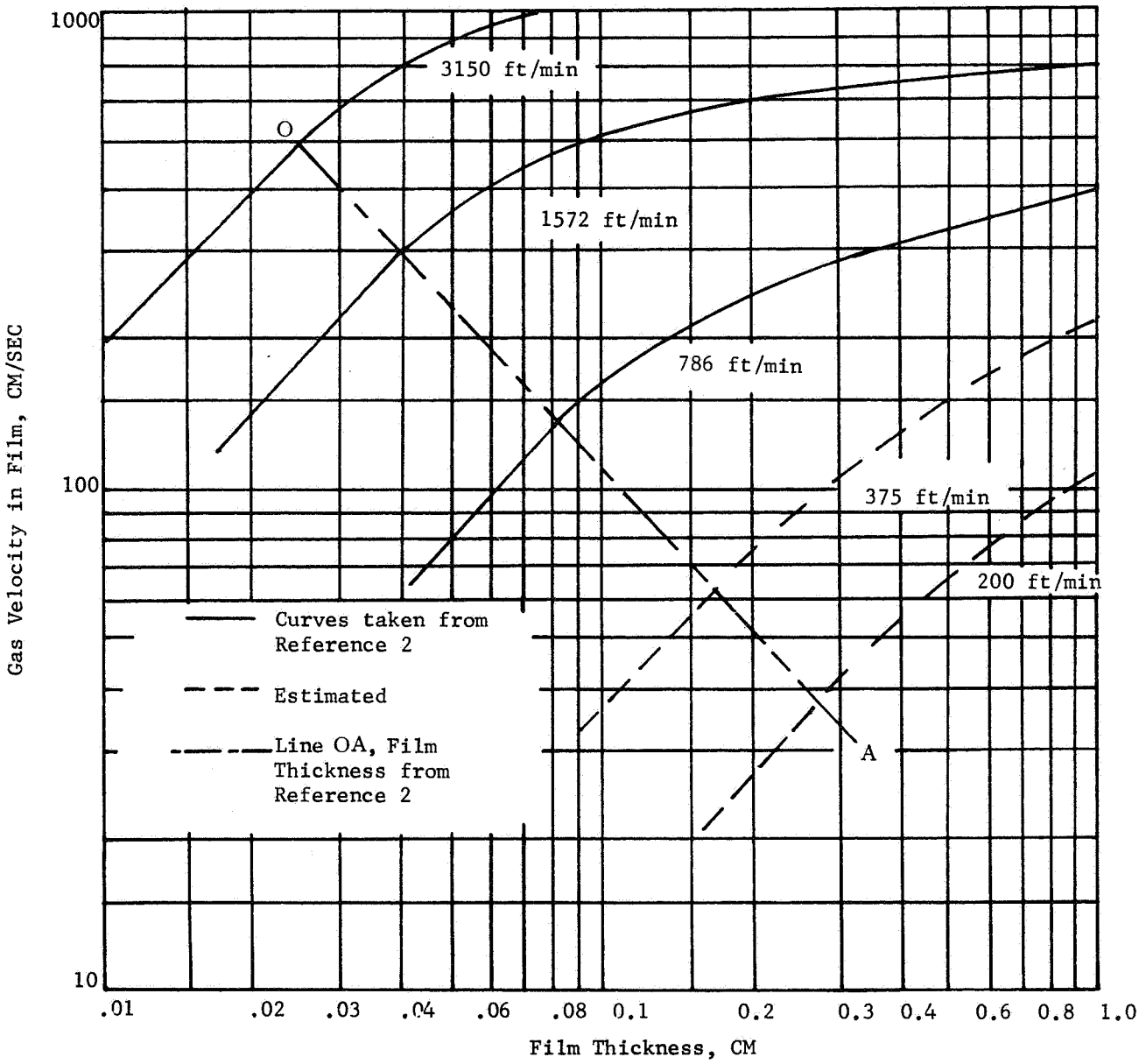

Figure 17. Gas Velocity vs. Film Thickness

layer. The air velocities were measured by a calibrated hot-wire anemometer, 0.005 cm in diameter. The intersection of line OA with the velocity curves defines the thickness (Z) of the boundary layer in equation 6a. The three curves at 786-, 1572-, and 3150-ft/min and the line OA are taken directly from reference no. 2. The two curves at 200- and 375-ft/min are extrapolations to the conditions of this study.

Comparison of Data With the Diffusion Model

Molecular Sieve as a CO_2 Adsorber. - Due to the large number of tests involved in the adsorption study a detailed discussion of each will not be attempted. Test runs selected exemplify how a given variable affects the overall diffusion process. Performance predictions based upon the model show reasonable correlation with the performance observed in the actual test runs. The data for all tests is summarized in tables of test blocks 1 through 9.

With reference to table 7 and figure 18, test runs no. 1 and no. 2 show the difference in adsorption rates caused by a change in flow velocity. The higher value of 200-ft/min is estimated to be in the turbulent flow region while the lower value of 25-ft/min is estimated to be in the laminar flow region. Substituting the test conditions of run no. 1 into equation 6(a):

$$N_{CO_2} = \frac{(0.139\ cm^2/sec)\ (1\ ATM)\ (21/760\ ATM)}{(82.06\ cm^3 atm/mol^oK)\ (298^oK)\ (0.26\ cm)\ (0.985\ ATM)}$$

$$N_{CO_2} = 6.14 \times 10^{-7}\ gm\text{-}mols\ CO_2/cm^2 sec$$

where 0.26 cm is the layer thickness predicted from figure 17.

Noting that the plate sample contains 1 square foot of surface and using the initial adsorption rate for test run no. 1 we find:

$$N^1_{CO_2} = 0.131\ lb/hr\text{-}ft^2 \times \frac{1\ hr}{3600\ sec} \times \frac{454\ gr}{lb} \times \frac{gr\text{-}mol}{44\ gr} \times \frac{1ft^2}{928\ cm^2}$$

$$N^1_{CO_2} = 4.0 \times 10^{-7}\ gm\text{-}mols\ CO_2/cm^2\ sec$$

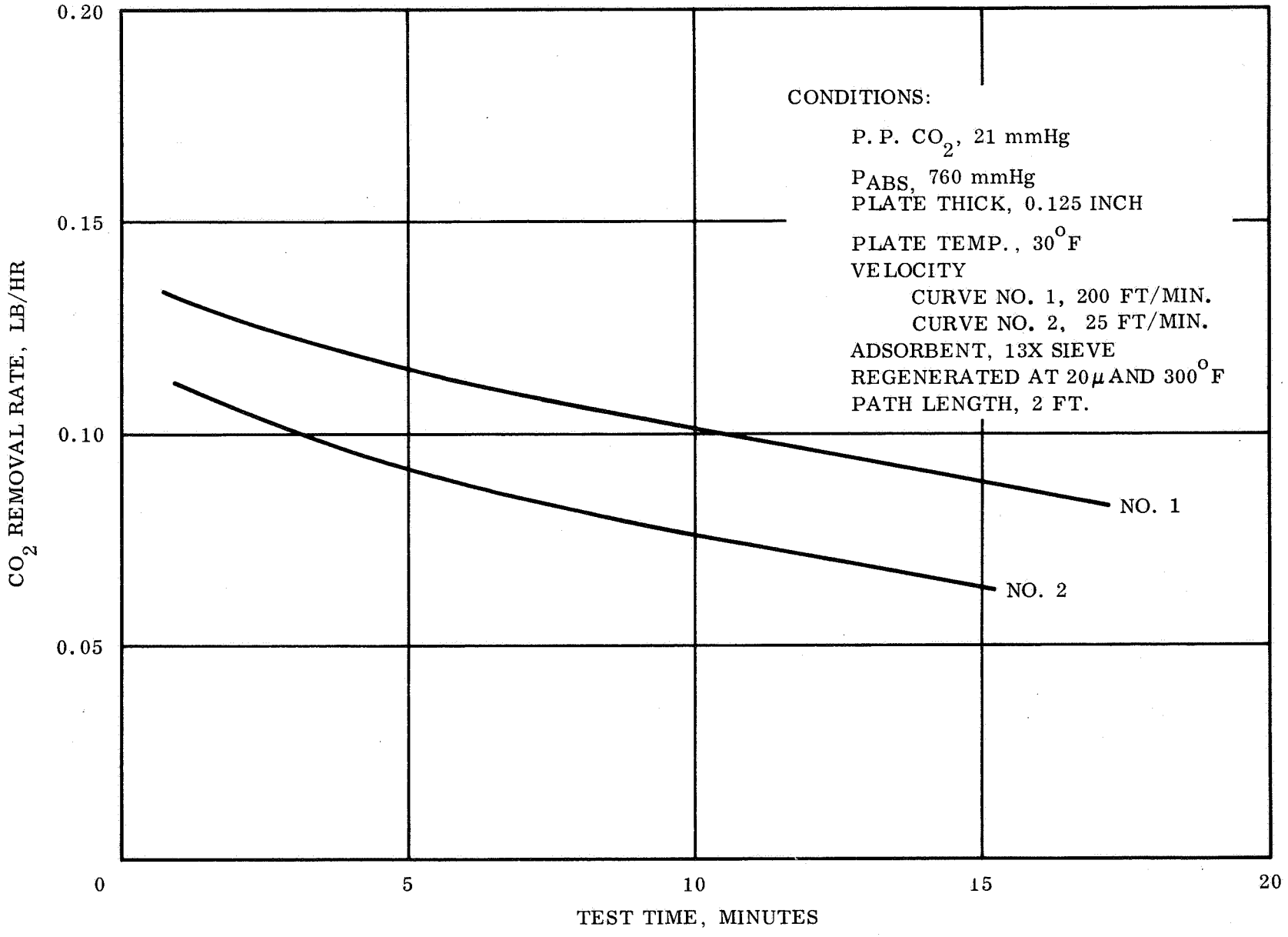

Figure 18. CO_2 Removal Rate as a Function of Adsorption Time at Various Velocities

The difference between theory and experiment can be attributed to several factors. First the theoretical prediction is for the initial adsorption rate at t = 0 or the instant where the full CO_2 partial pressure differential of 21 mm is realized. The test value of 0.131 pound/hour-foot^2 is an average rate measured over the first two minutes of the testing sequence. Extrapolation of the curve back to t = 0 would bring the values closer together. This deviation can also be attributed to localized differences in flow conditions on the plate surface due to reversal of gas flow at the rear of the canister and the inlet/outlet manifolding configuration of the gas delivery lines. This causes uneven film thicknesses on the plate surface with a resultant change in the CO_2 adsorption rate.

The CO_2 adsorption rates for test no. 2 (see figure 18) are lower than the rates measured in test no. 1. This was caused by the increased film thickness at the lower velocity of 25 ft/min. Equation 6a shows the CO_2 adsorption rate to be inversely proportional to film thickness which corroborates the test results.

A comparison of the CO_2 removal efficiencies for the two tests shows that the plate removed larger percentages of CO_2 during test no. 2. A comparison of the efficiencies at t = 1 minute shows the plate to be 70.46/9.53 = 7.4 times more efficient at the lower flow velocity of 25-ft/min. This can be explained by relating the efficiency to contact time (defined as path length over velocity or L/V). For a constant path length, the efficiency is seen to be inversely proportional to velocity. The ratio of the velocities in the tests is 200/25 or 8.0 which is less than a 10 percent difference from the efficiency ratio of 7.4. The relationship of efficiency with path length will be discussed in a later paragraph.

Several tests at the low flow rate of 25-ft/min showed removal efficiencies of greater than 100 percent for portions of the test run (see test no. 4, table 7, and test no. 22, table 22). Test no. 4, for example, had an initial removal efficiency of 133 percent. This efficiency was calculated by dividing the weight of CO_2 removed by the plate, by the total weight of CO_2 passed over the plate. The weight of CO_2 removed by the plate was obtained from the test data. The total CO2 passed over the plate was calculated from the following equation:

$$W = (V)\ (A)\ (\rho)\ (C) \qquad (7)$$

where

V = gas velocity, ft/min

A = canister flow area, ft^2

ρ = gas density, lbs/ft^3

C = concentration of inlet gas, lbs CO_2lb gas

The most likely cause of the high efficiency appears to be the measurement of gas velocity. To lower the efficiency from 133 to 100 percent, an actual gas velocity of 33.3-ft/min (calculated from equation 7) is required during the test. From the discussion of flow measurement at 25-ft/min contained in the "Instrumentation" section, it follows that 33.3-ft/min was probably the actual velocity during test no. 4.

Prediction of the decay of the transfer rates with time is based upon the following method. Table 7 data contains a column marked "Total CO_2 Adsorbed in 10 Minutes". The listed values were determined by a computer methods program which graphically integrates the area under the rate curves up to the 10 minute mark. This gives the plate loading (which can be calculated by dividing the weight of sieve on the plate into the total CO_2 on the plate, 0.0191/0.68 = 0.0281-lb CO_2/lb sieve). Reference to figure 11, curve C, shows the equivalent equilibrium pressure to be approximately 2.4 mm Hg. Noting the full pressure differential across the film is now 21. - 2.4 = 18.6 mm, a new rate of 0.116-lb/hr was determined from equation (6a). This compares favorably with the value of 0.105-lb/hr at 10 minutes shown on figure 18. The predicted value was higher than the test data because the pressure differential of 18.6 mm was assumed to be constant at all points on the plate surface. In actuality, the inlet partial pressure of 21.0 mm decreases as the gas flows along the plate, resulting in the lower measured rates.

The next parameter to be investigated was the effect of partial pressure on adsorption rate. Figure 19 shows the comparison of runs made at CO_2 partial pressures of 21.0 and 5.3 mm Hg respectively. Equation (6a) indicates that the initial CO_2 rate for the 5.3 mm run would be lower than the 21 mm run by a factor of 21/5.3 or 3.9 times lower. A comparison of the actual test points, 0.069 and 0.131-lbs/hr shows the rates to differ only by a factor of 1.9. The difference is due most probably to the assumption that the diffusion constant D is independent of CO_2 concentration. Over the relatively wide range of 5.3 to 21. mm covered by the tests, this does hold true (see p. 18, reference 1) primarily for the following reason. At the higher partial pressures more CO_2 molecules are impinging on the plate surface per unit area. This increases the probability that two CO_2 molecules will simultaneously reach an adsorption site on the plate surface. The collision between the CO_2 molecules results in one or both of the molecules being driven away from the site resulting in adsorption rates which are lower than those predicted by equation (6a). It is realized that under operational conditions cabin atmosphere partial pressures will be maintained below 7.6 mm. But, tests were run at CO_2 p.p. up to 21 mm Hg so that plate performance could be investigated over a wider range to aid in the prediction of interactions.

CO_2 removal rate as a function of plate temperature is shown by figure 20 for test runs 21 and 23 at two levels of temperature, 30° and 75°F, respectively. The curves show that the higher temperature gave a slightly higher initial removal rate of 0.037-lb/hr compared with 0.035-lb/hr. This is predicted by kinetic theory which shows the average velocity of a gas molecule to increase in proportion to the absolute temperature. The fact that the rates for the two plates cross over shows also that the sieve layer at 75°F approaches equilibrium loading capacity more rapidly than the cooler one which results in a higher equilibrium pressure on the surface side of the gas film. This in turn lowers the effective ΔP across the film and accounts for the lower removal rates as the test progresses. It should be noted that the absolute difference in the rates are quite small and in fact approach the accuracies of the test equipment and instrumentation. Based on these considerations it would appear that plate temperature over the range tested is not a dominant variable in the rate of CO_2 removal.

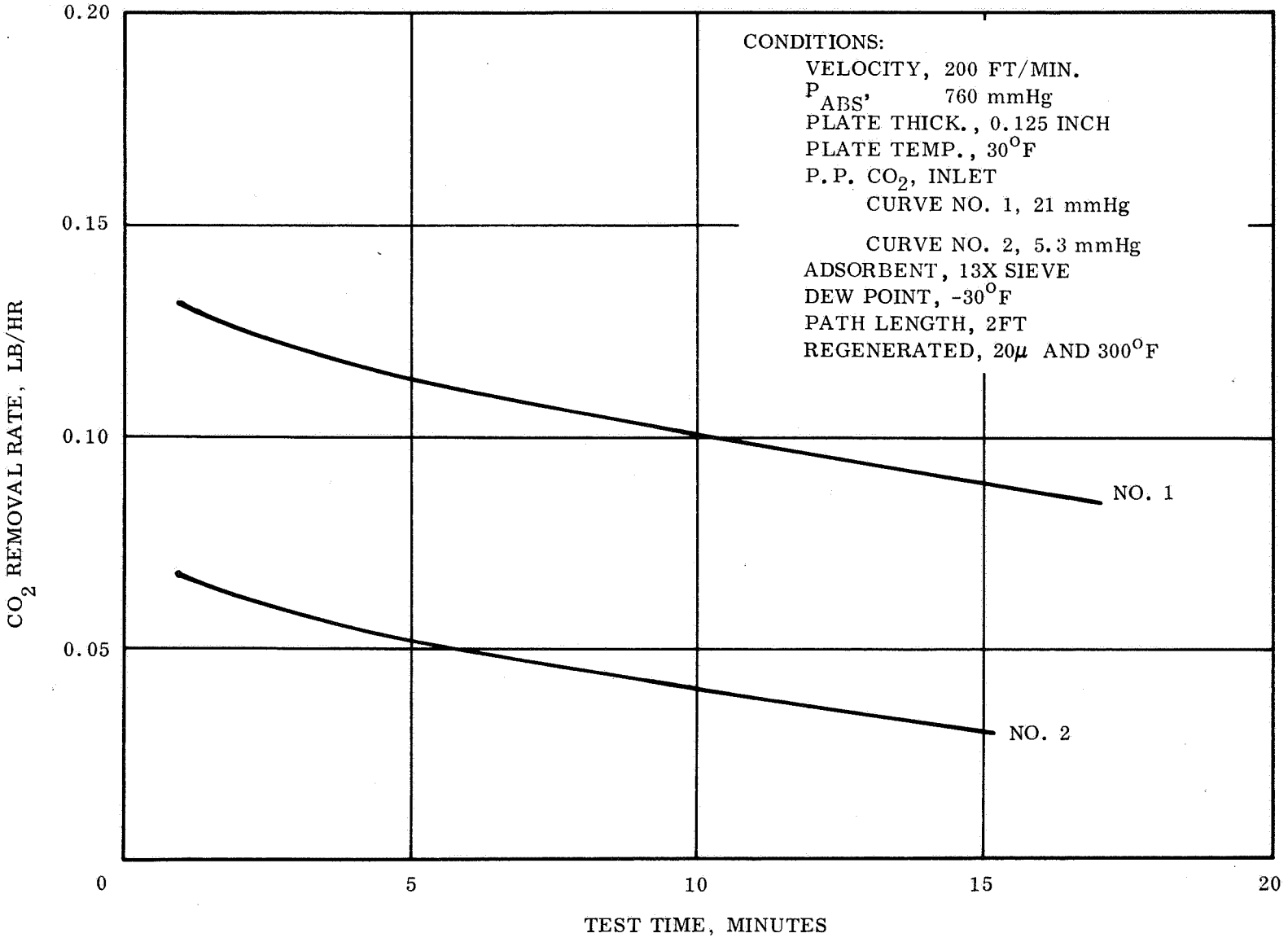

Figure 19. CO_2 Removal Rate as a Function of Time and Inlet CO_2 Partial Pressure

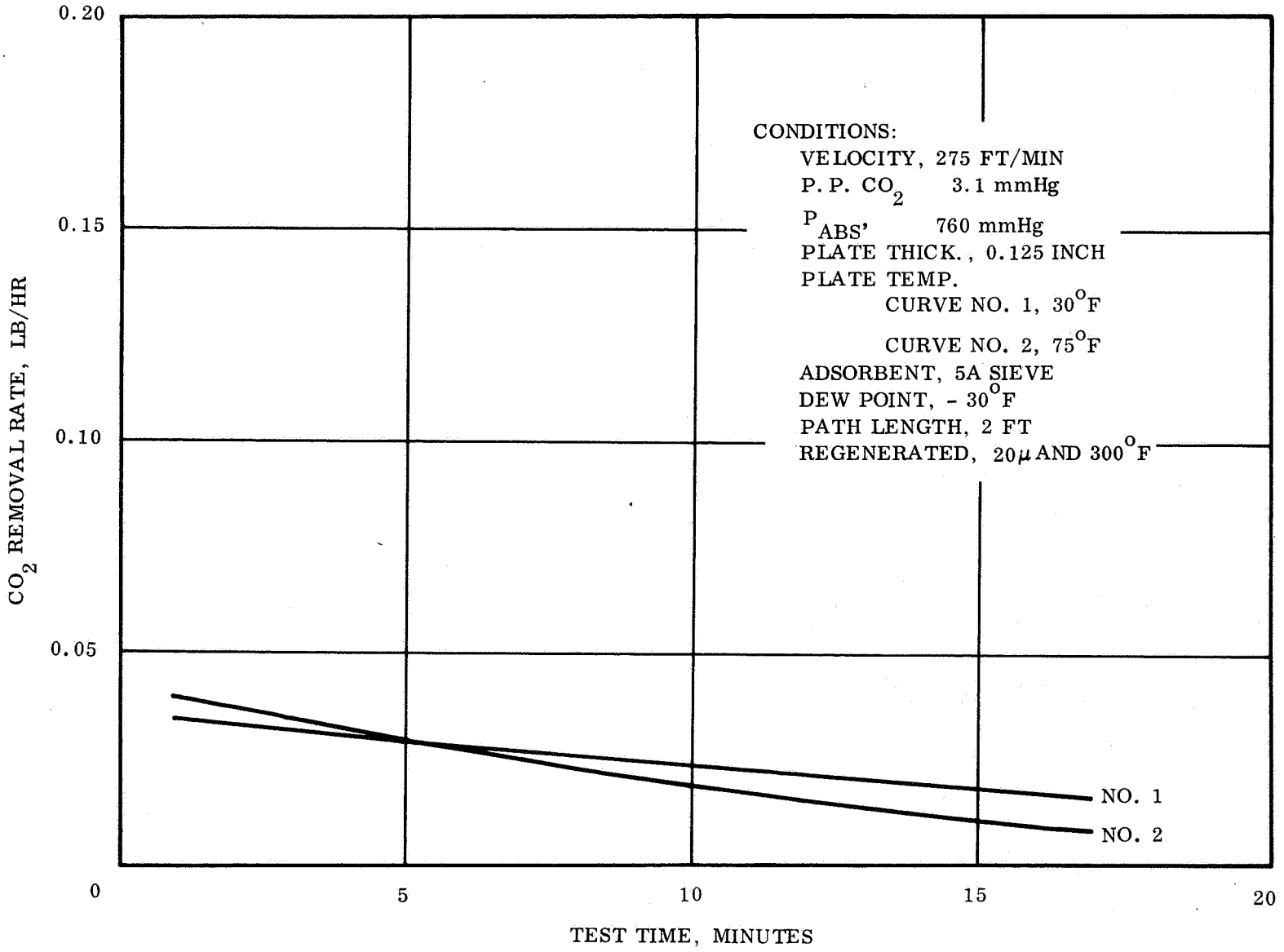

Figure 20. CO_2 Removal Rate as a Function of Time and Plate Temperature

The next parameter to be tested was the effect of plate or path length on CO_2 adsorption. Two plates were mounted in series, doubling the path length to a total of four feet. A comparison of curves 1 and 2 in figure 21 shows a significant increase in removal rates is realized because of the increased path length. Again using equation (6a) and figure 21 as a basis, the predicted rate is:

$$N_{CO_2} = \frac{(0.139\ cm^2/sec)\ (1\ ATM)\ (4/760\ ATM)}{(82.06\ cm^3\ ATM/mol\ ^oR \times 298^oK)\ (0.16\ cm)\ (0.985\ ATM)}$$

$$N_{CO_2} = 1.9 \times 10^{-7}\ gm\text{-}mol\ CO_2/cm^2\ sec$$

A comparison of the test data from figure 21, curve no. 2, shows an initial average rate of 0.11-lb/hr. Converting to equivalent units and dividing by the effective surface area we find:

$$N^1_{CO_2} = \frac{0.11\ lb}{hr.\ 2\ ft^2} \times \frac{1\ hr.}{3600\ sec} \times \frac{454\ gm.}{lb} \times \frac{gm\text{-}mol}{44\ gm.} \times \frac{1\ ft^2}{928\ cm^2}$$

$$N^1_{CO_2} = 1.7 \times 10^{-7}\ gm\text{-}mol\ CO_2/cm^2\ sec$$

A previous discussion on velocity effects related CO_2 removal efficiency to contact time (defined as length over velocity, L/V). To show this relationship, a comparison is made between two test runs from table 19 at constant velocity and different path lengths. For example, tests no. 92 and no. 110 have initial efficiencies of 11.1 and 21.0 percent. The ratio of the efficiencies, 11.1 to 21.0 percent or 0.528 percent compares to a path length ratio of 2 to 4 ft or 0.50 percent. A similar comparison can be made between tests no. 99 and no. 109. Comparing the efficiency ratio of 22.0 to 42.1 percent or 0.522 percent with the path length ratio of 0.5 percent, the direct relationship of efficiency with path length can be seen. This analysis in combination with the previous discussion of velocity effects on removal efficiency is the basis for relating efficiency to contact time (length/velocity). The efficiency can be used in determining system sizing requirements since choice of a value for efficiency and CO_2 removal rate defines the required process gas flow rate and also the L/V ratio for the adsorbent plate.

The effect of regeneration temperature was investigated at the two levels of 150° and 300°F. A comparison of curves no. 1 and no. 2, figure 22, shows the plate regenerated at the lower temperature of 150°F to give slightly lower CO_2 removal rates and also to become loaded more quickly due to the increased residual CO_2 and water being present on the plate. The removal rate differences are small enough that this parameter does not materially affect the adsorption process in a test where plate water loading is less than 0.01-lb H_2O/sieve.

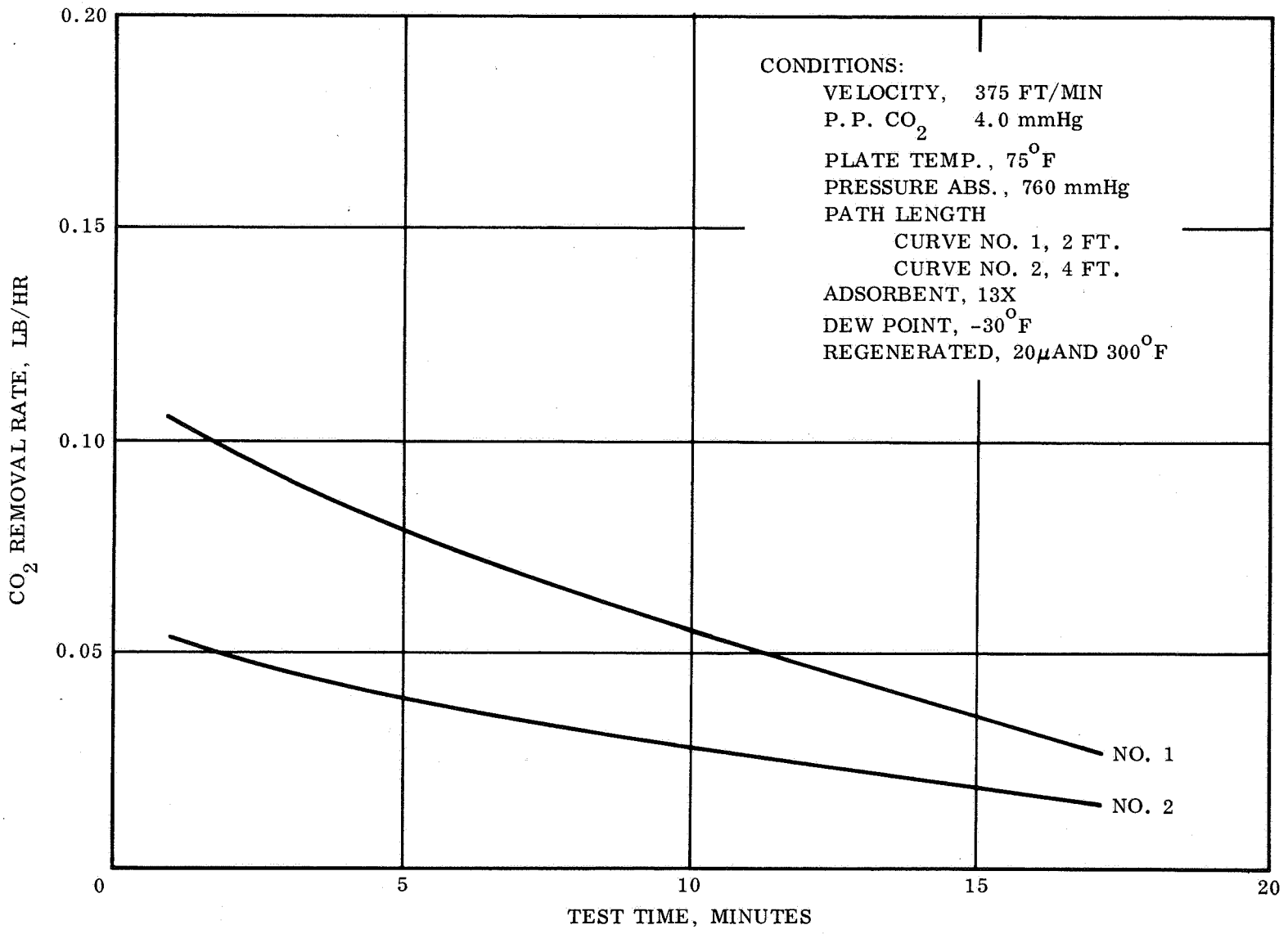

Figure 21. CO_2 Removal Rate as a Function of Time and Path Length

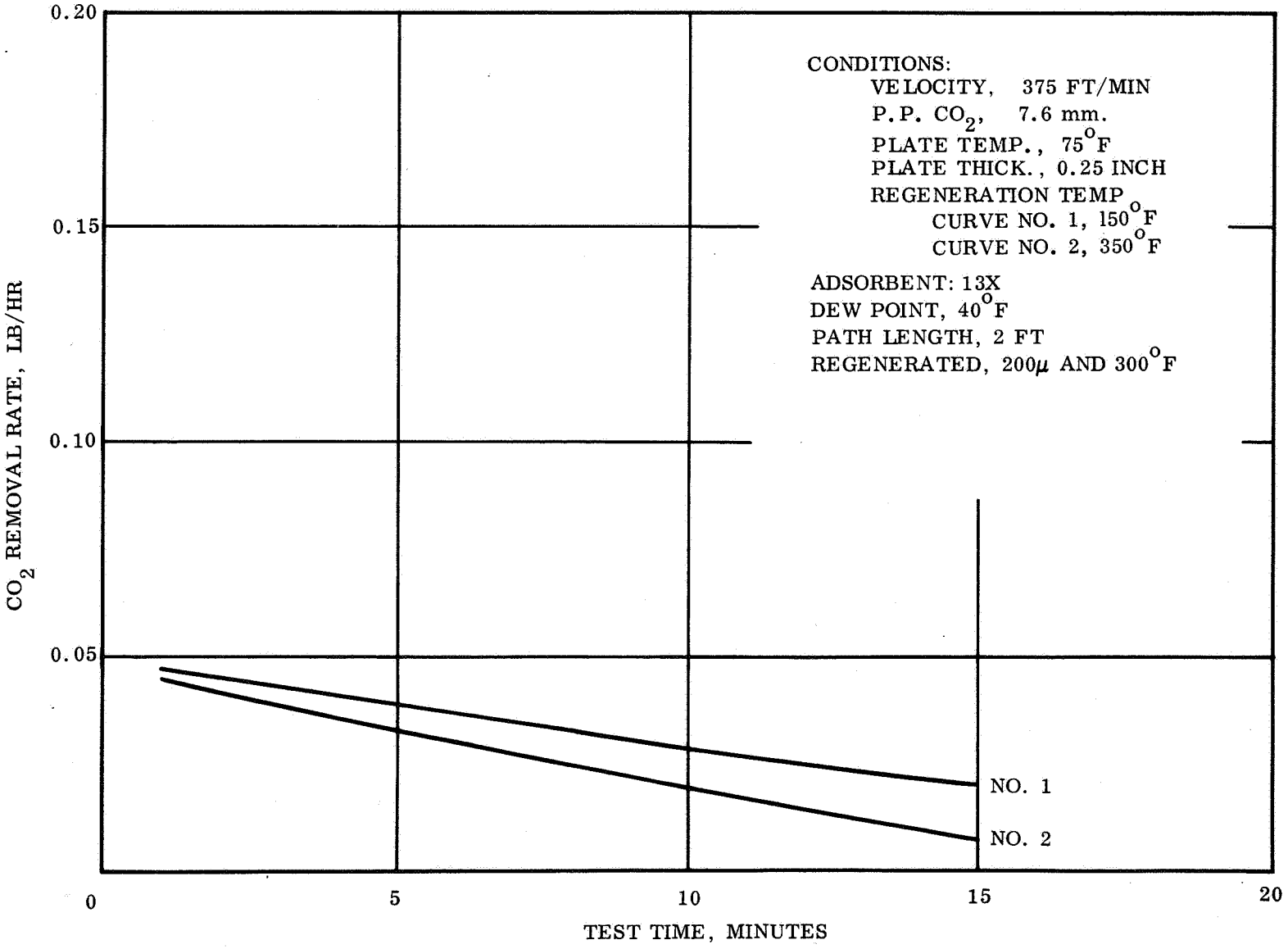

Figure 22. CO_2 Removal Rate as a Function of Time and Regeneration Temperature

Another factor to be considered is the effect of absolute pressure on the adsorption process. Figure 23 summarizes two tests performed at different total pressure, one at atmospheric or 760 mm and a second at 380 mm. A comparison of the two tests shows the rates to be equivalent with observed differences being within the accuracy of measurement. The results also agree with data from equilibrium testing discussed previously. Absolute pressure, therefore, was eliminated as a major variable in subsequent testing.

Silica Gel as a Water Vapor Adsorber. The water vapor removal tests for silica gel are summarized in table 25. The tests were carried out with an inlet dewpoint varying from 40^{o} to 43^{o}F, which correspond to inlet partial pressures of 6.3 and 7.1 mm Hg respectively.

CO_2 partial pressure was maintained at a constant 4.0 mm pressure throughout the tests. As anticipated no adsorption of CO_2 by the gel was observed. Corroboration between measured and theoretical rates of adsorption was good as evidenced by the example given below.

Using a diffusion constant of 0.258-cm^2/sec from reference no. 1 for water vapor diffusing through air, and a gas film thickness of 0.26-cm from figure 17 for a velocity of 200-ft/min, the rate of water adsorption can be predicted from equation (9).

Substituting the data for test 84:

$$N_{H_2O} = \frac{(0.258\ cm^2/sec)\ (1\ ATM)\ (6.3/760\ ATM)}{82.06\ cm^3\ atm/mol\ ^{o}K)\ (298^{o}K)\ (0.26\ cm)\ (0.985\ ATM)}$$

$$N_{H_2O} = 3.41 \times 10^{-7}\ gm\text{-}mol/cm^2\ sec$$

Converting the initial measured removal rate for test 84 to the correct units gives:

$$N^{1}_{H_2O} = \frac{0.041\ lb}{hr\ ft^2} \times \frac{1\ hr}{3600\ sec} \times \frac{454\ gm}{lb} \times \frac{1\ mol}{18\ gm} \times \frac{1\ ft^2}{928\ cm^2}$$

$$N^{1}_{H_2O} = 3.1 \times 10^{-7}\ gm\text{-}mol\ H_2O/cm^2\ sec$$

The lower measured rate can be attributed mainly to the fact that the silica gel layer contains approximately 5 percent of an inert epoxy binder.

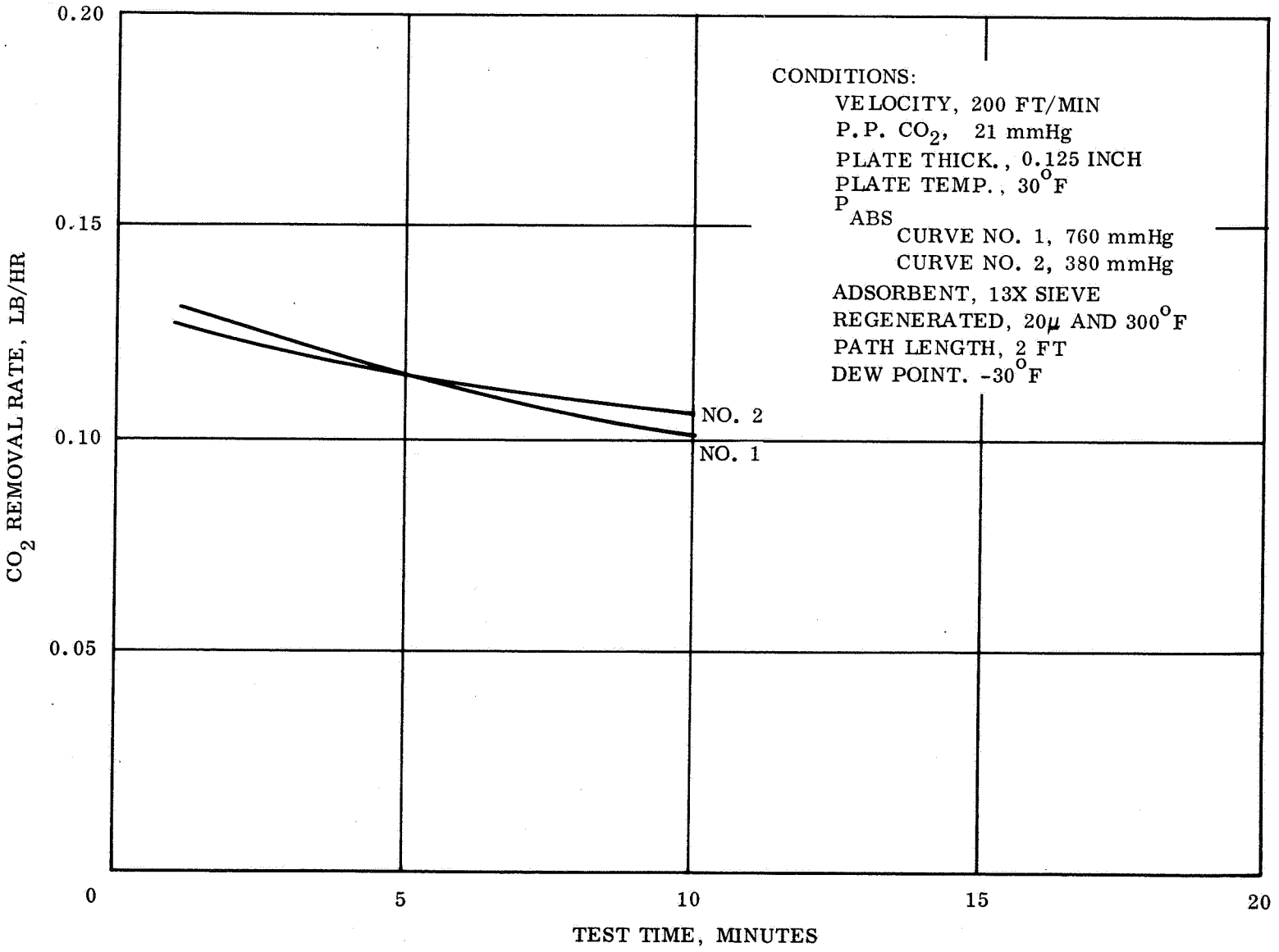

Figure 23. CO_2 Removal Rate as a Function of Time and Pressure

TABLE 25 BLOCK 6.

H_2O ADSORPTION ON SILICA GEL AS A FUNCTION OF VELOCITY PLATE TEMPERATURE AND THICKNESS

No.	Velocity ft/min.	Plate temp. °F	Plate thick. in.	Avg. inlet dewpoint °F	Test time min.	Initial H_2O removal rate lb/hr	Final H_2O removal rate lb/hr	Total H_2O adsorbed in 10 min. lb	H_2O inlet rate lb/min.	Removal efficiency per pass %	Avg. outlet dewpoint °F
84	200	30	0.125	41	14	0.041	0.035	0.00598	0.00294	20.4	35
85	375	30	0.125	43	16	0.049	0.042	0.00723	0.00592	12.22	40
86	200	75	0.125	40	14	0.038	0.032	0.00603	0.00277	21.75	35
87	375	75	0.125	40	16	0.051	0.040	0.00704	0.0052	13.53	36
88	200	30	0.25	41	16	0.035	0.032	0.00544	0.00246	22.10	35
89	375	30	0.25	41	16	0.052	0.045	0.00773	0.00551	14.05	36
90	200	75	0.25	41	16	0.035	0.030	0.00517	0.00246	21.05	35
91	375	75	0.25	41	16	0.048	0.043	0.00733	0.00551	13.33	36

Constants: Regeneration at 300°F and 200μ
Abs. pressure, 760 mm Hg
PP CO_2, 4.0 mm Hg

There appears to be no real advantage for using an adsorbent in the thin film configuration as a predryer, since the lowest outlet dewpoint observed during the tests was $35^{o}F$. In order to achieve outlet dewpoints commensurate with those required by predryer applications exhorbitant path lengths would have to be utilized.

Desorption and Energy Balances

Upon completion of the adsorption half-cycle, the canister is isolated from the flow circuit and the vacuum pump is turned on. Hot oil flow is initiated into the plate coils and continued until a steady state condition is reached. Figures 24 to 27 show typical pressure and temperature traces for the regeneration period. The discontinuities in the pressure decay curves are pressure surges caused by cutting in of the roughing and diffusion pumps.

A comparison of figures 24 and 25 shows the relationship between different plate thicknesses during the regeneration cycle. The thicker plates were found to take approximately 5 minutes longer to reach the final pressure. This is due in part to the greater thermal mass of the bulkier 1/4-inch plates. Additionally, the time required for diffusion of a CO_2 molecule from the bottom of the layer to the open surface is obviously greater for the thicker layer.

Temperature profiles for various locations on the panels during desorption heating are shown in figures 26 and 27. The cycle times indicated can be reduced by further optimization of the heat transfer characteristics of the panels. Several possibilities for optimization are discussed below. Substitution of a metal honeycomb structure for the wire mesh in the sieve layer would increase the contact area between the sieve and substrate over the presently used wire mesh screen. The honeycomb is also lighter in weight than an equivalent thickness of screening. Another alternative for improving the heat transfer characteristics is the replacement of stainless steel with aluminum as the substrate material, which has a thermal conductivity of 119-Btu/hr-ft^2-^{o}F/ft against 26-Btu/hr-ft^2-^{o}F/ft stainless steel. The material change requires the development of an alternate sieve layer bonding process. The process utilized for the test panels requires bonding cure temperatures in excess of $1500^{o}F$ which precludes the use of most common materials except stainless steel. Bonding process temperatures less than $1200^{o}F$ would permit use of aluminum with a resultant decrease in weight and thermal capacitance as well as an increase in thermal conductivity, all of which will improve desorption cycle time.

Figure 28 shows the effect of water vapor on a typical regeneration cycle. Although the time required to reach a final steady state pressure was not significantly increased when compared with the dry system of figure 25, the minimum pressure reached was observed to be within a range of 200μ to 600μ resulting in a greater retention of residual gases within the sieve layer. This in turn lowers plate capacity since lesser quantities of gas are removed before reaching equilibrium.

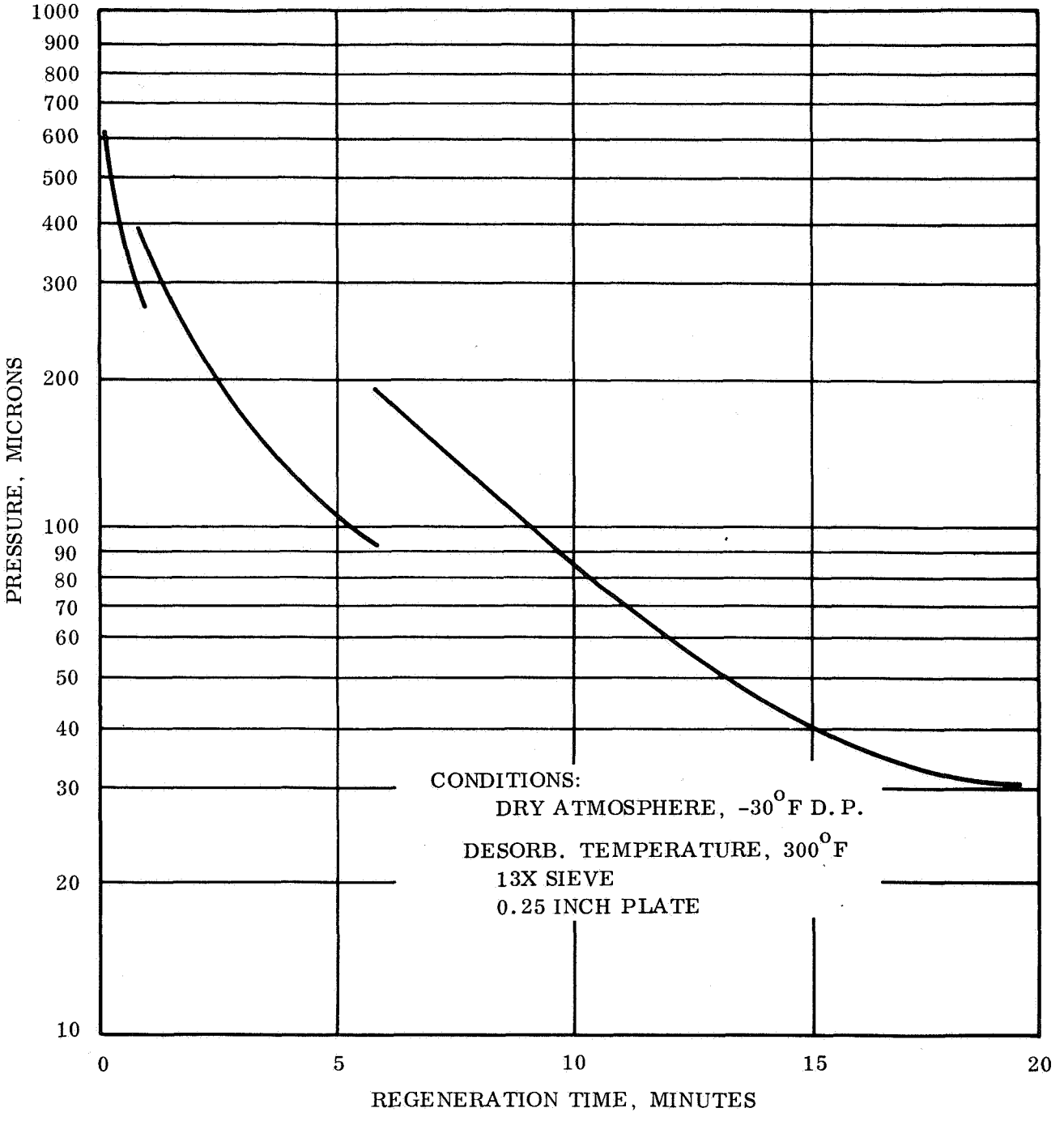

Figure 24. Pressure Decay During CO_2 Desorption, 1/4 inch Plate

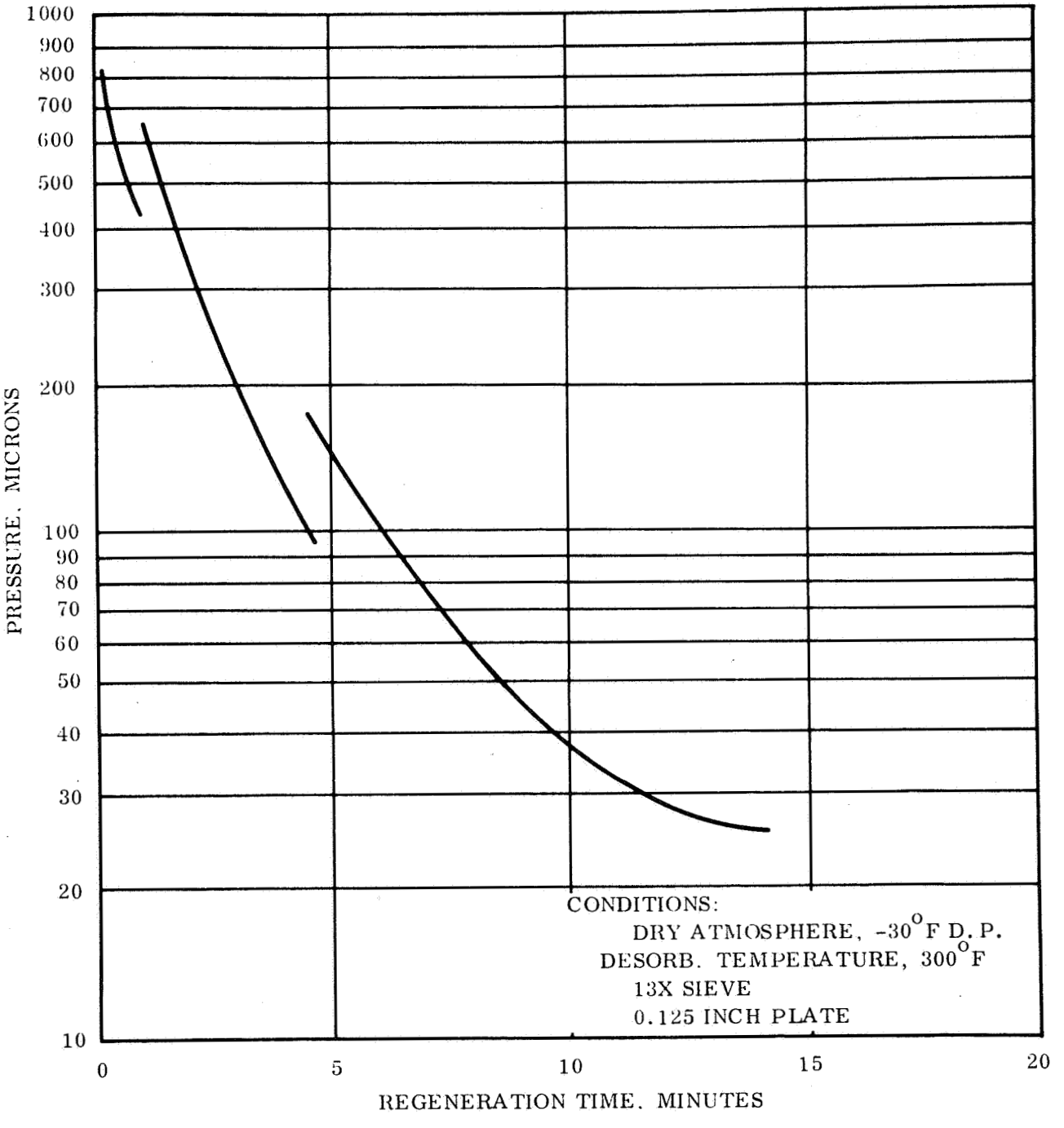

Figure 25. Pressure Decay During CO_2 Desorption, 1/8 inch Plate

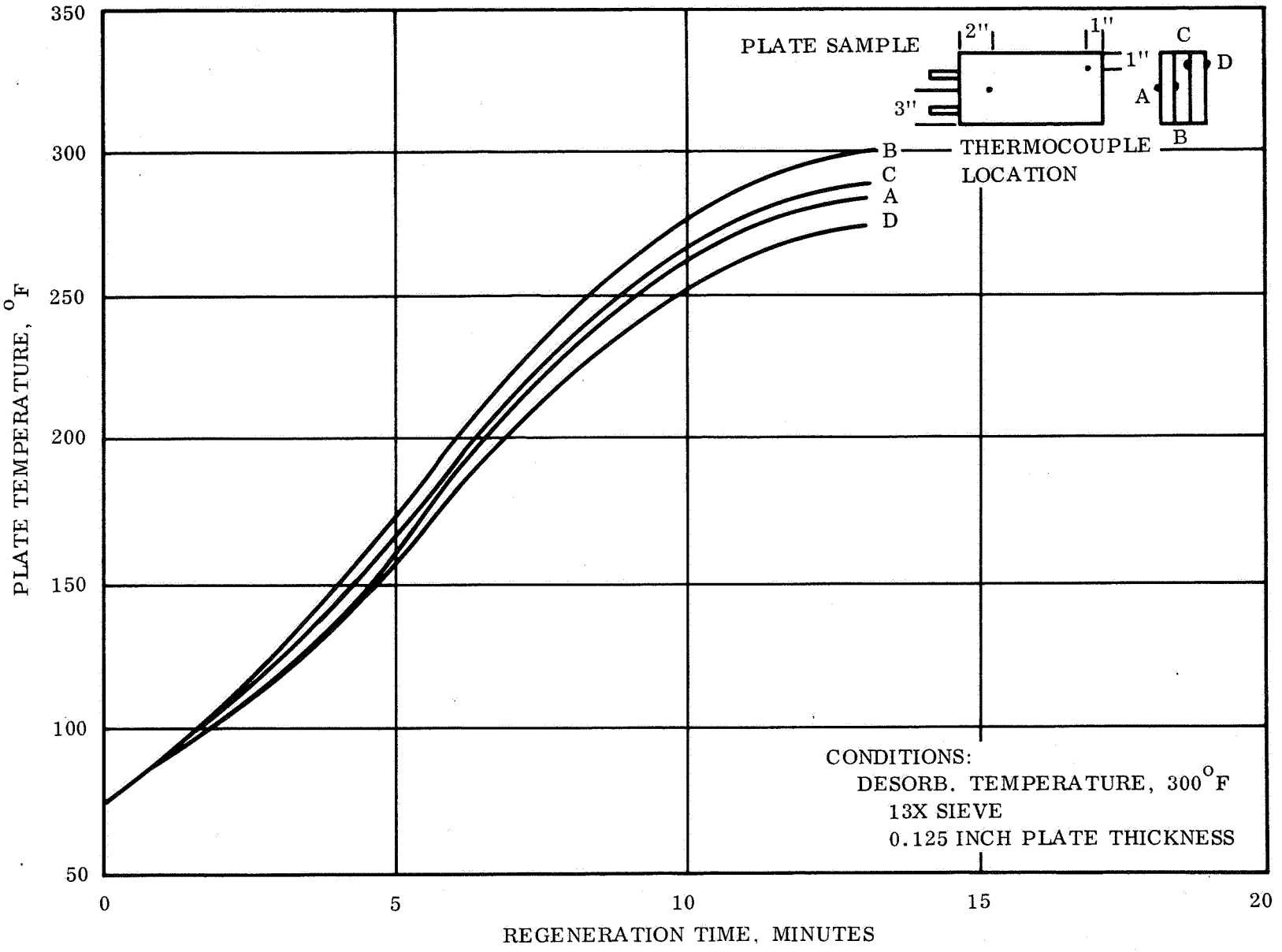

Figure 26. Plate Temperature History During Regeneration

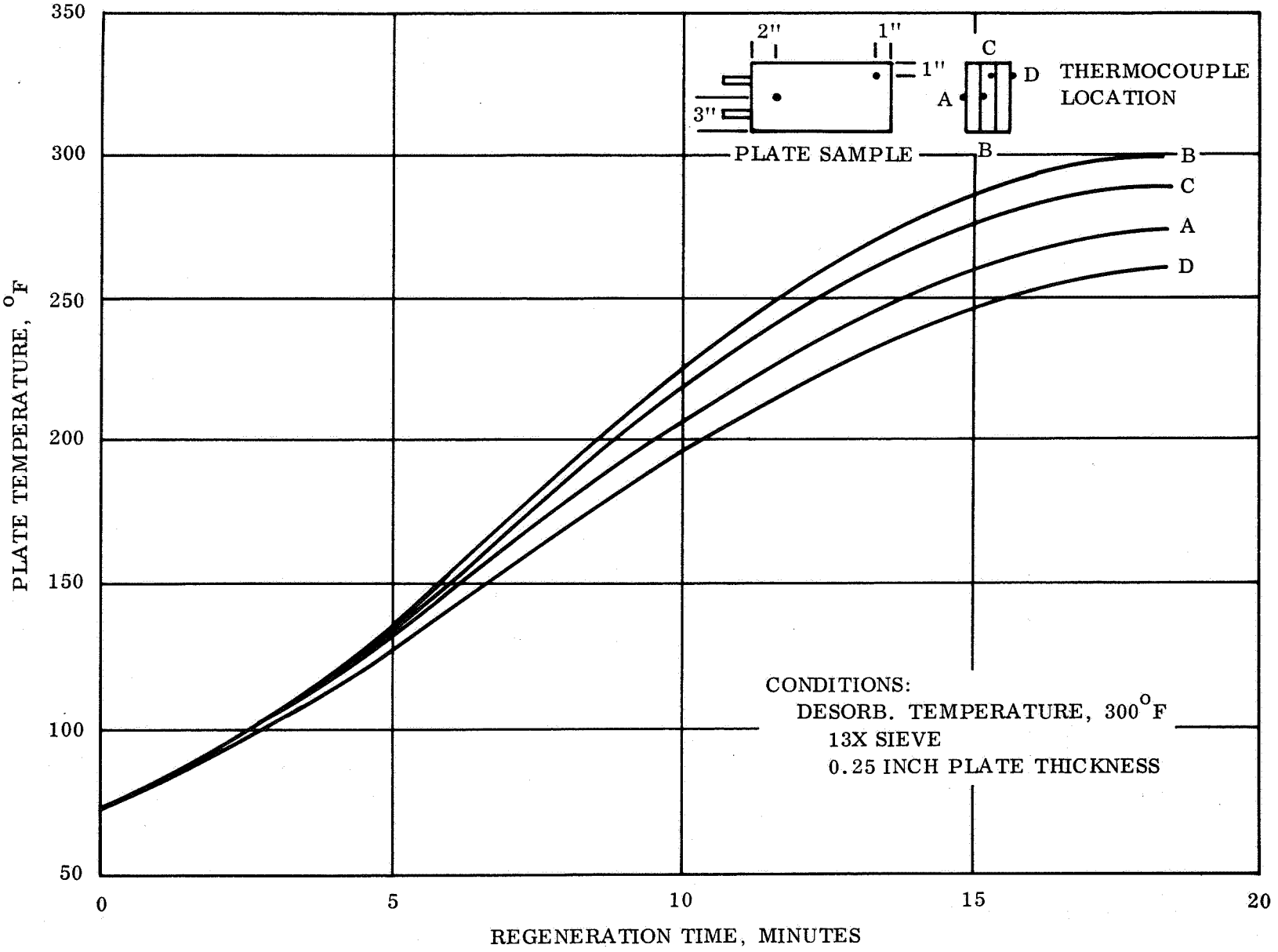

Figure 27. Plate Temperature History During Regeneration

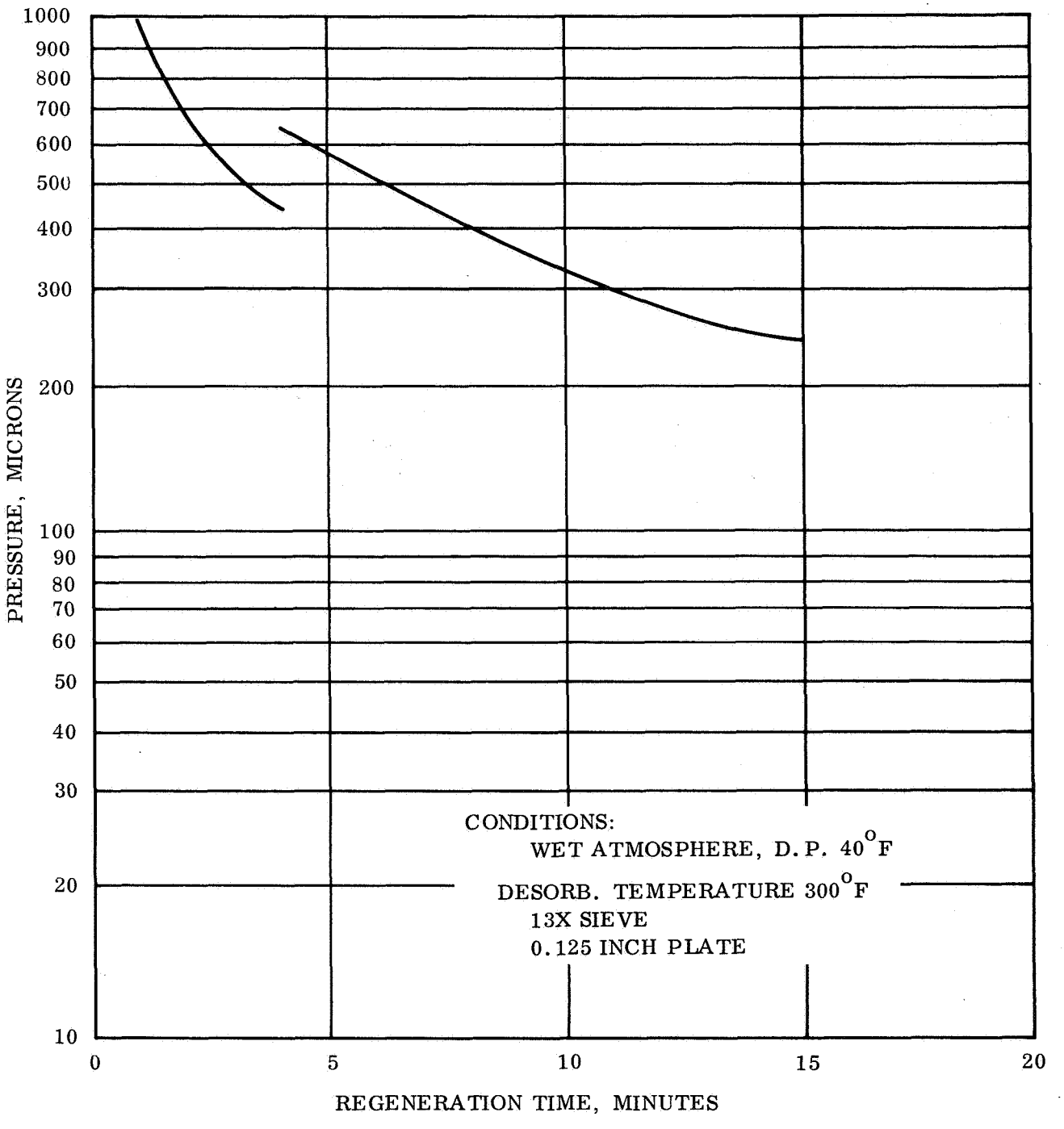

Figure 28. Pressure Decay During CO_2 Desorption

In order to investigate desorption properties of the plates at a lower temperature, several tests were performed at a regeneration temperature of 150°F. Figure 29 summarizes the results for regenerations of 1/8-inch and 1/4-inch sieve thickness where CO_2 desorption and CO_2/H_2O co-desorption take place. As expected the thinner plates heated more rapidly and desorbed more rapidly than the thicker ones. The presence of water vapor does not appear to affect significantly the time required to reach equilibrium, however, the minimum pressure reached during regeneration is noticeably raised when water is being desorbed. This is due to a loading of the vacuum system with water vapor during desorption. Comparison of total cycle times required for desorption of 1/8-inch plates were observed to decrease from approximately 35 minutes at 300°F to about 22 minutes for the 150°F temperature. A similar comparison for 1/4-inch plates shows the total cycle time to be 45 minutes at 300°F and about 32 minutes at 150°F.

Figure 30 shows a series of eight vacuum desorption tests which were performed under the general test conditions listed in table 26. To give a common basis for evaluation, a time required to remove 90 percent of the CO_2 gas during desorption is measured. These values for each test are listed in the final columns, "Desorption time". Water loading on the plates was less than 0.01-lb H_2O/lb adsorbent during the test. Again plate thickness is seen to be a significant factor during desorption with the thicker sieve layers requiring longer time periods. The 1/8-inch plates averaged less than 6 minutes per desorption and the 1/4-inch plates about 12 minutes.

A comparison can be made with vacuum regeneration for a pelletized bed contained in reference 3 (see table 27). The data is for Linde 5A molecular sieve pellets. The average desorption time was found to be more than 20 minutes, showing that pelletized adsorbents require longer regeneration cycles than the plates. This is due primarily to the longer path lengths traversed by an individual gas molecule moving through the pellet bed. On the other hand, the maximum path length traveled by gas molecules in the solid layer adsorbent is limited only by the thickness of the layer itself which for the table 26 tests is a maximum of 1/4-inch.

A second parameter affecting the desorption time is the amount of CO_2 on the plate at the beginning of the regeneration cycle. The CO_2 loading for the table 26 tests varied from 0.026 to 0.084-lbs/lb sieve which was a somewhat higher range than the 0.0037 to 0.062 lb/lb sieve reported for the pelletized sieve in table 27. Using table 26, a comparison of desorption times as a function of plate loading can be made by comparing tests no. 36 and no. 37. The ratio of the initial loadings is 0.033 to 0.026 = 1.27 while a ratio of the desorption times is 5.5 to 4.5 = 1.22, indicating that initial loading is directly proportional to desorption time.

The effect of plate thickness on desorption time is illustrated by comparison of tests no. 37 and no. 40. These tests have nearly the same initial loading, 0.026 vs 0.027-lb CO_2/lb sieve. The desorption time ratio was found to be 4.5 to 9.5 = 0.474

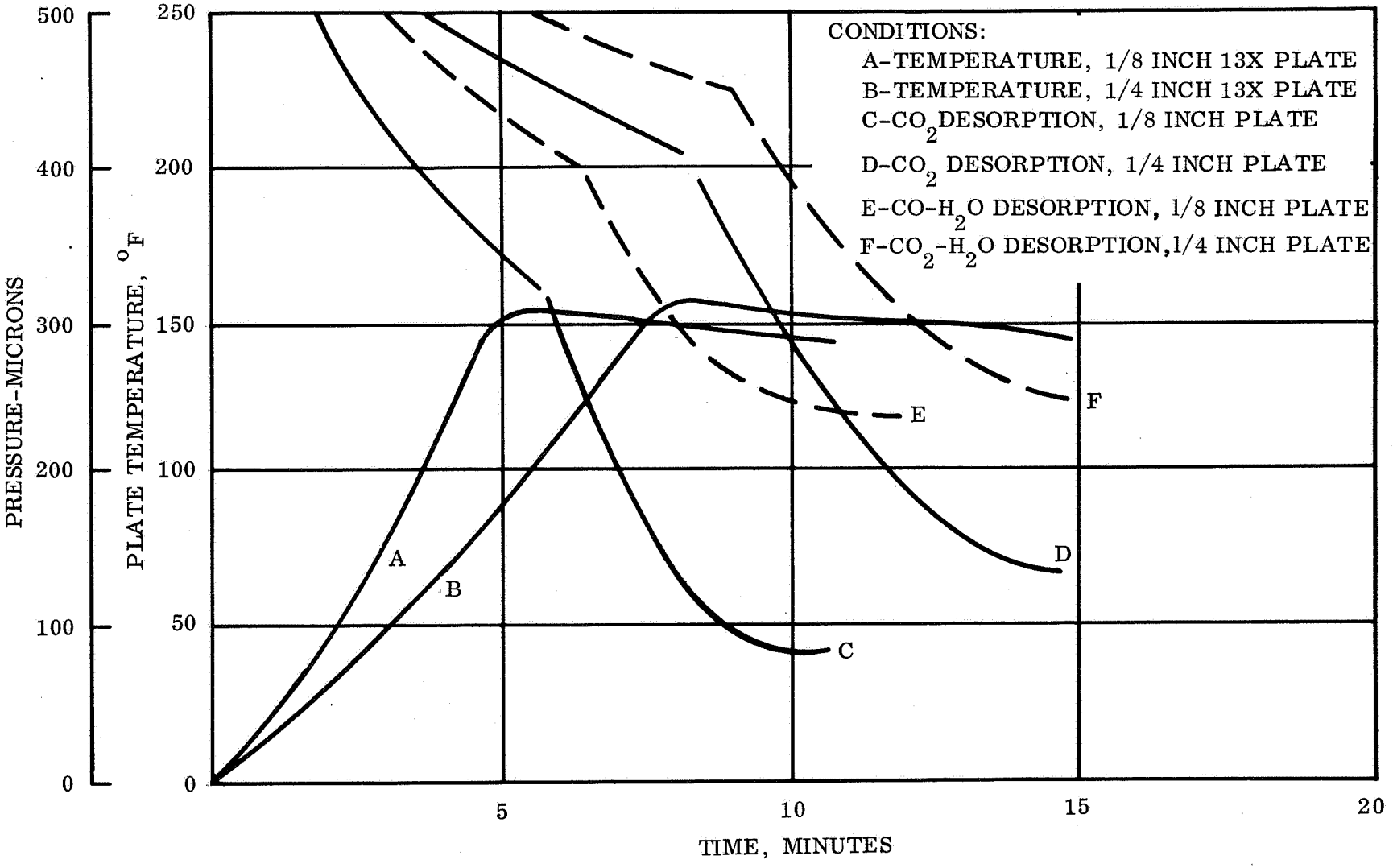

Figure 29. Desorption Characteristics of 1/8" and 1/4" Plates at 150°F Regeneration Temperature

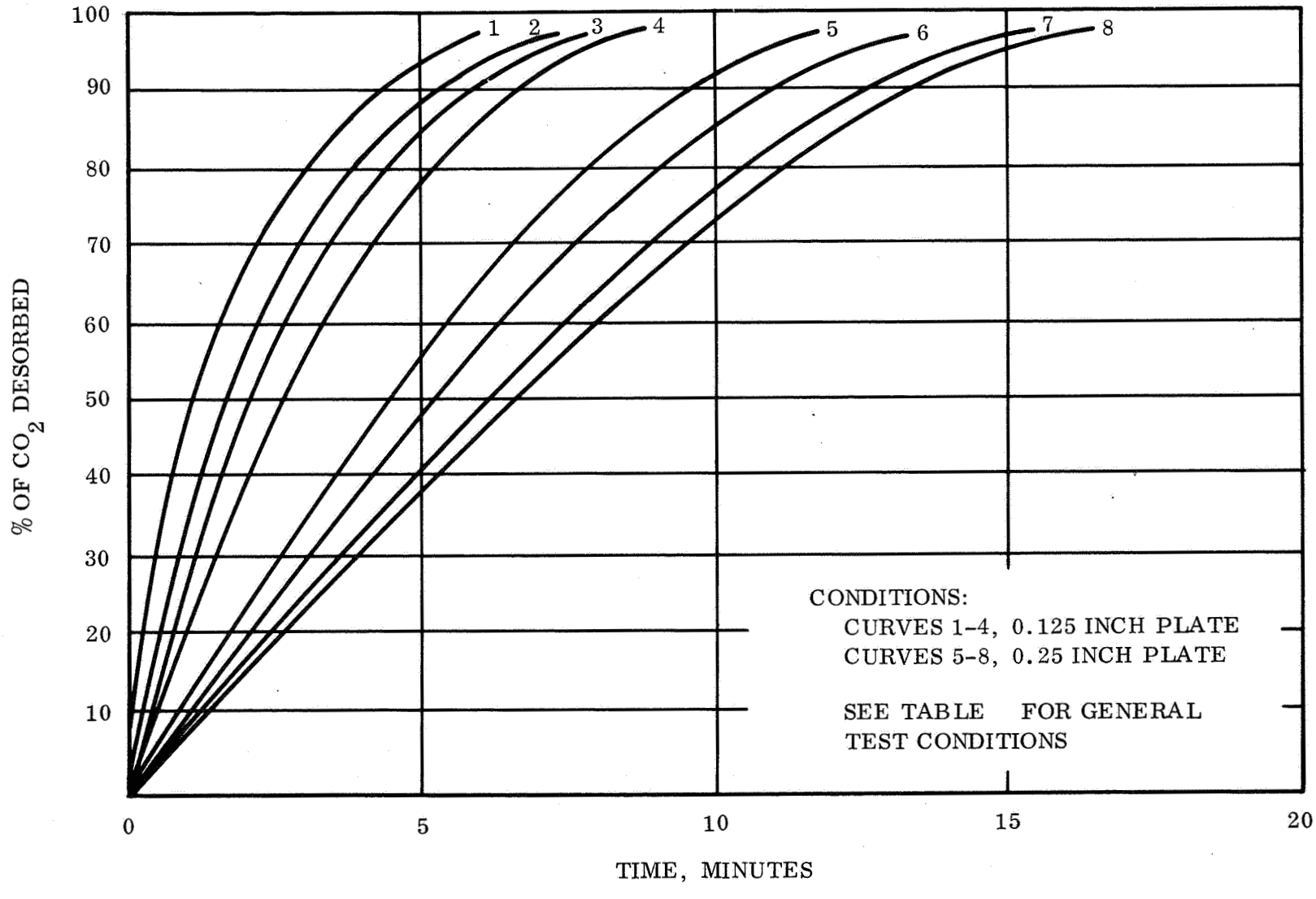

Figure 30. Vacuum Desorption of CO_2 from 13X Sieve ($72^{o}F$)

TABLE 26.

VACUUM DESORPTION CHARACTERISTICS OF CO_2 FROM 13X SIEVE

Test no.	Plate thick, in.	Temp. desorb, ^oF	Initial loading lb CO^2/lb	Final loading lb CO^2/lb	Final press, micron	Desorb time min. (a)	Curve no.
36	0.125	72	0.033	<0.005	20	5.5	2
37	0.125	72	0.026	<0.005	25	4.5	1
38	0.125	72	0.052	<0.005	20	6.0	3
39	0.125	72	0.066	<0.005	30	7.0	4
40	0.25	72	0.027	<0.005	30	9.5	5
41	0.25	72	0.084	<0.005	50	14.0	8
42	0.25	72	0.0685	<0.005	40	13.0	7
43	0.25	72	0.054	<0.005	30	11.5	6

(a) Time required to desorb 90% of total CO_2 on the plate.

TABLE 27

VACUUM DESORPTION OF 5A MOLECULAR SIEVE PELLETS

Run no.	Initial CO_2 LDG, lb CO_2/lb sieve	Final CO_2 LDG, lb CO_2/lb sieve	% CO_2 removed	Pellet size, dia. in.	Desorption time min
1	0.062	0.007	88.9	1/16	30
8b	0.025	0.007	72.0	1/16	25
9c	0.010	0.0055	45.0	1/16	13
11d	0.007	.0037	47.2	1/8	13

a) Data taken from reference 3 for desorption at 77°F.

b) Desorption times are times required to remove listed percentage of CO_2.

which compares closely with the plate layer thickness ratio of 0.125 to 0.25 = 0.5 and indicates that desorption time is also directly proportional to layer thickness.

Effect of Cycling on Plate Performance

The method chosen to determine the effect of cycling on plate performance was to compare plate equilibrium loadings at several intervals throughout the testing sequence. Figure 31 shows the change in performance of the plates as a result of cycling. The plate chosen for analysis is the 1/8-inch plate coated with 13X molecular sieve. This particular plate was exposed to 51 cycles during the test program, greater than any other plate specimen and should give the best indication of cyclic effects.

Decay tests were performed after test no. 51 and test no. 108. At these points the plate had a total of 32 cycles and 51 cycles on it respectively. The decay test was performed in the following manner. The system was loaded to approximately 18 mm Hg CO_2 partial pressure. CO_2 flow was terminated and the plate was allowed to remove CO_2 continuously from the system until equilibrium was attained. Knowing the difference in the CO_2 partial pressure between the beginning and end of the test and the void volume of the system (9.9 ft^3), the amount of CO_2 adsorbed by the plate was calculated by using the perfect gas laws. The calculated equilibrium loading for the plate under these conditions was 0.031-lbs CO_2/lb sieve at 2.6 mm and 0.033-lbs CO_2/lb sieve at 3.0 mm pressure. The points when plotted in figure 31 shows a relatively small change (less than 10 percent) over the 51 cycle period.

Comparison of 5A and 13X Adsorbents

Figure 32 shows a comparison of 5A and 13X sieve adsorbents for the same operating conditions. As can be seen from the curves the 13X gives an initially higher rate with the difference in removal rates diminishing as the test progresses. The 5A sieve according to Linde data and verified by the equilibrium tests, has a greater CO_2 loading capacity than 13X. This would indicate that the CO_2 removal rate for the 5A sieve would not decrease as rapidly as for the 13X, a fact which is substantiated by the lesser slope of the 5A curve. The difference in the initial rates is most probably explained by adsorbent poisoning.

Immediately prior to test no. 21 on the 5A sieve, the blower motor windings were burnt out. The resultant combustion products actually permeated the sieve plate before it could be isolated from the system. The plate was removed from the canister for inspection where a noticeable discoloration of the plate surface was noted. The surface was sanded lightly with emery paper to remove as much of the contaminant layer as possible and a prolonged regeneration of 4 hours at 350°F was also performed to rid the plate of any deep-seated contamination. As evidenced by the decreased removal rates in subsequent testing some trace "poisioning" was still present.

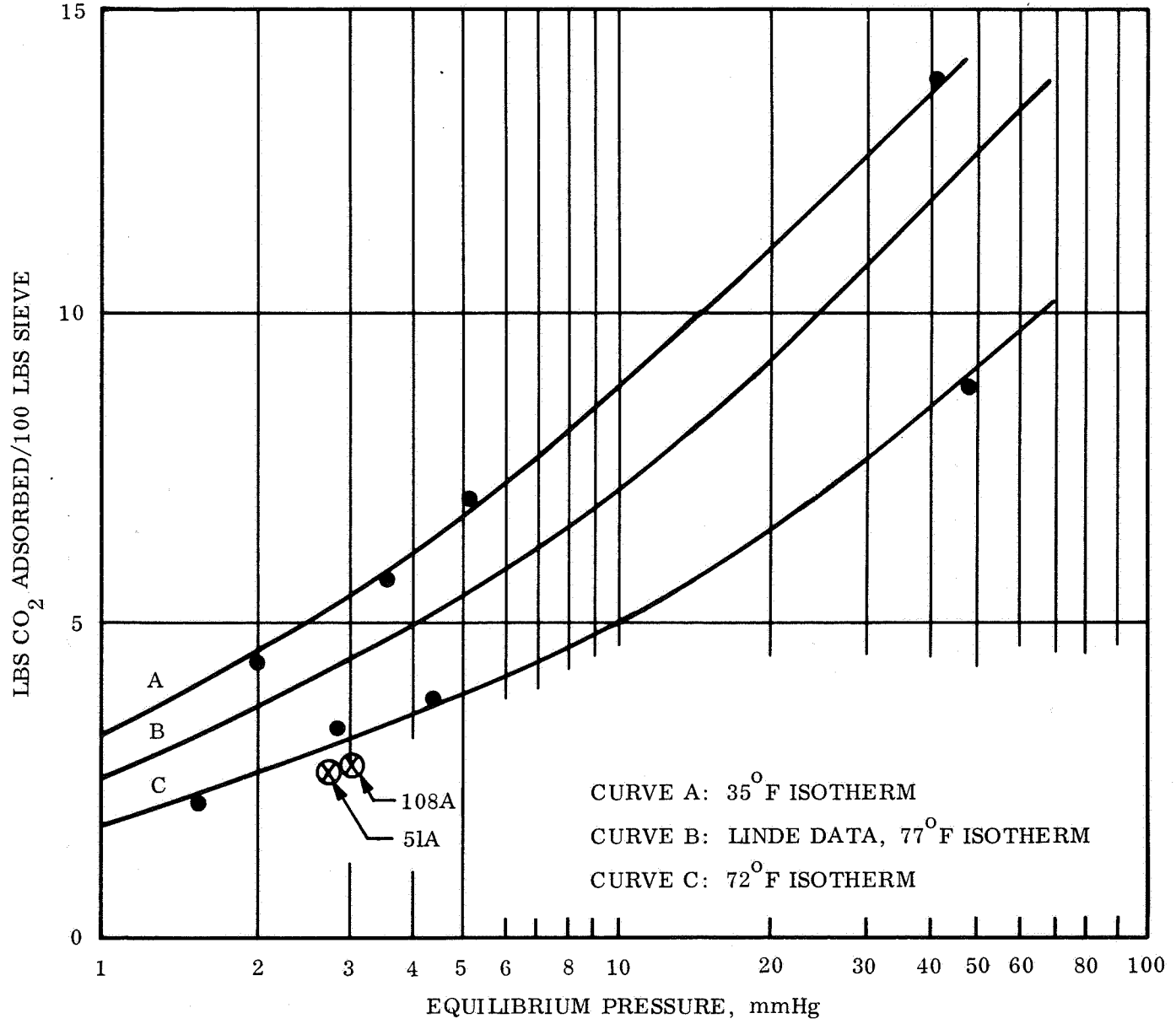

Figure 31. CO_2 Equilibrium Loading on 13X Sieve

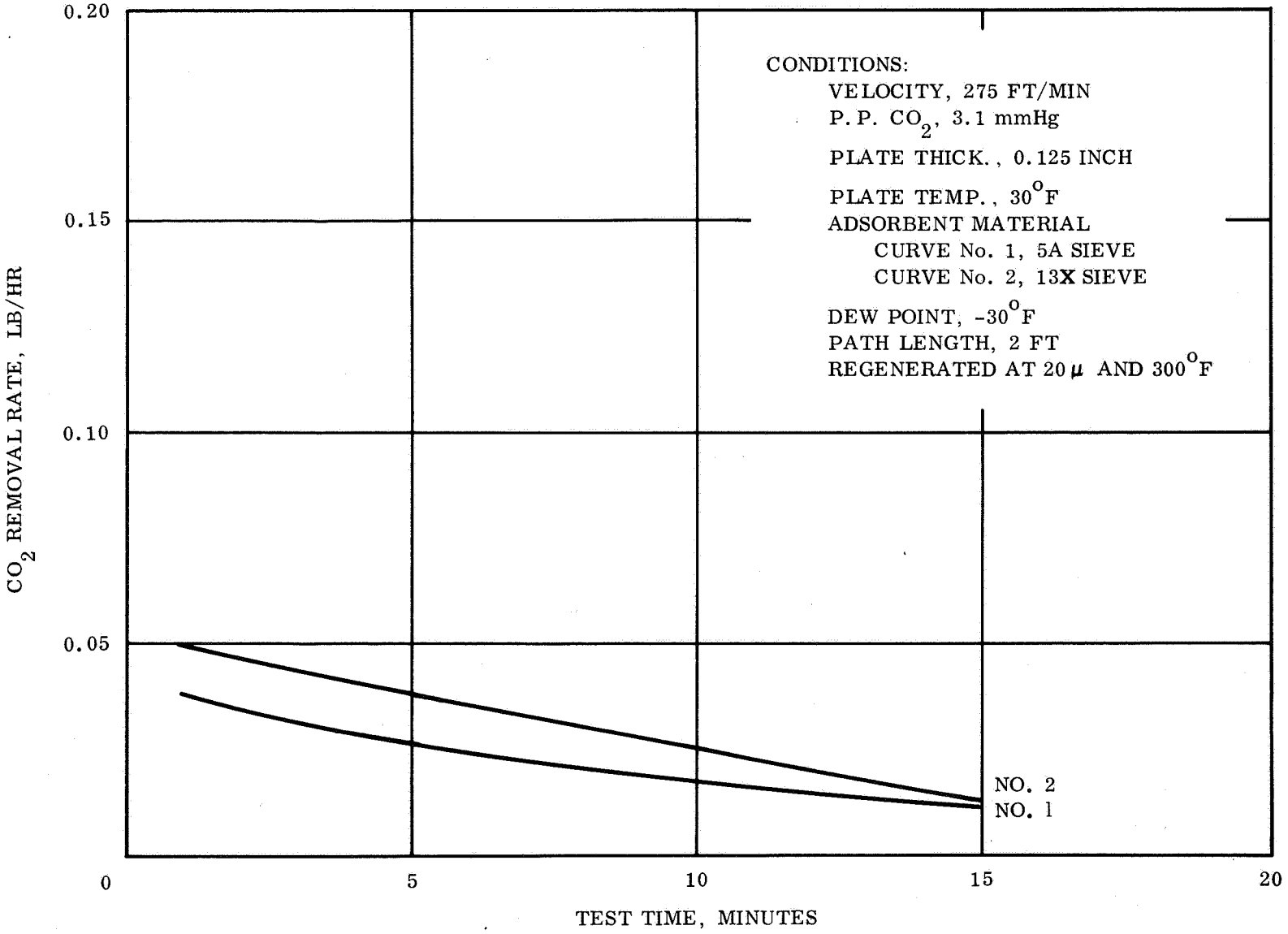

Figure 32. CO_2 Adsorption Rates for 5A and 13X Plate Samples

Only one series of CO_2 adsorption tests were run on the 5A as a result and no coadsorption tests of H_2O and CO_2 were performed. Before eliminating entirely the use of 5A, further analysis would seem to be in order.

CO_2 Recovery Tests

A series of tests was performed to investigate the recovery of the CO_2 regenerated from the plate. The flow setup for the adsorption cycle is the same as used for the previous tests. The modifications for the regenerating cycle consisted of the removal of the large vacuum pumping system from the apparatus and the addition of two diaphragm pumps in series. The lowest pressure which the pumps were capable of attaining during regeneration was between 30 and 50 mm Hg. With reference to table 21, it can be seen that as anticipated desorption temperature appears to have the greatest affect on the CO_2 removal rate.

The CO_2 recovery tests also provided a direct means of observing the effect of regeneration pressure on CO_2 adsorption rate. Tests 92 and 100 were regenerated at pressures of 25 microns and 50 mm Hg respectively. The lower removal rate for test 100 regenerated at the higher pressure level (50 mm) is evident. A better indication of CO_2 recovery system performance is to compare the total amount of CO_2 adsorbed in a ten minute period. The values, taken from tables 19 and 21 are found to be 0.0116-lbs CO_2 for test no. 92 and 0.0083-lbs CO_2 for test no. 100. This would indicate that approximately 30 percent less plate surface area and sieve weight are required for the plate regenerated at the lower pressure.

A typical regeneration cycle is shown in figure 33. The time to reach equilibrium is equivalent to that realized for the larger vacuum pump system (see figure 25) which would appear to indicate that desorption time is more a function of the rate at which energy is added to the plate during regeneration rather than the properties of the pumping system.

Coadsorption

Tables 15A and 15B show a series of 16 tests (block 5) performed at a constant inlet dewpoint of $+40^{\circ}F$. The four variables investigated were velocity, pp CO_2, plate thickness and regeneration temperature. The tests regenerated at $300^{\circ}F$ are listed in table 15A and those regenerated at $150^{\circ}F$ are listed in table 15B. A comparison of initial adsorption rates for velocities of 200 and 375-ft/min shows the rates to be less at the lower velocities (except for test no. 72 and no. 73 where the rates differ by 0.002-lb/hr.). These observations agree with the previous discussion on CO_2 adsorption in a dry ($-30^{\circ}F$ dewpoint) environment which also showed adsorption rates to increase with increasing velocity. A theoretical prediction of CO_2 and H_2O adsorption rates was not made for the coadsorption tests since a rigorous model for diffusion of two gases in a third non-diffusing gas could not be formulated.

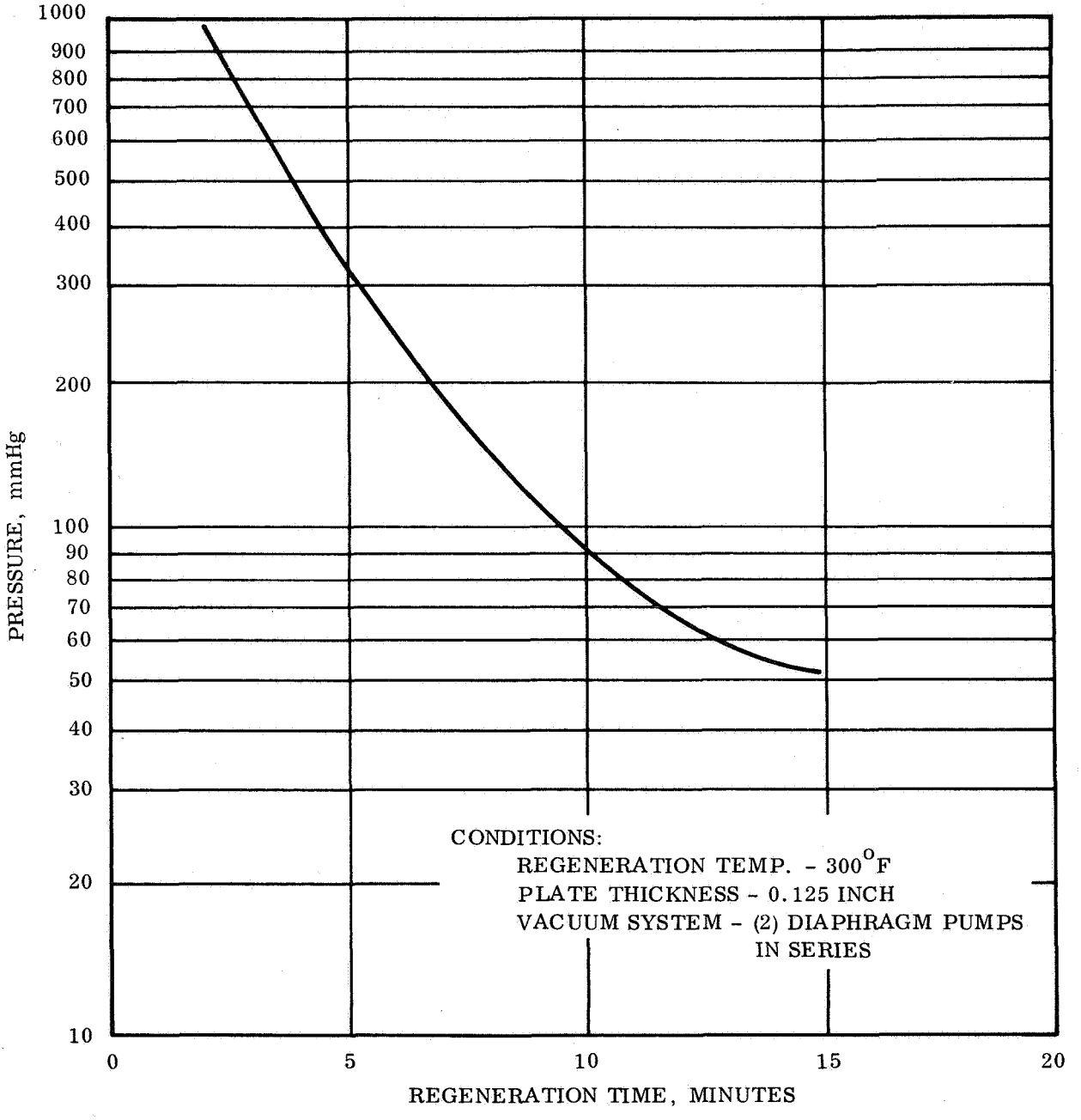

Figure 33. Regeneration Characteristics - CO_2 Recovery System

The effect of partial pressure was determined by measuring the difference in CO_2 adsorption rates at 4.0 and 7.6 mm Hg. The tests at the higher partial pressure also showed the higher adsorption rates. For example, tests no. 68 and no. 70 had a partial pressure ratio of 7.6 to 4.0 = 1.9. The adsorption rates differed by 0.44 to 0.42 = 1.05 which shows that during coadsorption, CO_2 removal rates are not directly proportional to partial pressure. This is due to the inhibiting effect of water vapor in the system.

The effect of plate thickness on adsorption rates gave varying results. Comparison of tests no. 68 and no. 72 (at 4.0 mm Hg) show adsorption rates to be greater for the 1/8-inch plate. Comparison of tests no. 70 and no. 74 (at 7.6 mm Hg) show the 1/4-inch plate to give the higher adsorption rates, thus indicating the probability of an interaction between partial pressure, plate thickness, and degree of regeneration. One possibility is that a higher initial CO_2 partial pressure gives higher CO_2 adsorption rates which would cause the plate loading (i.e., lb CO_2/lb adsorbent) to increase at a faster rate than for the thicker plates. This results in a decreased CO_2 pressure gradient across the film and thus a lower measured adsorption rate for the 1/8-inch plate as the test progresses. The same circumstance could result for an incompletely regenerated panel.

The effect of regeneration temperature is shown by comparison between tests no. 68, table 15A and no. 76, table 15B. The lower temperature of 150°F results in lower adsorption rates caused by the greater residual amounts of H_2O and CO_2 remaining on the plate after regeneration. The water loading after regeneration was estimated from Linde data to be 0.06-lb H_2O/lb sieve at 300°F and 0.10-lb-H_2O/lb sieve at 150°F. The residual CO_2 was estimated from Linde data to be 0.01-lbs CO_2/lb sieve at 300°F and 0.02-lbs CO_2/lb sieve at 150°F.

From an operational standpoint, the coadsorption of CO_2 and water results in weight and volume penalties. This can be shown by comparing the operation of the plates in tests no. 94 and no. 97 (tables 19 and 17) which show that one 6" x 12" plate in a dry atmosphere (-30°F inlet dewpoint) gives the same performance as two plates in a mosit (40°F inlet dewpoint) environment. The effect of inlet dewpoint on performance can be explained by figure 34 which shows the H_2O vapor pressure in the inlet process gas as a function of dewpoint. From the curve, it can be seen that the H_2O vapor pressure in inlet gas increases slowly with dewpoint up to approximately 0°F where the changes become more rapid.

One other reason for the low CO_2 adsorption during the 40°F dewpoint tests can be explained by the conditions during regeneration. The lowest pressure achieved during desorption of the "wet" plates was 200 μ, absolute due to loading of the vacuum pump. As previously noted, the residual moisture was estimated to be 0.06-lb H_2O/lb sieve. Such a high water content would tend to inhibit CO_2 adsorption and account for the lower observed CO_2 adsorption rates. The best method for increasing the CO_2 adsorption would appear to be an improvement in the vacuum pumping system during

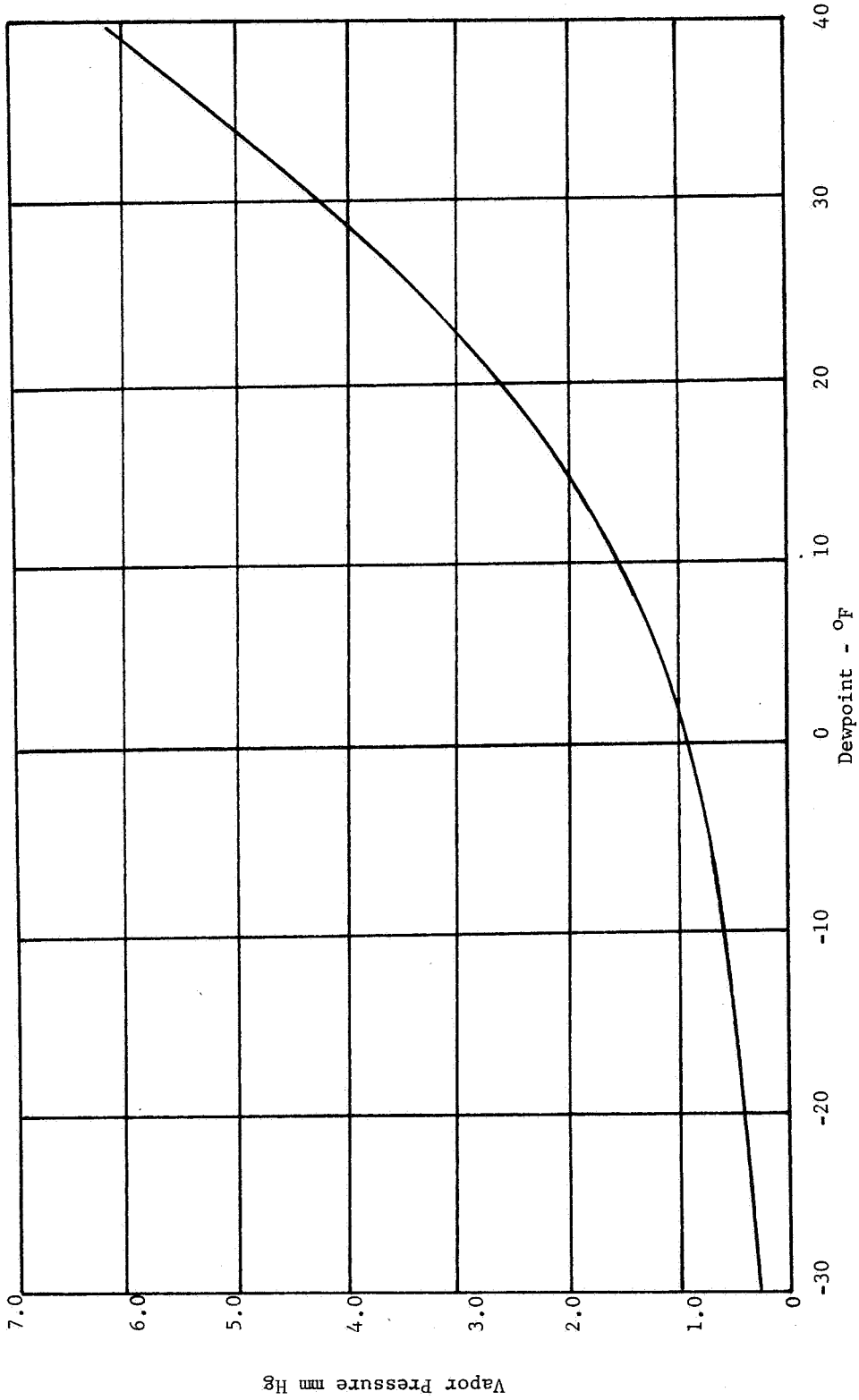

Figure 34. Water Vapor Pressure vs. Dewpoint

regeneration. Inclusion of a cold trap in the vacuum lines would freeze out the water vapor as it was pulled off of the plate. This would permit the pump to reach a lower system pressure thereby achieving a lower water loading on the plate.

The basic conclusion reached during the coadsorption tests was that the $40^{o}F$ inlet dewpoint effectively doubles the amount of plate surface area required to maintain the same CO_2 removal rate on a plate exposed to a $-30^{o}F$ dewpoint.

Table 28 is a summary of the coadsorption tests previously discussed. The tests were chosen at a partial pressure of 4.0 mm to approximate actual operating conditions. The regeneration conditions of $300^{o}F$ and 200μ, also approximate the heat and vacuum sources available in a typical space environment. These tests will be used in a later section as a basis for sizing a plate adsorber canister.

TABLE 28

COADSORPTION OF CO_2 AND H_2O ON 13X MOLECULAR SIEVE

	Variables			Weight of CO_2 and water coadsorbed			
				t = 10 minutes		t = 15 minutes	
Run no.	Velocity, ft/min	Plate thickness, inches	Path length, ft.	Wgt. CO_2, lbsx10^3	Wgt. H_2O, lbsx10^3	Wgt. CO_2, lbsx10^3	Wgt. H_2O lbsx10^3
68	375	0.125	2	5.81	7.64	7.12	11.6
69	200	0.125	2	4.64	6.47	5.28	10.0
72	375	0.25	2	3.85	7.96	4.33	12.3
73	200	0.25	2	3.81	5.91	4.27	9.0
97	200	*	4	6.48	14.0	7.80	24.1
98	375	*	4	6.9	12.7	8.47	21.0

Constants: P. P CO_2, 4 mmHg

Regeneration at 300°F and 200

Inlet Dew point, 40°F

* One 0.125" plate and one 0.25" plate connected in series to obtain 4 ft path length.

DESIGN CRITERIA

Preceeding sections of this report have presented details pertinent to the test program design and performance, and the techniques and results of data analysis. In this section, the results will be re-evaluated to present the same information in the form of preliminary design criteria. The data presented shall be extracted from the body of data in the preceeding sections to summarize the more positive results of the program, i.e., performance obviously not applicable to typical spacecraft CO_2 control systems will not be repeated here.

The characteristics of primary interest in establishing design criteria may be generally defined into two functional categories; namely, those concerned with the adsorption phase, and those primarily pertaining to the desorption or regeneration phase of an operational cycle. It is to be recognized however, that in actuality these functional phases are not separable, their being important interactions between the two which greatly affect overall performance. The following discussion will, for organizational purposes, discuss each phase separately noting areas of interaction as they occur.

Guidelines

Prior to formulation of CO_2 adsorber design criteria the basic performance guidelines for spacecraft systems must be considered. The spacecraft design parameters and their anticipated ranges are tabulated in table 29. The adsorber system design criteria as developed are formulated within the framework imposed by the anticipated spacecraft system design parameters.

Adsorption Cycle

Formulation of design criteria for the adsorption phase of the cycle requires that relationships between adsorber size and CO_2 production rates (or removal rates); and size and adsorber panel capacity be determined. Sizing characteristics of the panels tested can be expressed in two ways, that is,

(1) pounds of CO_2/pound of sieve (loading)

(2) pounds of CO_2/unit time (rate)

As previously indicated loading is primarily an equilibrium characteristic which is a function of adsorption temperature and CO_2 partial pressure. Selection of these operating levels then dictates the loading characteristic. For purposes of establishing system design criteria the levels selected are a pCO_2 of 4.0 mm Hg and an adsorber temperature of 70^o to 75^oF.

TABLE 29

TYPICAL SPACECRAFT PERFORMANCE GUIDELINES

Mission duration	30-200 days
Cabin atmosphere ambient temperature	65-85°F
Cabin atmosphere ambient pressure	300-760 mm Hg
Cabin atmosphere pO_2	160-180 mm Hg
Cabin atmosphere pCO_2	3-12 mm Hg
Cabin atmosphere pH_2O	5-15 mm Hg
Cabin volume	100-200 ft^3/man
Carbon dioxide production rate	2.3 lb/man/day
Crew size	2-6 men
Waste heat temperature	350°F (max.)
Process air temperature	45-49°F
Process air dewpoint	40-44°F
Waste heat penalty	0.1 lb/Btu/hr

The weight of sieve required for a given cycle time has been defined by the loading characteristics. As noted in the data, the 1/8 inch thick test panels were regenerated more readily than the 1/4 inch panels (as evidenced by the greater quantities of CO_2 adsorbed by the thinner panels). For a 1/8 inch thick plate the approximate sieve loading is 0.65 pounds of 13X per square foot of panel.

The rate of CO_2 removal for the adsorber panel system is dependant upon the area of sieve exposed and the velocity of process gas over the sieve. It is useful then to express the rate of adsorption as pounds of CO_2/hour/ft^2 thus permitting a direct computation of the area required for any given CO_2 removal rate.

The curves shown in figure 35 are a summary of the relationship noted between velocity and adsorption rates. Data are plotted for both coadsorption (water vapor and carbon dioxide) and straight CO_2 adsorption at an inlet pCO_2 of 4.0 mm Hg, and 7.6 mm Hg.

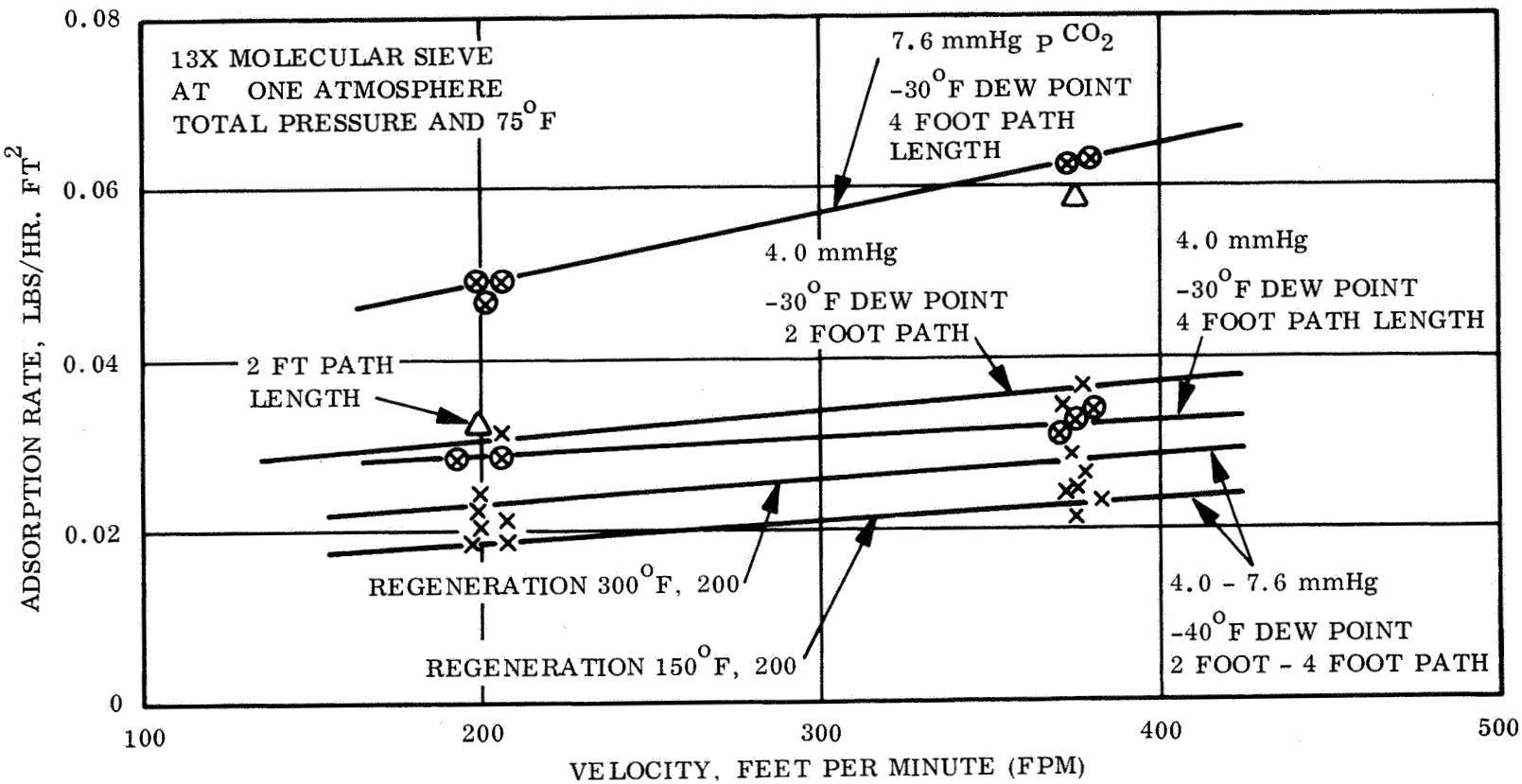

Figure 35. Relationship Between Observed Adsorption Rates and Velocity at Various Operating Levels (Blocks 5, 7, 8)

In the coadsorption mode the high dewpoint as previously indicated is the dominant factor in setting the performance of the panels. There is still however, an increase in CO_2 adsorption rate with an increase in velocity (from approximately 0.022 lbs/hr/ft^2 at 200 FPM to 0.025 lbs/hr/ft^2 at 375 FPM). The panel criteria are thus established nominally as:

4.4 square feet/man at 200 fpm

3.8 square feet/man at 375 fpm

From the adsorption efficiencies presented in the tables (ranging from 7 to 14 percent CO_2 removed per pass) and the minimum flow rates required to move 2.3 pounds of CO_2 per man day (as shown in figure 36) the panel spacing for a system is also determined. Since adsorption rates are a function of velocity and area exposed (not path length) then the adsorber can be designed for minimum volume, minimum weight rather than for any specific path length.

Desorption Cycle

Adsorber panels were regenerated at 150° and 300°F and concurrently exposed to pressure levels of 20-200 microns and 30 to 50 mm Hg in order to determine the resulting regeneration characteristics (as evidenced by the subsequent adsorption performance). Since these criteria are concentrating on a coadsorption system it should be noted here that regeneration at 150°F and 200 micron reduces the average adsorption rate by less than 10 percent as shown in figure 35. These data are not conclusive since they represent only a few points but they are consistant with other performance data obtained.

Regeneration of a straight CO_2 adsorption system at 30-50 mm Hg and 150° and 300°F was also performed. The resulting adsorption rates are presented in figure 37 for information and comparison with the coadsorption system performance.

Conclusions

The conclusions to be reached at this point are that sufficient rate and capacity data are available at the present time to establish a design for a 13X molecular sieve, coadsorption system where flow rates, adsorption and desorption temperatures, carbon dioxide partial pressures, desorption pressures, and cycle times can be defined with a reasonable degree of accuracy.

Information on cycle life accumulated during the test program (approximately 100 cycles) indicates that operation as a "panel" does not change the life characteristics. What remains to be seen is the residual loading curve for water in a coadsorption system for operating life in excess of that tested (i.e. more than 50 cycles).

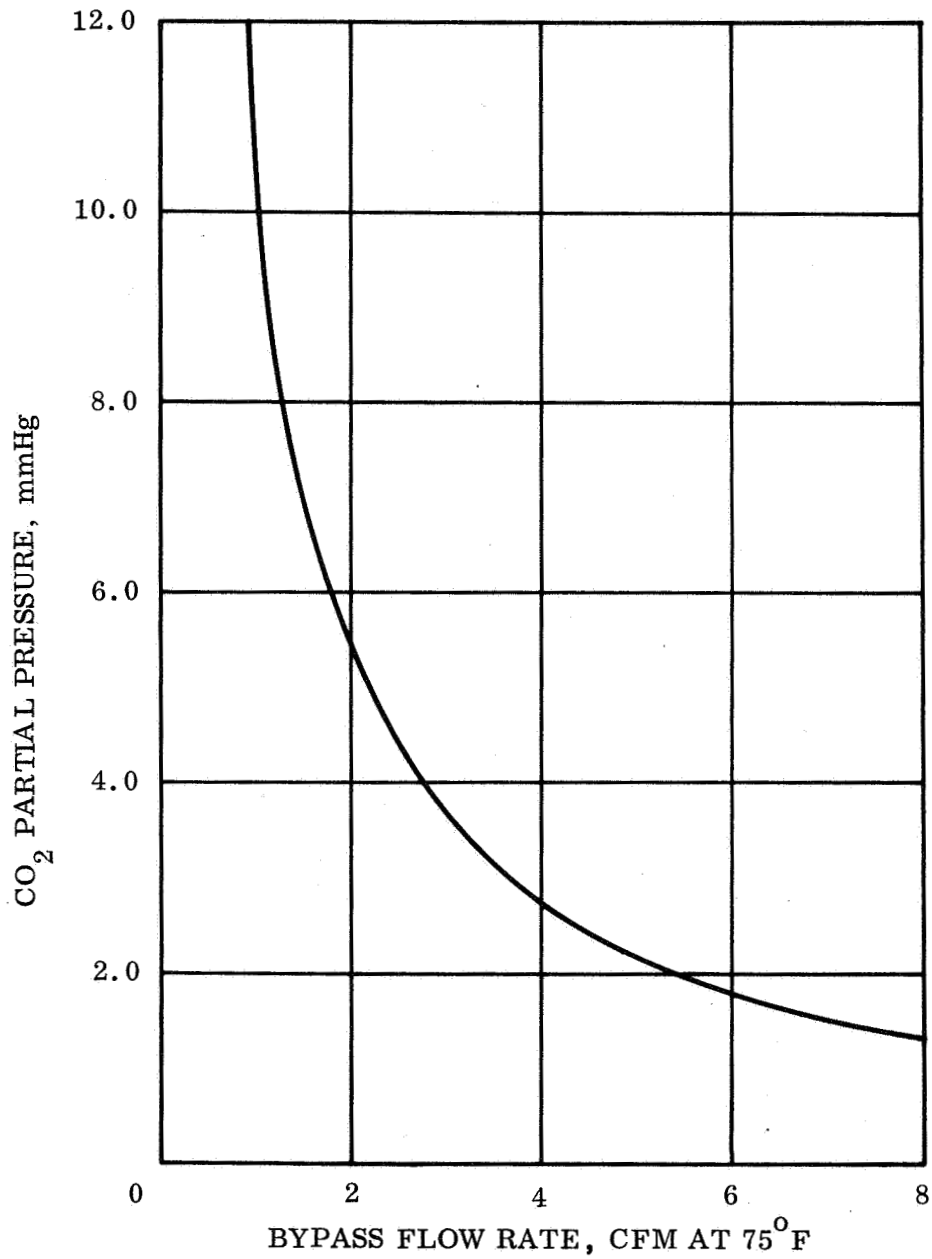

Figure 36. Minimum Flow Rate of Air at 760 mm Hg and 75°F Required to Move 2.3 Pounds of CO_2 Per Day

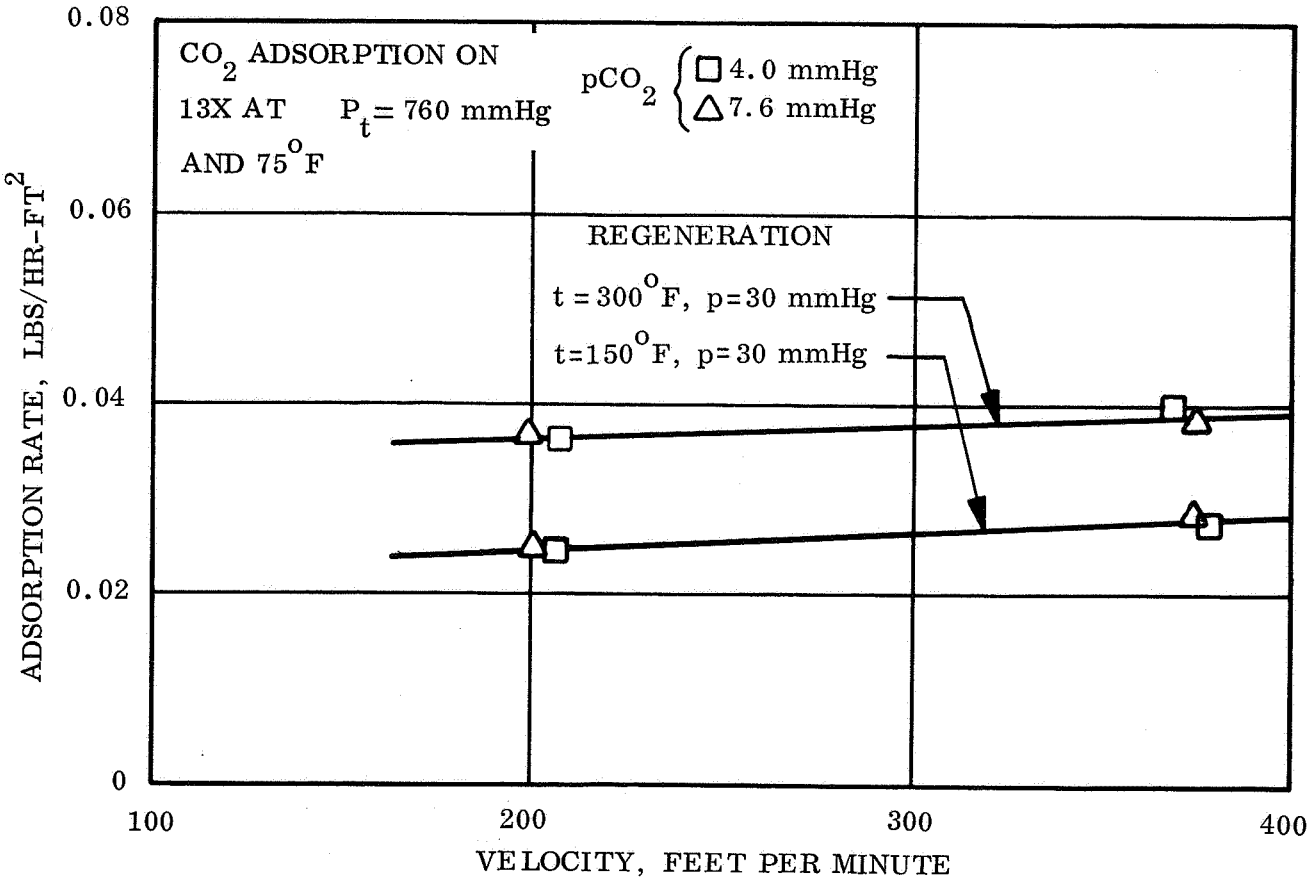

Figure 37. Adsorption Rate as a Function of Velocity at Various Regeneration Temperatures and Pressures (Block 9)

COMPARISON OF RESULTS WITH PACKED COLUMN ADSORBENT SYSTEMS AND RECOMMENDATIONS

In conclusion a tabulation of characteristics is presented in table 30 that compares a thin film adsorbent canister (based upon performance criteria presented herein) with a comparably sized prototype packed column canister. Auxiliary equipment requirements (e.g. valving, structure, and controls) for both concepts is assumed to be equal for a given application. The packed column data was supplied by the contract technical monitor and is for a system that vacuum desorbs both the predryer (silica gel) and the CO_2 adsorbent (5A sieve). Both adsorbents are packed in series within a common canister. Correspondingly thin film coadsorption performance data was utilized for the sizing indicated in the table. Although the ventilating mass flow rate for the thin film concept is higher the water loss penalties as a result of this operating mode (i.e. dumping CO_2 and water vapor to space) are comparable for both systems because of the lower removal efficiency inherent to the thin film concept. A comparison between other characteristics tabulated for the two concepts favor the thin film concept. The weight and volume estimates for the thin film concept are predicated upon an adsorber panel configuration that embodies the design improvements iterated previously. Regeneration temperature for the packed column canister was stated as 120°F. The thin film canister characteristics indicated are based on adsorbent regenerative temperature of 150°F.

Therefore based upon the comparison presented in the table it appears that the thin film concept for regenerable adsorbent applications is worthy of further investigation. A prototype canister should be designed, fabricated and tested to permit verification of the performance capabilities projected by the data. However, it will be necessary to perform additional experimental and design investigation task efforts before the fabrication of a full scale prototype canister can be undertaken. The following is a breakdown of the recommended further areas of investigation:

Design Optimization of Adsorber Panel. - This would include investigations into such areas as:

(1) Alternate porous binder compositions that would permit curing of the zeolite layer at temperatures below 1000°F; this in turn would permit use of lighter substrate materials (e.g. aluminum).

(2) Implementation of honeycomb structures for the retention of the zeolite layer to further improve thermal conduction paths and bond strengths between binder and substrate.

(3) Optimization of the liquid side heat transfer characteristics for the panel assembly by implementation of embossed fluid flow passages that are integral with

the substrate panel. A weight reduction would also be realized by implementation of this "platecoil" configuration.

(4) Reduction of canister weight by instituting minimum weight "flight oriented" seal and structural configurations.

Performance of Additional Experimental Tests:

(1) Coadsorption testing at a lower regeneration temperature (e.g., 120°F). - The thin film canister performance projected in table 30 is extrapolated from 150°F regeneration temperature data since lower regeneration temperature performance is not available directly from existing test program data.

(2) Performance of extended duration cyclic testing (greater than 100 cycles) of 5A sieve as a coadsorber. - As mentioned previously, a test equipment failure (burn out of blower motor windings) resulted in irreversible poisoning of the 5A sieve test panel that terminated prematurely the evaluation of this adsorbent.

(3) Evaluation of Poisoning of Zeolites as a result of Fire. - Fire within a space vehicle is a definite possibility and its effects on operational equipment should be pinpointed. As evidenced by the above mentioned test failure, this area should be explored further to determine in fact fire effects on the adsorber are in fact irreversible.

(4) Design, Fabrication, and Operational Tests on a full scale thin film canister. - Tests to be performed under actual operational conditions including dynamic environment testing to verify structural adequacy of the concept during simulated launch, orbital and re-entry conditions.

TABLE 30

CANISTER CHARACTERISTICS COMPARISON

Characteristic	Thin film concept	Packed column pellet bed
CO_2 removal rate, lbs/hr.	0.3	0.27
Inlet pCO_2, mm Hg	4.0	4.0
1/2 Cycle time, min.	20	40
Sieve wt., lbs.	7.4	3.0
Substrate wt., lbs.	12	---
Canister wt., lbs.	9.5	30
Predryer wt., lbs.	---	11.0
Power weight penalty, lbs.*	3.0	1.0
Air flow rate, lbs./hr.	60.0	10.0
Total canister wt., lbs.	31.9	45.0

* Based upon a power weight penalty of 0.1 lb/watt.

APPENDIX

Equipment List
Instrumentation List

Equipment Photographs

EQUIPMENT LIST

	Nomenclature	Manufacture	Part no.	Size
1.	Rotameter	Brooks	Model 1355	0-840 cc/min.
2.	Flow controller	Brooks	Model 8940	5000 cc/min. (max)
3.	Elapsed timer	Automatic Timer and Controls	5701A	0-9999 min.
4.	Solenoid valve	Hoke	B90A34OR	1/4 inch
5.	Ball valve	Hoke	30206-5	1/4 inch
6.	Ball valve	Smith	125	1 inch
7.	Blower	Rotron	RS-3501	12 inch H_2O
8.	Silicon oil	G.E.	SF-96 (20)	-
9.	Ball valve (auto)	Jamieson	900-242-28	1 inch
10.	Insulation	Armstrong	9390-20	3/8 inch
11.	Vacuum valve	F. J. Stokes	2-ST-3	2 inch
12.	Controller	API Instrument	503-K	0-50 MV.
13.	Molecular sieve plate	Union Carbide	9999-00	13X & 5A
14.	Alumina plate	Bowser-Briggs	5050-1	H-151 Alumina
15.	Silica GEL plate	Alco Control	-	Davison GEL
16.	Oil pump	Eastern Ind.	DH-11	20 psi (max)
17.	Metal substrate	Wall-Colomony	9999	-
18.	Regulator	Matheson Co.	8-320	2000 psi (max)
19.	Diaphragm pump	Air Control	08-423-71	115 Volt
20.	Oil heater	Chromalox	NWHO-3451	4.5 Kw.

EQUIPMENT LIST (Cont)

Nomenclature	Manufacture	Part no.	Size
21. Thermostat	Fenwal	21170	-20° to 120°F
22. Compressor	Tecumseh	C7T16LT	3/4 HP
23. Vernier valve	Hoke	1RB280	1/8 inch
24. Rheostat	General Radio	W5MT	0-130 V
25. CO_2 gas	Matheson Co.	1A	99 percent
26. Vacuum pump	Stokes	149-H	3 stage
27. Generator	CML Corp.	1431 A	400 cycle

INSTRUMENT LIST

Part no.	Nomenclature	Manufacture	Identification
FA-160	Pressure gauge	Wallace and Tiernan	0-800 mm
20660	Venturi	Brooks Instrument	0-14 SCFM
6081-1	Transducer	EOS	0-0.1 PSIA
DHG-L-3P	Hygrometer	Bendix	$-100^{o}F$ (min)
992C1T1R1	Hygrometer	Cambridge Ins.	$-100^{o}F$ (min)
6702	Recorder	Weston Ins.	0 to 300 $\pm$ $2^{o}F$
6702	Recorder	Weston Ins.	-100 to 150 $\pm$ $2^{o}F$
6702	Recorder	Weston Ins.	0 to 100 $\pm$ $2^{o}F$
6702	Recorder	Weston Ins.	0 to 100 $\pm$ $2^{o}F$
Series S	Recorder	Esterline-Angus.	0 to 1 V $\pm$ 1/2%
1355	Rotameter	Brooks Inst.	0-840 cc/min
8940	Flow controler	Brooks Inst.	5000 cc/min (max)
	Thermocouples	Thermo Electric	Cu-Con
300	Gas analyser	Mine Safety	0-3%
200	Gas analyser	Mine Safety	0-3%

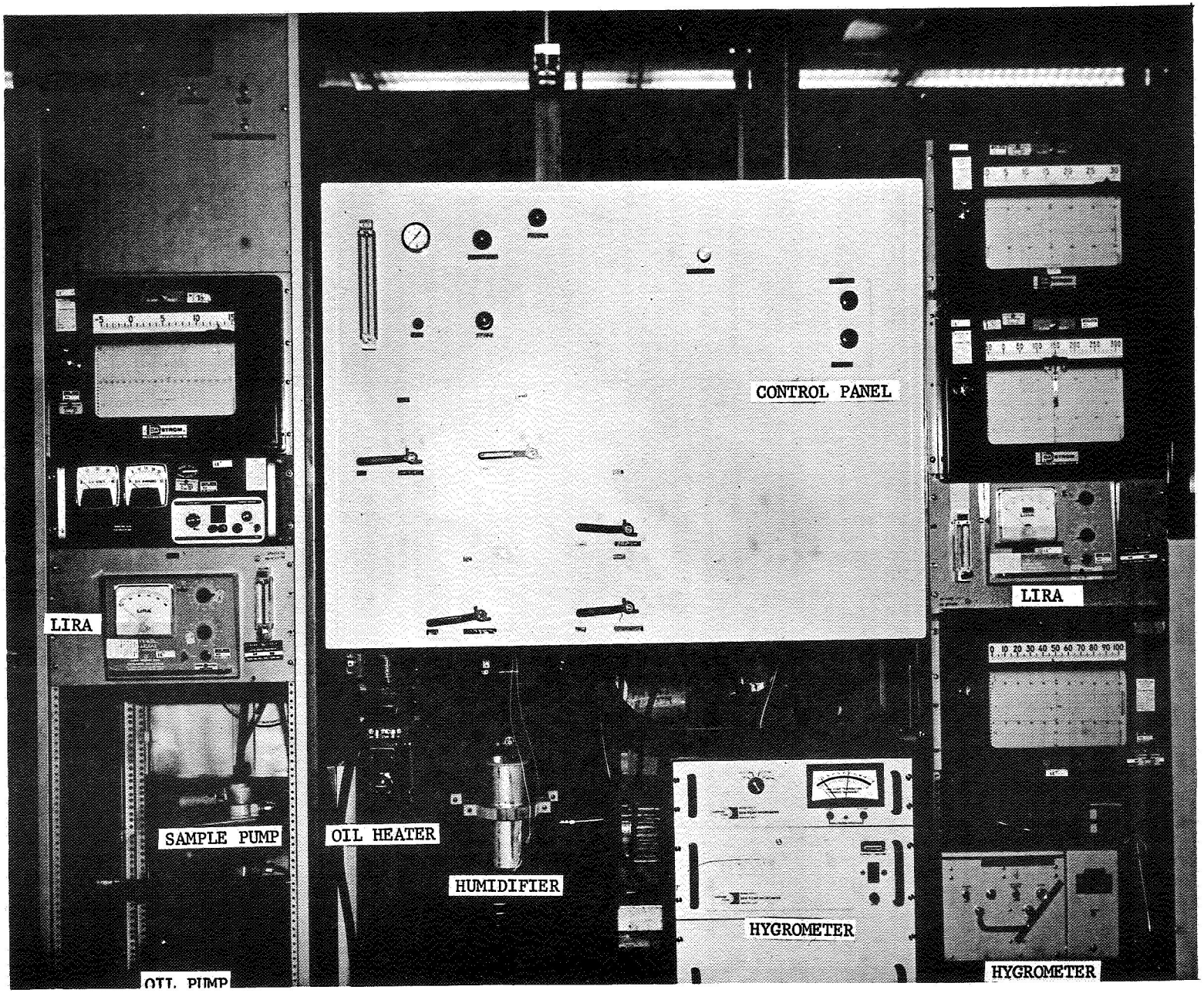
CONTROL PANEL
LIRA
LIRA
SAMPLE PUMP
OIL HEATER
HUMIDIFIER
HYGROMETER
HYGROMETER

Test Setup

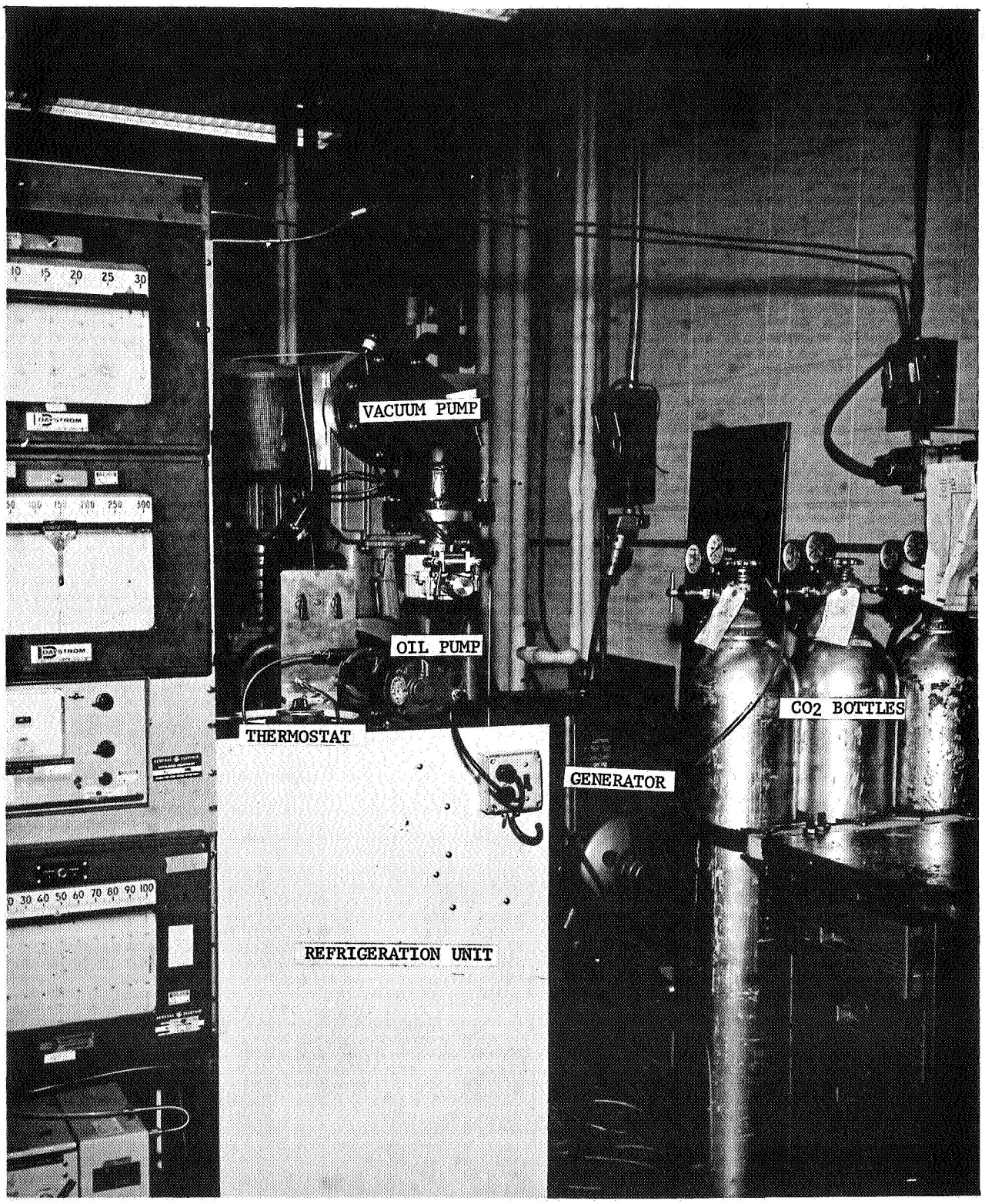
VACUUM PUMP
OIL PUMP
THERMOSTAT
GENERATOR
CO2 BOTTLES
REFRIGERATION UNIT

Test Setup

REFERENCES

1. Treyball, R. E.: Mas Transfer Operations. McGraw-Hill Book Co., Inc., 1955.

2. McAdams, W. H.: Heat Transmission. McGraw-Hill Book Co., Inc., 1954.

3. Data for Pellet Beds supplied by R. Martin, Contract Monitor. Langley Research Center, Hampton, Va.